1791 Tullie Circle, N.E./Atlanta, GA 30329
404-636-8400

DRAFT

TC/TG/MTG/TRG MINUTES COVER SHEET

(Minutes of all Meetings are to be distributed to all persons listed below within 60 days following the meeting.)

TC/TG/MTG/TRG No. TC 9.10 DATE May 24, 2024

TC/TG/MTG/TRG TITLE Laboratory Systems

DATE OF MEETING January 23, 2024 LOCATION Chicago

VOTING MEMBERS PRESENT	YEAR APPTD	MEMBERS ABSENT	YEAR APPTD	CORRESPONDING MEMBERS AND ADDITIONAL ATTENDANCE (INCLUDING VIRTUAL ATTENDEES)
Robert Weidner	2022	Danny Sanchez	2023	Roland Charneux (CM)
John Varley	2020	Ken Crooks	2021	Mike Carl (PCM)
Kelley Cramm	2022	Wei Sun	2021	John Castelvecchi (CM)
Glenn Friedman	2020			Tyler Kee (PCM) (V)
Kishor Khankari	2020			Jason Atkisson (CM)
Ryan Parker	2023			Pierre-Luc Baril (CM) (V)
Rachel Romero	2022			Christine Benga (CM)
Mark Malkin	2023			Brendon Burley (CM)
Guy Perreault	2022			Pat Carpenter (CM) (V)
Justin Garner	2021			Brad Cochran (CM)
Jim Coogan	2023			Brendan Dingman (CM)
Anne Juran	2023			Jake Edmondson (CM)
Chris Kirchner	2022			Kris Geyson (CM)
				Duncan Green (CM) (V)
				Greg Gross (CM)
				Keith Hammelman (CM)
				Charlie Henck (CM)
				Lloyd Le (CM)
				Paul Lemestre (CM)
				Scott MacMurray (CM) (V)

				Kurt Monteiro (CM)
				Victor Neuman (CM)
				Dave Rausch (CM) (V)
				Christine Reinders-Caron (CM)
				Kurt Rindoks (CM)
				Ali Salim Shirazi (CM)
				Gordon Sharp (CM)
				Tom Smith (CM)
				Ryan Soo (CM)
				Brooks Stout (CM)
				Bill Stump (CM) (V)
				Mitchell Swann (CM)
				Mark VanderKooy (CM)
				Danny McGrail (G)
				Chen-Wei Liu (G)
				Rachel Peters (G)
				Kirstin Thibodeaux (G)
				Otto VanGeet (G) (V)

DISTRIBUTION: ***All Members of TC/TG/MTG/TRG plus the following:***	
TAC Section Head: Brad Cochran	SH9@ashrae.net
All Committee Liaisons As Shown On TC/TG/MTG/TRG Rosters (Research, Standards, ALI, etc.)	See ASHRAE email alias list for needed addresses.

Mike Vaughn, Manager Of Research & Technical Services	MORTS@ashrae.net

CM = Corresponding Member
PCM = Provisional Corresponding Member
V = Attended on-line (virtual)

Note: These draft minutes have not been approved and not the official, approved record until approved by the TC.

CALL TO ORDER
Bob Weidner called the meeting to order at 3:30 PM CST.

CODE OF ETHICS COMMITMENT
In this and all other ASHRAE meetings, we will act with honesty, fairness, courtesy, competence, inclusiveness and respect for others, which exemplify our core values of excellence, commitment, integrity, collaboration, volunteerism and diversity, and we shall avoid all real or perceived conflicts of interests.
(Code of Ethics: https://www.ashrae.org/about/governance/code-of-ethics)
(Core Values: https://www.ashrae.org/about/ashrae-s-core-values)

TITLE, PURPOSE, SCOPE for TC9.10
Bob W. read our Title, Purpose, and Scope:
TC 9.10 is concerned with HVAC components for laboratory systems and their use therein. These components include but are not limited to air intakes, supply air conditioning systems, air distribution methods, laboratory fume hoods, biological safety cabinets, exhaust systems and exhaust discharge. The technical committee will address the unique requirements of all types of laboratories. These laboratories include but are not limited to nuclear, pharmaceutical/medical, general chemistry, and teaching. Additional TC 9.10 concerns are; (1) the reduction of energy usage in laboratory systems, (2) the monitoring of government regulations affecting laboratory operation.

SELF INTRODUCTIONS
The group did not do self-introductions in the interest of time.
.
MEMBERSHIP
Took roll call for voting members. 12 of 16 voting members are present. Quorum achieved. Note that Kishor Khankari joined the meeting late, bringing the total of voting members present to 13.

MEETING MINUTES
Guy Perreault moved and Charlie Henck seconded to approve the minutes from the last meeting as amended. The meeting date needs to be corrected. The minutes were approved unanimously.

WEBSITE
Jim Coogan reported that the recent minutes have been posted to the website. There is a lot of legacy stuff on the website but he is not planning to remove any of it.

Jim led a group on a tour of brewpubs on Sunday evening. It was a lot of fun and a good time.

ANNOUNCEMENTS
None

SECTION HEAD REPORT
Brad Cochran, Head for Section 9 gave his report. Activity forms need to be submitted after this meeting. Brad will work with the TC to get this done.

New roster is due end of February. Hopefully, ASHRAE will get it corrected.

Brad asked for a show of hands of those who participate in their chapter. It has been reported that only 10% of TC members participate in their chapter and only 2% of chapter members participate in TCs. Would like ideas on how to get more people involved in TCs. Now have a virtual attendance option but it hasn't increased participation.

A new MTG has been approved, MTG Generative AI. Will coordinate technical activities around AI. They have 3 tasks; look at how we can make sure ASHRAE publications are being referenced by AI but also properly referenced. Set up society standards for how we interact with AI. We don't want seminars generated by AI.

How can ASHRAE help develop AI as a tool in the development of HVAC systems? MTG will be meeting between now and the summer meeting. TC 9.10 needs to decide whether we want a liaison to that committee. Two years ago we approved TG9.Space. They have been active over the last 2 years. They have become a full TC: TC 9.13 Space

Only about 1% of ASHRAE members are fellows. Would like to increase this. Need more people to step up and nominate members for fellow. Fellow is not about ASHRAE participation, it's about contribution to the industry. Brad encouraged current Fellows to consider nominating someone.

Fellow Qualifications:

Section 16.2 – Honors & Awards Manual of Procedures

1. Requirements for eligibility for election to the grade of Fellow by the Board of Directors:
   - A. Good standing as a Full Member grade for at least ten (10) years.
   - B. Participation or service to ASHRAE is not a metric to be evaluated.
   - C. Attained distinction and made substantial contribution in HVAC&R and the built environment such as:
     1. Education and/or research
     2. Engineering design/consulting/forensics
     3. Invention/original work
     4. Engineering executive on projects of unusual or important scope.
     5. Sharing knowledge and contribution through outreach activities such as mentoring, publications, oral presentations and involvement in industry activities.
     6. Other activities leading to advancement of the arts and sciences of HVAC&R and the built environment including that of contractors, manufacturers and their representatives
   - D. Distinction is interpreted to mean: seen by their peers in the industry as a person of excellence
   - E. Substantial contribution is interpreted to mean: one or more contributions to the industry which had a notable, unique, and positive impact in the advancement of the arts and/or sciences of HVAC&R, the built environment and a sustainable world.

Second year in a row Hightower award went to a section 9 participant. It went to Erich Binder this year. This is related to contributions to society.

You can contact Brad at:
SH9@ashrae.net
For general questions email:
Asktac@ashrae.net

PROGRAM SUBCOMMITTEE REPORT

Rachel Romero provided a report. TC 9.10 Program committee met earlier this month. We had 4 sessions (2 seminars, a forum, and a panel) and a paper session at this meeting. Justin Garner and Ryan Soo's seminar was sold out and standing room only.

For Indianapolis, looking at a session for the Codes, Standards, etc. Track. Have one or two more ideas that are being developed.

For Orlando, thinking about a debate for the RP1780 results.

See attached report for more information.

RESEARCH SUBCOMMITTEE REPORT

Bob W gave a report:

RP1573 – "Determination of suitable replacement of SF6 when used as a tracer gas in accordance with ANSI/ASHRAE Standard 110" was completed. If you'd like more information, talk to Tom Smith.

RP1780 – “Test method to evaluate cross-contamination of gaseous contaminants within total energy recovery wheels” is complete but may spur additional research, programs, etc. See detailed report below.

RP1835 – “Characterizing the performance of induced flow stacks”. Brad gave a report. We are measuring plume rise and spread from induced flow fans to see if it aligns with what is characterized for utility set fans. May have some data to present by Indianapolis.

RTAR 1963; Survey of sources of contamination in existing labs. Roland and Tom are looking for some help with this. If you are interested, please contact Tom or Roland. RAC feedback is that the topic needs to be narrowed down.

Potential future projects to submit RTARS: duct velocity, using AI, demand ventilation in labs, hourly data on lab equipment use, 3D printers.

CO-RP 08 – Proposed Research Project: “Evaluation of impact of air change rate (ACR) and airflow patterns on the ventilation performance of indoor spaces”. Price Industries has committed to support this project financially.

SPC 129 – Measuring Air-Change Effectiveness – (this is not sponsored by TC9.10) but Tom reported that their objective is to measure air change effectiveness. Doesn’t lend itself to a field test. Plan to add a field test and a CFD analysis. Committee met yesterday and formed subcommittees. Field testing, CFD analysis, and Metrics.

RP 1780 - Test method to evaluate cross-contamination of gaseous contaminants within total energy recovery wheels

Carey Simonson, the Principal Investigator from the University of Saskatchewan gave a report. Their final report has been published. Looked at xylene and SF6. Noted significant cross contamination for both chemicals. The full report is available on the Technology Portal. Roland suggested that they publish an article in the ASHRAE Journal to report these results so the scope of the cross contamination is understood. Brendan said he is responsible for curating content for the IAQ column in the ASHRAE Journal and asked Carey to write a 4 page article and he will see if he can get it published.

Tom Smith asked if they had an opinion on how the results might be different if the wheel were older and degraded. The research used a new wheel. The researcher can’t predict how this might affect performance.

See attached report.

LAB CLASSIFICATION SUBCOMMITEE

This committee met. Danny Sanchez was not present. See attached report.

STANDARDS SUBCOMMITTEE

Justin Garner reported: Wade Conlan used to be liaison to SSPC 241 but Justin needs a new liaison due to Wade being busy. Tom suggested Brandon Burley.

Jim Coogan is still the best liaison for Z9.5.

Guideline 36: Jim is on the committee. Ryan Soo has been involved also. Jim reported that the Guideline 36 committee has proposed an addendum for lab room sequences. The draft was voted for public review a month ago. The committee was asked if they want TC9.10 review and the committee said no. They designated Kelley Cramm as the reviewer. Jim and Ryan have prepared a review also. When it goes for public review, the TC

may want to coordinate public comments. Guy agreed to help. They added a sequence for what to do if the supply fails, for whatever reason, the exhaust sequence to allow people to safely exit the building.

Standard 170: Justin has had a hard time getting the committee to work with us. Bob said he will follow up on this item.

STANDARD 110
Tom Smith gave a report.

DESIGN GUIDE
Ann Juran is the chair of this subcommittee. See attached report. Table of contents is being revised now. Once this is done, they will open it up for chapter reviewers to work on chapters. Looking for cover artwork or photography. If anyone wants to give artwork or photography, contact Ann.

HANDBOOK SUBCOMMITTEE
Mark Malkin reported they had their on-line meeting two weeks ago. He had 4 people volunteer to help. There is no hurry; they will roll design guide changes into the handbook. It is the 2027 version they are working on so they have some time. Looking for suggestions from the committee. Send Mark an email if you have suggestions.

ASHRAE JOURNAL
Roland Charneux reported since the last meeting the September issue had an article by Kelley Cramm; Designing Safe, Healthy Science Labs in Schools.

ALI COURSES
Laboratory Design Course – The Basics and Beyond – John Varley reported he taught the course Sunday but that will be his last. He has been teaching for 12 years. Had over 30 pre-registered attendees plus several walkups so attendance was good. New instructor(s) will be Danny McGrail and maybe Rachel Romero.

Laboratory Exhaust Course – Safe and Energy Efficient Design – Brad said this course was not held in Chicago. It's on hold until he rolls off TAC.

Laboratory Controls Course –.John C reported It's ready to go.

LIAISON REPORTS

TC 1.4 Control Theory and Application – Jim Coogan: See Jim's TC 1.4/Guideline 36 report.

TC2.2 Plant and Animal Environment- Henry is not present. No report. Bob noted that the Animal Environment might move to TC9.10 since TC 2.2 is focusing more on Plant environments.

TC 4.3 Ryan Parker reported– They are excited about the lab fan research. Chapter 24 will be available soon and they are looking for reviewers.

TC5.1 Fans – No report

TC5.3 Room Air Distribution–Kishor reported they don't have anything to report related to TC 9.10

TC7.6 Building Energy Performance – Pat Carpenter reported he was not at the meeting but they have a lot going on around decarbonization. They have an ongoing performance standard effort. They had a discussion on the monitoring of energy code. There seems to be a large discrepancy in how AHJs across the country apply and enforce the energy code. In general, energy use in laboratories is not consistently addressed. Benchmarking is not addressed well for laboratories.

TC7.9 Building Commissioning –Justin Garner will provide a report. Rachel asked if 7.9 would pursue a lab Cx program with 9.10 for a future meeting.

TC9.2 Industrial Air Conditioning and Ventilation. Scott MacMurray said they had a discussion on the exhaust demand research.

TC9.6 Healthcare Facilities – Brendan Dingman reported that there wasn't much in 9.6 pertaining to laboratories.

TC9.7 Educational Facilities – Keith Hammelman reported they updated their scope and purpose. Discussion on how they can add information on their website on the Inflation Reduction Act. Also looking at how to address Maker Spaces.

TC9.11 Clean Spaces – Roland Charneux reported there is a big push on energy efficiency and demand control ventilation since these spaces are very large energy users.

MTG ACR –Jim Coogan said the research project is the point of this. It is a very ambitious project involving both field testing and CFD modeling. Also trying to add to the list of potential bidders.

62.1 Ventilation for Acceptable IAQ – Brendon Burley left for the airport so he did not report.

90.1 – Jason Atkisson indicated he is now on TAC so he did not attend the 90.1 meeting. He asked if someone else would liaison. Justin Garner said he is the liaison to another committee so he may be able to address issues pertinent to TC9.10.

SMACNA – No report

NFPA 45 – Ken Crooks reported that the 2024 edition was released in fall of last year. The 2027 edition has entered public input phase. It will be open for comments until January, 2025. Health Care laboratories are now covered by NFPA 45.

NSF – No report

ISPE – CJ Blair is a member and would like to see better coordination between ISPE and TC9.10 in the future. Nothing to report at this time.

ASTM Z9.5 – Jim Coogan stated they are looking for new people to help with this for future versions. Most of those who worked on the last edition may be retired when the next effort starts. Other main purpose is getting this standard integrated with ASTM since it's now under ASTM's purview.

AIHA Lab Health & Safety – Tom Smith reported they have a group working on fume hood monitors. They tried to survey EH&S people on what issues they have on fume hood monitors, but they have not received any feedback.

I2SL – Gordon shared a short presentation. They have new branding. No superscript. Conference next year is in St. Louis in September. Last year they had one of the highest attendances ever. Will have an international conference in April. Have two new chapters (UK and Australia). Big effort is on Labs2Zero. Planning for more training and accreditation in the future. I2SL is stepping into the benchmarking area since DOE doesn't cover labs. Looking at operational emissions also. Also working on embodied carbon. See attached report.

Title 24 – Brad reported the version that will come out in 2026 which will take effect in 2027 will have a lot more exhaust fan requirements. It will be a major change regarding how you operate and turn down laboratory exhaust systems. Glen F also reported that Standard 100 – "Energy and Emissions Building Performance Standard for Existing Buildings" is being adopted and other jurisdictions have also begun adopting this. It

includes laboratories as one of its building types. Standard 100 covers actual building data to see if the target is being met.

NEW BUSINESS

Pat Carpenter asked if anyone followed what TC9.9 is doing this year. They are putting their publications on line in a single document and making them searchable. Brad stated that they have 14 books they are putting on a single Wiki and making them searchable. They are implementing a subscription service for these documents. Pat asked if this is a model we should be looking at for the future. Should we think about doing this with the Design Guide? Brad said TC9.9 is being the “Guinea pig” for this and we should definitely keep an eye on how this works for them.

Rachel suggested we take a TC picture after the meeting.

Kishor said he presented two papers yesterday on residential kitchen ventilation. The topic of gas stoves has been covered by the media recently. He did some analysis on this and found some surprising results. He found that the buoyancy of the air from the stove and the buoyancy of heat from the person standing in front of the stove affects the hood capture.

ADJOURN

It was moved and seconded to adjourn at 5:27 PM CST

ASHRAE 9.10 Research Subcommittee – Chicago Meeting Report – Research Summary

1.23.24

Completed 9.10 Research Projects:

1. RP-1573 Replacement of SF-6
2. RP-1780 Cross contamination in Heat Recovery/Enthalpy Wheels
    a. U of Saskatchewan paper presented here in Chicago
    b. Overview of paper in 9.10 meeting
    c. Considering other follow up research on sensible heat recovery wheels, different velocity ranges, etc. – **1780 Part 2?**

On going 9.10 Research Projects:

1. RP-1835 Induced air exhaust fans Characterizing the Performance of Entrained Flow Stacks) Brad C. (CPP)

9.10 RTARS (Research Topic Acceptance Request) and Work Statements in the works

a. RTAR 1963 - "Survey of sources of contamination in existing labs" Roland C. and Tom Smith. A "heavy re-write" is needed based on comments - ***Looking for help from TC!***

Future Research Projects under consideration:

1. 1780 – Part 2
2. Duct velocity in exhaust ducts
3. Using AI for lab control
4. Hazardous emissions in vivariums
5. Demand ventilation in labs to reduce air flow rates
6. Hourly data on lab equipments
7. 3-D printing emissions (TC 9.7 as co-sponsor)
8. Validating Plug Loads in Labs

Related Research Project Work

1. Ventilation Effectiveness for Labs – WS 1936n (CO-RP-08) – Almost completed (Kishor, Jim, Roland,) Co-sponsor by Price Jim C. is liaison from 9.10.

ASHRAE 9.10 Research Subcommittee - 2024 Winter Meeting Agenda & Minutes (1/8/24)

2. **1780-RP Research Project** (Test Method to develop a Methodology to Evaluate Cross Contamination of Gaseous Contaminants within Total Energy Recovery Wheels) - University of Saskatchewan – Easwaran Krishnan
    a. Status of Research Project
        i. Project is complete!
        ii. Presentation of Final Paper (Chicago); Future Seminar or Debate (Indianapolis or Orlando)
        iii. 1780 Part 2 – Sensible Wheels; Higher Velocities
3. **1835-RP Update** (Characterizing the Performance of Entrained Flow Stacks) – Brad C. (CPP)
    a. Brad Update – Full scale testing of actual lab exhaust stacks to compare to analytical calculations;
    b. Next summer – Initial Results
    c. PI – Using drones for data collection

4. Research Projects under consideration

a. RTAR: "Survey of sources of contamination in existing labs" Roland C. and Tom Smith. RTAR draft is written; awaiting review from Tom Smith. RTAR 1963 – responses to comments – "heavy re-write" Looking for help from TC

b. Ventilation Effectiveness for Labs – Variety of Groups doing this work - I2SL, ASHRAE MTG ACR, SP 129; Kishor – RTAR is approved; research has some industry support; Work Statement in process and close to completion. WS 1936n (CO-RP-08) – Almost completed (Kishor, Jim, Roland,) Co-sponsor by Price Jim C. is liaison from 9.10.

c. Using AI to help better operate buildings – Future research – Jim Coogan to provide input. RHW to follow up with Jim.

d. Carbon Emissions within labs - NA

e. Duct velocities in Lab exhaust – transport velocities required for chemical removal, prevention of condensate, etc. – Tom S. commented – heated acid vapors – condenses and rains back into hood – guidance needed; 110 committee members to be asked (RTAR

f. Tom Smith – AIHA – Hazardous emissions in Vivariums; nuisance odors, air changes – historic design practices; advances in technology. ALAC criteria – 10AC without protective environment. Should be more research. "Hot topic" liaison (Henry Hayes 2.2) – put on back burner; TC 9.10 to take over animals – Discussion w/ TC 2.2

g. Potential research needed following forthcoming Program Initiatives:
    i. Demand Control Ventilation in labs to reduce air flow rates – Forum or Seminar; Kishor ready to present – Need 2 more speakers – Gordon Sharp? Overview of DCV – Tom Smith; What is it, How does it work? Avoid commercialism. Tom follow up! Paul Fusson, Amanda, Rachel – potential chair: Chicago or Indianapolis? RHW to follow up w/ Rachel; Kishor simulations
    ii. Hourly data on lab plug loads needed; are metrics available? Database follow up from Labs21 may be helpful – Future Program – Lab2Zero? My Green Lab has this data. May be a data collection project to consolidate this data. RHW to look into this. Check w/ Rachel; IS2L – data should be reflective of type of lab -

5. Review of pertinent on-going research outside 9.10

a. RP 1833 – Air Change Rates – Research is Complete; Future program should come out of this. Sets basis for future research. Completed – RHW to check for report
b. Work Statement 1936 – Air Change Rates vs. Effectiveness – In development – co-funded by Price; MTG ACR;
c. 3D Printing Hazardous Issues (nano particles, chemicals, fumes, etc.) – TC 9.7 discussing; Roland to follow up and also Jason Atkisson – Protocol for investigation for contaminant emission could be used for 3D. (Keith Hammelman was mentioned) RHW

6. Open to floor for Research Topics:
    a. No discussion

Attendees: Bob Weidner, Brad Cochran, Christine R., Chris Kirchner, Tom Smith, Ryan Soo, Ken Crooks, Glenn Friedman, Roland C., Tyler Kee, Kevin Gebke, Chen Wie, Otto NREL; Bill Stump; Jason A., Guy P., Ryan Parker, Ryan Soo

Summary of Proposed ASHRAE Research Project (CO-RP-8)

ASHRAE MTG.ACR

Title

Evaluation of impact of air change rate (ACR) and airflow patterns on the ventilation performance of indoor spaces.

Hypothesis

Layout and selection of supply diffusers and returns can have larger impact than ACH on ventilation performance.

Summary

The main purpose of heating, ventilation, and air conditioning (HVAC) for buildings is to maintain an acceptable indoor environment for occupants, products, and processes. Air Changes per Hour (h-1) is often used as a metric for specifying the supply airflow rates for critical spaces including healthcare facilities, cleanrooms, and laboratories. Although high ACH can enhance dilution and rate of decay of contaminants, it cannot ensure effective distribution of clean air and removal of contaminated air from the critical zones such as the breathing zone of occupants.

Air is the primary carrier of heat, moisture, and airborne contaminants in indoor spaces. The distribution of clean supply air and resulting airflow patterns, therefore, play a crucial role in determining indoor air quality. The indoor airflow patterns can depend on several factors including the number, location, and type of supply diffusers; supply airflow rates and associated diffuser throws; supply air temperature; number, size, and locations of return/exhaust grilles for certain fixed location and strength of heat sources and furniture arrangement which will present obstructions to airflow. Previous studies indicate that proper layout of supply diffusers and returns not only improves ventilation performance but also reduces the required supply airflow rate.

The proposed research aims to evaluate the relative impact of air change rates and airflow patterns in indoor spaces and verify that an optimized HVAC layout can improve ventilation performance without excessive high supply airflow rate. Both experimental and computational fluid dynamics (CFD) approaches will be employed to test the impact of the type and number of supply diffusers, number and location of return/exhaust grilles, and supply air temperature. These tests will be conducted for three different room sizes for various ACH levels for each size. Obstructions to airflow will be placed in the room to represent equipment and furniture. These tests and analyses will be performed for a certain specified release rate of a gaseous contaminant surrogate at a certain location. Experimental tests will involve transient measurements of air velocity, temperature, and contaminant concentration at various locations. CFD analyses will be performed to guide the experimental setup and sampling locations. The ventilation performance will be evaluated by employing suitable metrics for ventilation effectiveness.

The research will help ASHRAE develop guidelines and standards for specifying HVAC layout and selecting ventilation rates that achieve a better combination of indoor environment, first cost, operating cost, carbon emissions, and energy efficiency.

Preliminary Test Matrix

Tests matrix CO-RP-8		
Physical Settings		
Room Sizes (Feet)	10 x 10, 10 x 20, 20 x 30	
Room Height (Feet)	9	
Diffusers and Return grilles locations	2 different locations per room size	
Movable obstacles in room	Potential movable partitions at every 200 sq-ft to adjust room size and blocks that could pose obstruction to airflow in the room	
Diffusers types		
Square 4 ways		ACR 3, 4, 6, 8
Round/square high induction		ACR 6, 8, 10, 15
2 x 4 perforated laminars		ACR 8, 10, 15, 20
System operational conditions		
ACR	3, 4, 6, 8, 10, 15, 20, as per diffuser types	
Supply Temp (°F)	55, 75, Thermal laods will be required in the room	
Contaminant	gaseous contaminant	
Contaminants sources locations	One location in breathing zone	
Measurements		
Measurements	Temperature, air velocity, contaminants concentration at each sampling points	
Sampling locations	At every 40 sq-ft in the breathing zone, minimum 10 per room, and at the return	
HVAC System characteristics		
VAV system that could provide the required ACR (+/- 2 000 CFM) and varying temperature from 55°F to isothermal conditions.		
100% outside air to avoid contaminant re-entrainment in the supplied air to the room		
Airflow measuring station in the supply and the return		
Ducted supplied and returned air.		
Location of diffusers as per manufacturer recommendation. Ability to relocate supply diffusers and return grilles in a room.		
Cooling loads in the rooms (+/- 12 kW Heating load to creat cooling need and 55°F supply temperature)		

ASHRAE Research Project Report 1780-RP

TEST METHOD TO EVALUATE CROSS-CONTAMINATION OF GASEOUS CONTAMINANTS WITHIN TOTAL ENERGY RECOVERY WHEELS

"

Approval: June 2023

Contractor: University of Saskatchewan

Principal Investigator: Carey Simonson

Authors: Easwaran Krishnan , Mehrdad Torabi, Melanie Fauchoux, Jafar Soltan
Author Affiliations, University of Saskatchewan

Sponsoring Committee: TC 9.10, Laboratory Ventilation

Co-Sponsoring Committee: TC 2.3, Gaseous Air Contaminants and Gas Contaminant Removal Equipment; TC 9.6, Healthcare Facilities; SSPC 62.1, SSPC 62.1, Ventilation for Acceptable Indoor Air Quality

Co-Sponsoring Organizations: N/A

Shaping Tomorrow's Built Environment Today

FINAL REPORT

TEST METHOD TO EVALUATE CROSS-CONTAMINATION OF GASEOUS CONTAMINANTS WITHIN TOTAL ENERGY RECOVERY WHEELS

ASHRAE RESEARCH PROJECT 1780

Easwaran Krishnan[1]
Mehrdad Torabi[1]
Melanie Fauchoux[1]
Jafar Soltan[2]
Carey Simonson[1]

[1]Department of Mechanical Engineering, College of Engineering, University of Saskatchewan, Saskatoon, Canada.
[2]Department of Chemical and Biological Engineering, College of Engineering, University of Saskatchewan, Saskatoon, Canada.

June 6, 2023

EXECUTIVE SUMMARY

The main goal of ASHRAE RP-1780 was to develop a test method to evaluate gaseous contaminant transfer in total energy recovery wheels. The project had the following objectives:

(i) Review current testing methodologies and relevant research data available.

(ii) Develop a draft test methodology and establish minimum specifications for the test facility and instrumentation.

(iii) Evaluate the draft test methodology with various gaseous chemicals representative of contaminants of concern and operating conditions representative of a laboratory, vivariums and similar facilities. Also consider various incoming outside air temperatures and humidity.

(iv) Validate the test methodology based on the test results collected under laboratory conditions.

(v) Produce a final test method for establishing gaseous cross contamination rate measurement that is reliable and effective for manufacturers/test laboratories to employ.

This report describes the research undertaken at the University of Saskatchewan to meet the objectives and goals of this project. Overall, the test method developed, evaluated, and validated in this report builds on existing test methods in the literature (i.e., ASHRAE Standard 84-2020) and will allow manufacturers and test laboratories to accurately quantify gaseous contaminant transfer in energy exchangers.

Objective 1: *Literature review*

The literature review on experimental studies on contaminant transfer in energy exchangers revealed five mechanisms that contribute to gaseous contaminant transfer: (1) carryover, (2) leakage, (3) adsorption, (4) absorption and (5) frosting/condensation. Carryover and leakage are due to bulk air transfer, while adsorption, absorption and condensation/frosting are due to phase change. Gaseous contaminant transfer due to air leakage and carryover has been studied and measured extensively using inert gases, and established test methodologies exist in ANSI/ASHRAE Standard 84-2020 (ANSI/ASHRAE 2020) and Canadian Standards Association C439- 2018 (Canadian Standard Association 2018). In these standards, contaminant transfer due

to air leakage and carryover (i.e., bulk airflow from the exhaust side to the supply side of the exchanger) is quantified using the exhaust air transfer ratio (EATR), which quantifies the fraction of exhaust air that is transferred into the supply air.

The literature review showed that several researchers have measured the contaminant transfer of non-inert gases in energy exchangers but very few have conducted an uncertainty analysis. While these contaminant transfer measurements inherently include all transfer mechanisms, no test method exists in the literature to quantify and determine the uncertainty of gaseous contaminant transfer due to mechanisms other than carryover and leakage. Researchers have published gaseous contaminant transfer ratios between 0% and 75%. The highest transfer ratios were measured for phenol, toluene, ammonia, acetic acid, and formaldehyde, which have high solubilities in water and may explain the high transfer rates. The literature review showed that the exchanger design parameters (effectiveness and face velocity) have a greater effect on EATR than the operating conditions (relative humidity and temperature).

Objective 2: *Development of a test method*

In this report, an experimental method is proposed to determine the transfer of gaseous contaminants in rotary energy wheels. The proposed methodology builds on ASHRAE standard 84, which is a rigorous, established method to determine the effectivenesses and exhaust air transfer ratio (EATR) of energy exchangers. A schematic of an energy wheel showing the four measuring stations are presented in Figure 1.

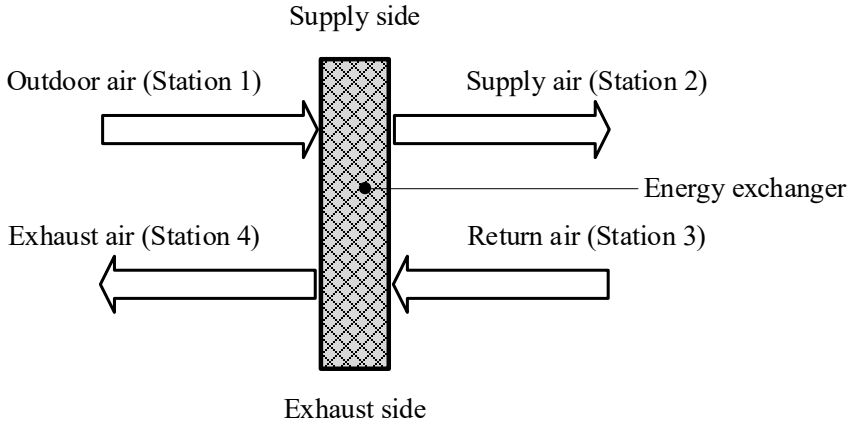

Figure 1. Schematic of an energy wheel showing four measurement stations corresponding to outdoor air (Station 1), supply air (Station 2), return air (Station 3) and exhaust air (Station 4).

The test method proposed in this report adopts all the methods, parameters and criteria from ASHRAE Standard 84 and introduces a new performance parameter, Exhaust Contaminant Transfer Ratio (ECTR), and associated criteria to ensure an acceptable test. ECTR is similar to EATR, but quantifies contaminant transfer rather than air transfer from the exhaust side to supply side of the wheel. ECTR is defined as the difference in the concentration of gaseous contaminants between the supply air outlet and the supply air inlet, divided by the concentration difference of gaseous contaminants between the exhaust air inlet and the supply air inlet, expressed as a percentage, as shown in Eq. (1).

$$ECTR = \frac{C_2 - C_1}{C_3 - C_4} \quad (1)$$

where C_1, C_2, C_3, and C_4 are the gas concentrations measured at Station 1 outdoor (outdoor air) Station 2 (supply air), Station 3(return air) and Station 4(exhaust air) airstreams, respectively.

ECTR quantifies the transfer of gaseous contaminants due to all the mechanisms, while EATR quantifies transfer due to carryover and leakage. The contribution of phase change mechanisms (adsorption, desorption and condensation/frosting) to contaminant transfer is $ECTR_{pc}$, which can be determined by subtracting the EATR measured using an inert gas (like SF_6) from ECTR, as shown in Eq. (2)

$$ECTR_{pc} = ECTR - EATR \quad (2)$$

To ensure high quality of data from an ECTR test, data that fails to meet the following criteria are to be rejected. These recommended criteria for the rejection of test data are similar to criteria for EATR tests in ASHRAE Standard 84.

(i) Steady-state inequality for the inlet air concentration measurement:

$$\frac{|\delta C_3|}{|C_1 - C_3|} < 0.05 \quad (3)$$

where δC is the maximum deviation of any concentration measurement from its time-averaged mean value.

(ii) Contaminant mass balance inequality:

$$\frac{|\dot{m}_1 C_1 - \dot{m}_2 C_2 + \dot{m}_3 C_3 - \dot{m}_4 C_4|}{m_{minimum\,(1,3)}\ |C_1 - C_3|} < 0.2 \quad (4)$$

where $\dot{m}_1$, $\dot{m}_2$, $\dot{m}_3$, and $\dot{m}_4$ are the mass flow rates measured from outdoor (measurement station 1 in ASHRAE Standard 84), supply (Station 2), return (Station 3) and exhaust (Station 4) airstreams, respectively.

(iii) Uncertainty in the contaminant transfer ratios:

$$U(ECTR) < 3\% \quad (5)$$

$$U(ECTR_{pc}) < 5\% \quad (6)$$

Objective 3: *Evaluation of the test method*

The proposed test method was evaluated by testing eleven gaseous contaminants in two energy wheels, one coated with silica gel (SG) and one with molecular sieve (MS), under a range of design and operating conditions. The method worked well for all gas tested and all design and operating conditions. For both wheels and all design and operating conditions, ammonia had the highest transfer (ECTR ≈ 70 - 80%) and carbon dioxide had the lowest transfer (ECTR ≈ 2 - 10%).

The method was also evaluated under a wide range of design and operating conditions. It was found that the effect of design parameters such as face velocity, desiccant material and pressure difference between supply and exhaust sides had a greater influence on ECTR than the effect of operating conditions such as outdoor and indoor air temperature and humidity. For example, the silica gel wheel tended to have slightly higher transfer rates and require longer test times to meet the mass inequality in Eq. (4) compared to the MS wheel.

The method was evaluated for six different face velocities ranging from 0.25 to 1.5 m/s (50 - 295 fpm). The contaminant transfer increased with decreasing face velocity similarly as water vapor transfer or latent effectiveness increases with decreasing face velocity. For example, with MS wheel, ECTR increased from 50% to 90% for the case of ammonia when the face velocity decreased from 1.5 to 0.25 m/s (or 295-50 fpm).

The method was shown to work for different pressure differences between the supply and return ducts. When the return duct pressure was higher than the supply duct (i.e., $P_{return} > P_{supply}$), the ECTR increased as the pressure difference increased due to increased air leakage. The measured

contaminant transfer due to phase change ($ECTR_{pc}$) was nearly constant for all pressure differences within experimental uncertainties.

The method was evaluated for a range of temperatures and humidities. The effect of temperature and humidity was found to be small unless there was frosting on the energy wheel. During frosting, ECTR increased, which means that frosting conditions need special attention in the final test method. The effect of outdoor air temperature on the contaminant transfer ratio was evaluated by varying the outdoor air temperature from -23°C (-10°F) to 32°C (90°F). The ECTR values measured at different temperatures were similar (within experimental uncertainties). However, as noted previously, there was a slight increase in ECTR during frosting, especially when the frosting experiments were run for a longer time (4-5 hours). To study the effect of outdoor humidity on contaminant transfer, the outdoor air humidity was varied from 30% RH to 85% RH and indoor humidity was varied between 10% RH to 70% RH. The measured ECTR values were nearly similar irrespective of the humidity conditions. These tests confirmed that air humidity does not have a significant effect on the contaminant transfer in energy wheels. Therefore, it is recommended to conduct ECTR tests under isothermal and equal humidity conditions, where both supply and return air temperature and relative humidity are equal to the conditions in the test lab.

Objective 4: *Validation of test method*

To validate the test method, the criteria that were proposed to ensure quality test data were assessed in all the tests. A total of 325 tests were completed in ASHRAE RP-1780 and the minimum, average and maximum inequality values for mass inequality (Eq. (4)), uncertainty in ECTR (Eq. (5)) and steady state inequality (Eq. (3)) were computed. Approximately 95% of tests were able to achieve the proposed inequality and uncertainty limits. The average values of contaminant mass inequality, uncertainty, and steady state inequality in ECTR were 12%, 2% and 3%, respectively. The tests that did not meet the criteria are highlighted in the report. The detailed statistics are summarized in Table 1.

Table 1. Maximum, minimum and average values obtained for contaminant mass inequality and ECTR uncertainty from the contaminant transfer experiments in ASHRE RP-1780.

Proposed criteria and limits		Statistics from 325 tests in RP 1780			
		Min	Max	Average	Standard deviation
Contaminant mass inequality	$\frac{\lvert \dot{m}_1 C_1 - \dot{m}_2 C_2 + \dot{m}_3 C_3 - \dot{m}_4 C_4 \rvert}{m_{minimum\ (1,3)}\ \lvert C_1 - C_3 \rvert} < 20\%$	0.5%	22%	12%	6%
ECTR uncertainty	3%	0.6%	4%	2%	0.7%
Steady state inequality	5%	0.2%	11%	3%	2%

Objective 5: *Final test method*

After evaluation and validation, the test method for contaminant transfer was finalized. The final test method follows ASHRAE Standard 84-2020 with an additional parameter to quantify the gaseous contaminant transfer (ECTR) and four additional criteria to ensure acceptable data as summarized in Table 2.

Table 2. Proposed parameters with their recommended maximum limits, uncertainty limits and the recommended test conditions for contaminant transfer experiments.

Proposed parameter	Equation and criterion	
Exhaust contaminant transfer ratio	$ECTR = \frac{C_2 - C_1}{C_3 - C_1}$	U(ECTR) < 3%
$ECTR_{pc}$	ECTR – EATR	U($ECTR_{pc}$) < 5%
Steady state inequality	$\frac{\lvert \delta C_3 \rvert}{\lvert C_1 - C_3 \rvert} < 5\%$	
Contaminant mass inequality	$\frac{\lvert \dot{m}_1 C_1 - \dot{m}_2 C_2 + \dot{m}_3 C_3 - \dot{m}_4 C_4 \rvert}{m_{minimum\ (1,3)}\ \lvert C_1 - C_3 \rvert} < 20\%$	
Test conditions	• All contaminants of interest with the wheel operating under isothermal and equal humidity conditions • A longer test during frosting conditions, if appropriate	

The final method quantifies contaminant transfer using the exhaust contaminant transfer ratio (ECTR), which is analogues to the exhaust air transfer ratio (EATR) in ASHRAE Standard 84-2020. It is recommended that the maximum allowable uncertainty in ECTR is ±3%. The uncertainty in $ECTR_{pc}$ depends on the uncertainty in ECTR and EATR, and the maximum

suggested value is ±5%. The recommended inequality limit for steady state conditions is 5%, and contaminant mass inequality is 20%.

ECTR tests are recommended for all contaminants of interest at isothermal and equal humidity conditions (where the conditions of the supply and return air streams are at equal temperature and humidity conditions). Typical indoor temperature and relative humidity are recommended for ECTR tests. A longer test should be conducted under frosting conditions, if the wheel is intended to be used in a cold climate where frosting is expected to occur.

TABLE OF CONTENTS

LIST OF FIGURES

LIST OF TABLES

NOMENCLATURE

Acronyms

AAEEs	Air-to-air energy exchangers
AHRI	Air-Conditioning, Heating, and Refrigeration Institute
ASHRAE	American Society of Heating Refrigerating and Air-conditioning Engineers
EA	Exhaust air
EATR	Exhaust air transfer ratio
ECTR	Exhaust contaminant transfer ratio
FTIR	Fourier transform infrared
HPLC	High performance liquid chromatography
HVAC	Heating, ventilating and air conditioning
IER	Ion exchange resin
ISO	International Organization for Standardization
LAMEE	Liquid-to-air membrane energy exchanger
MS	Molecular sieve
NI	National Instruments
OA	Outdoor air
OACF	Outdoor air correction factor
P	Liquid circulating pump
ppb	Parts per billion
ppm	Parts per million
PVC	Polyvinyl Chloride
RA	Return air
RAMEE	Run-around membrane energy exchanger
RFP	Request-For-Proposal
RP	Research project
SA	Supply air
SG	Silica gel
VOCs	Volatile organic compounds

Symbols

a	Absorptivity (m^2/mol)
A	Absorbance
b	Optical path length (m)
C	concentration (ppm)
Cr*	Heat capacity rate ratio
C_p	Specific heat capacity (J/kg. K)
dT	Maximum deviation from time-averaged temperature (°C)
dW	Maximum deviation from time-averaged humidity (g_w/kg_a)
δC	Maximum deviation of concentration reading from C, its time-averaged mean value (ppm)
fpm	feet per minute (ft/min)
h	Specific enthalpy (kJ/kg)
I	Intensity of infrared radiation that has passed through the sample gas (W/m^2)
I_0	Intensity of infrared radiation for background measurement (W/m^2)
$\dot{m}$	Air mass flow rate (kg/s)
NTU	Number of transfer units
P	Static pressure (Pa)
ΔP_{wheel}	Pressure drop across the energy wheel (Pa)
$P_{supply} - P_{exhaust}$	Pressure difference between supply and exhaust sides of the energy wheel (Pa)
q	Heat transfer rate (W)
RH	Relative humidity (%)
rpm	Revolutions per minute (rev/min)
T	Temperature (°C)
TR	Transmittance
U	Total uncertainty
V	Face velocity (m/s)
W	Humidity ratio (g_w/kg_a)

Greek symbols

ε	Effectiveness (%)
ω	Rotational speed (rad/s)

Subscripts

a	Measured results for EATR and face velocity
ad	Adsorption
b	Calculated EATR and face velocity due to dilution
exhaust	Exhaust airstream
high	High
inert	Inert gas (sulfur hexafluoride in this report)
l	Latent
low	Low
matrix	Matrix in energy wheel
min	Minimum
non-inert	Non-inert gas
pc	Phase change
return	Return airstream
s	Sensible
supply	Supply airstream
1, 2, 3, 4	Measurement station numbers in ASHRAE Std 84 (2020) at the inlets and outlets of the test section.

Chemical symbols

CO_2	Carbon dioxide
MIBK	Methyl isobutyl ketone
SF_6	Sulfur hexafluoride

ACKNOWLEDGEMENTS

The RP 1780: “Test method to evaluate cross-contamination of gaseous contaminants within total energy recovery wheels” was sponsored by the American Society of Heating, Refrigerating and Air-Conditioning Engineers (ASHRAE) Technical Committee 9.10, Laboratory Systems.

The Project Monitoring Subcommittee (PMS) members were Robert Weidner (chair), Roland Charneux (member), Nick Agopian (member), Brendon Burley (member), and Hoy Bohanon (member). We gratefully acknowledge the support, guidance, and feedback we received from the PMS members.

We would like to thank the manufacturers who supplied energy wheel samples for this project. We could not reveal their names because of the confidentiality reasons.

Our sincere thanks to Daniel Vessey, instrument maker at the Engineering shops, University of Saskatchewan (USask) for his assistance during the assembly of energy wheels.

We acknowledge the support received by Hayden Reitenbach, former research engineer at the USask for setting up the energy wheel test rig. Siddhartha Gollamudi and Ashwin Joseph Mathews, graduate students at the USask, contributed to this work by assisting with experiments during the last phase of this project.

CHAPTER 1

INTRODUCTION

1.1 Background

The background and need for this research were well articulated in the ASHRAE RP-1780 description, and is repeated in this section to set the background for this research report. *"The basic function of laboratory HVAC systems is the management of contaminant concentrations in the space in order to reduce the risk to the researchers of ingesting or being in contact with these contaminants. Unlike commercial spaces, energy-intensive laboratories use high volumes of filtered outdoor air to dilute airborne contaminants. In order to do this, a large amount of outside air must be cooled, dehumidified, heated, and humidified, resulting in very high energy consumption. According to DOE (Department of Energy, 2008), the US has about 9000 laboratory buildings covering 650 million square feet of work area. According to EPA, US laboratories consumed about 150 million MWhr/yr in 2005. Of this, approximately 60% (or 90 million MWhr/yr) was associated with the HVAC systems.*

Historically, the glycol loop, which utilizes a coil to transfer thermal energy between the exhaust and supply air streams, has been considered the safest energy recovery system for laboratory HVAC systems. This technology eliminates the risk of contaminant transfer in the incoming air from the exhausted air stream. However, this technology is only about 40-45% efficient in winter and even lower in the summer, since it does not recover the latent heat of the exhausted air. It also provides no heating season humidification.

ASHRAE Standard 90.1 (ANSI/ASHRAE, 2019) now mandates the use of total energy recovery devices for most buildings. To determine compliance with ASHRAE Standard 62.1 (ANSI/ASHRAE, 2022) for most building types, 62.1 provides Classification of Air and acceptable Exhaust Air Transfer Ratios (which are certified by AHRI). However, for laboratory applications, 62.1 directs the user to environmental health and safety experts and these experts needs to establish the degree of contaminant transfer air exhibited by a given product in a specific ERV installation. This research will provide tools for use by these experts and is essential for all building types, not just laboratories, since transfer contaminated air cannot be considered outdoor

air. To determine the proper outdoor air correction factor (OACF) the approximate degree of contaminant transfer air must be known.

As ASHRAE 62.1 (ANSI/ASHRAE, 2022) now permits the use of total energy recovery wheels under certain conditions for laboratory hood exhaust. The ASHRAE community needs qualitative data and tests procedures on the potential cross contamination of these devices.

Over the past 20 years, some manufacturers have developed specialized desiccant transfer surfaces and advanced purge sections to limit the transfer of airborne particulate and gaseous contaminants contained within the exhaust air stream. Field data of cross-contamination levels has been reported at various technical conferences, including ASHRAE. However, a standard test procedure does not exist, so the validity of the results is always in question. Therefore, ASHRAE should address the concern of contaminant transfer within total energy devices by developing a standard testing procedure" (ASHRAE TRP-1780, 2019).

There are several types of energy exchangers available, notably rotary energy wheels, membrane exchangers, flat plate exchangers and heat pipes. Comparing these exchangers, the rotary energy wheels have many advantages such as high effectiveness (up to 85%), ability to transfer heat and moisture simultaneously, low maintenance and less susceptibility to frost formation. Energy wheels are made of metal matrix coated with solid desiccants. Molecular sieve and silica gel are the commonly used desiccants. As the wheel rotates, heat and moisture continuously transfer between the supply and exhaust, as shown in Figure 1.1.

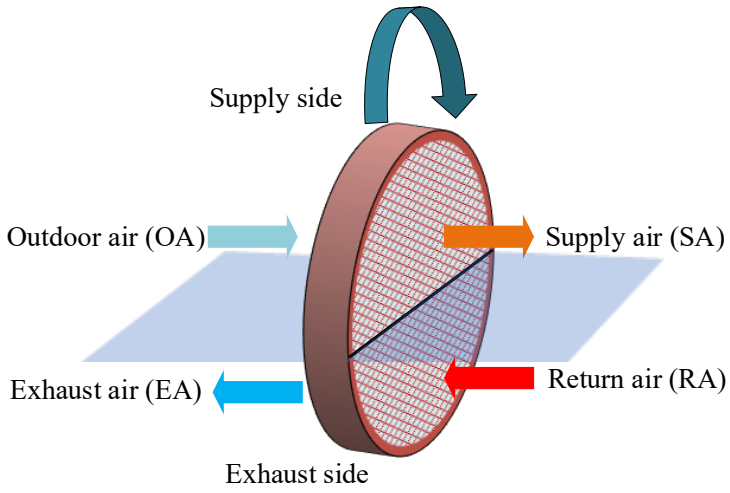

Figure 1.1. Schematic of an energy wheel showing the airflow and measurement stations.

The major concern with the operation of energy wheels is that they may also transfer indoor contaminants from process / building exhaust to the supply airstream. Studies have shown that the contaminant transfer in wheels depends on wheel material properties, physio-chemical characteristics of the contaminant and the operating conditions. A few contaminants reported in the literature having high transfer rates (above 30%) are: ammonia (Okano et al., 2001a, 2008), acetic acid (Bayer, 2011; Okano et al., 2001a), xylene (Bayer, 2011; Roulet et al., 2002), phenol (Roulet et al., 2002), formaldehyde (Fisk et al., 1985; Hult et al., 2014; Okano et al., 2008), and toluene (Nie et al., 2015; Wolfrum et al., 2008). The study conducted by Patel et al. (Patel et al., 2014) found that the temperature and relative humidity does not affect contaminant transfer rates.

ASHRAE standard 84 (ANSI/ASHRAE, 2020) provides test methods to quantify the contaminant transfer in energy wheels due to carryover and leakage. However, there are other mechanisms, such as adsorption, absorption, frosting, and condensation, that are also responsible for this transfer (Torabi, 2021). The phase change mechanism responsible for the contaminant transfer at room operating condition is adsorption and the magnitude of adsorption depends on the physio-chemical properties of the contaminant, the properties of the desiccant material, and the operating conditions. Each of these mechanisms is discussed in detail in the next section.

1.2 Contaminant transfer mechanisms in energy exchangers

Carryover, air leakage, and adsorption/desorption are the three major mechanisms responsible for contaminant transfer in energy exchangers. The contaminant transfer is also possible because of absorption/evaporation and condensation/evaporation. All three of these mechanisms are present in energy wheels. These mechanisms are discussed in detail in the following sections.

1.2.1 Carryover

The contaminant transfer due to carryover occurs when return air flows through the energy wheel and part of the air transfers to the supply airstream through the wheel rotation. Figure 1.2 presents a schematic of carryover in an energy wheel. As shown in the figure, some of the air from the exhaust side remains in the matrix of the wheel as it rotates to the supply side. This exhaust air mixes with fresh incoming outdoor air and is supplied to indoor space. The contaminants present in the return airstream will also get transferred through this mechanism.

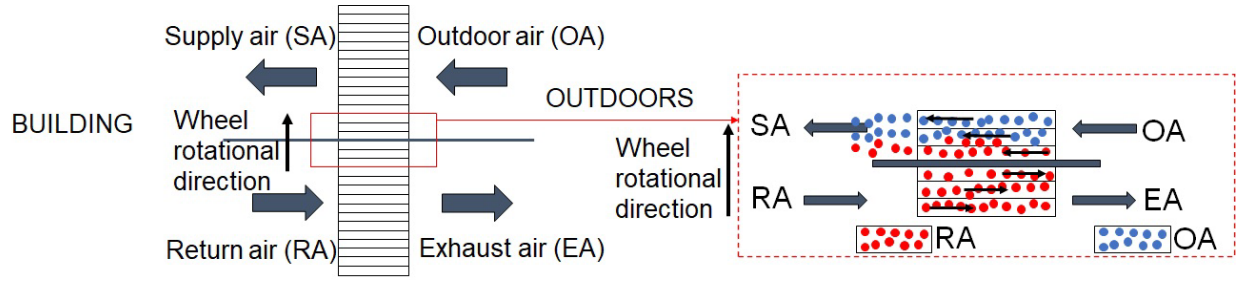

Figure 1.2. Schematic of carryover mechanism in energy wheels.

The carryover can be limited by using a purge section in the energy wheel, and with a good installation and proper maintenance of the energy wheel (Roulet et al., 2002; Shang & Besant, 2008). Figure 1.3 shows a schematic of a purge section in an energy wheel that prevents carryover from return airstream to supply airstream. The purge isolates a section of the wheel on the boundary between the supply and return airstreams and displaces the entrapped return air (from the exhaust side) along with some outdoor air to the exhaust side. Contaminant transfer due to carryover is independent of the gas since contaminants are simply carried in the air from one side to other.

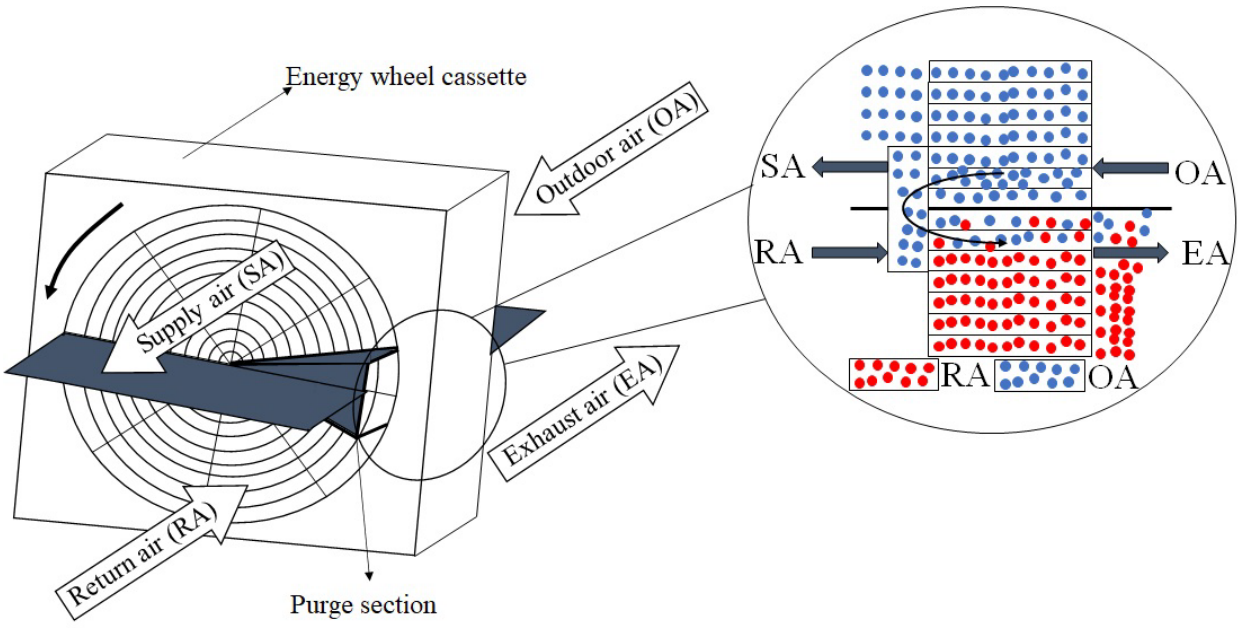

Figure 1.3. Schematic showing a purge section in an energy wheel that transfers outdoor air to exhaust air and prevents carryover from return air to supply air.

1.2.2 Air leakage

The contaminant transfer by air leakage occurs due to pressure differences between supply and return airstreams. In this case, air leaks through the interface (seals) of return and supply airstreams as shown in Figure 1.4. The leakage can occur either from supply to return airstream or vice versa, depending on the airstream pressure. The leakage to the supply side from the exhaust side can be minimized by maintaining high pressure on the supply side ($P_{supply} > P_{return}$). The locations of the fans in outdoor, supply, return, and exhaust airstreams play an important role in the direction of air leakage (Khoury et al., 1988). Figure 1.4 shows a schematic of the air leakage mechanism in an energy wheel, where the supply air has a higher pressure than return air.

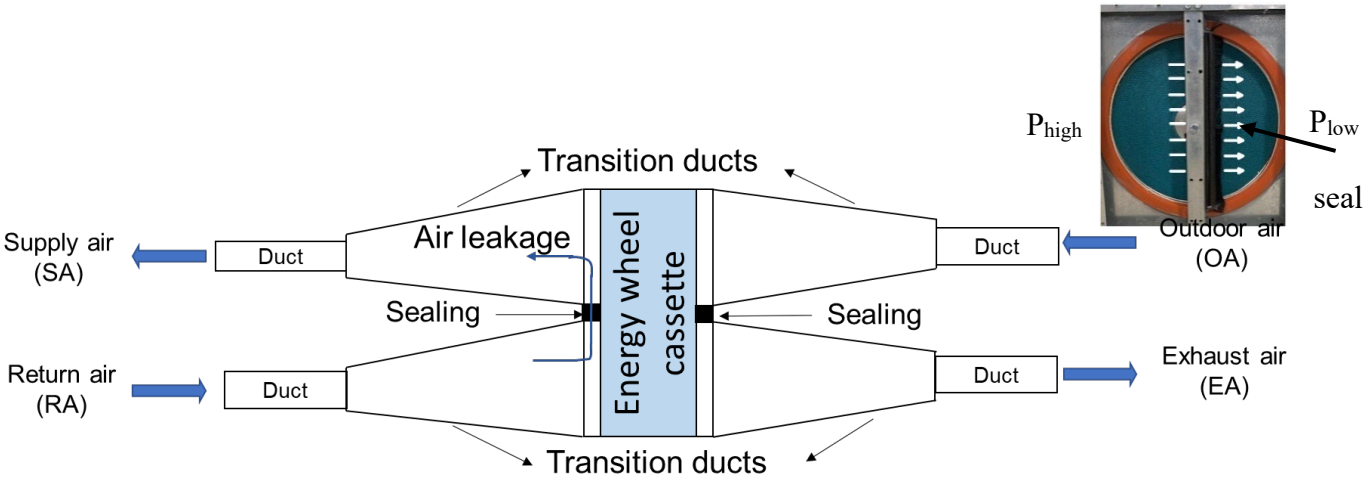

Figure 1.4. Schematic diagram showing air leakage from high pressure side of an energy wheel to the low pressure side of the wheel. Leakage occurs between the seal and the face of the rotating wheel.

1.2.3 Adsorption/desorption

Contaminant transfer due to adsorption/desorption occurs when the desiccant on the energy wheel has the capacity to adsorb the contaminant in one airstream and store the contaminant until it is desorbed in the other airstream (similar to transfer of water vapor). Figure 1.5 presents a schematic of adsorption/desorption mechanism in an aluminum sheet coated with desiccants.

The sorption capacity will vary for different contaminants and desiccants. Contaminant transfer between the airstream and the desiccant occurs because of the difference in the vapor pressure of the contaminant between the airstream and the desiccant (Okano et al., 2001b). Adsorption occurs when the vapor pressure is higher in the air than on the desiccant surface and desorption occurs when the vapor pressure is higher on the desiccant surface than in the air. Contaminant transfer in

energy wheels through the adsorption/desorption mechanism is expected to depend on many parameters such as the air conditions (temperature and humidity), the properties of the contaminants, desiccants (Kodama, 2010), and design of the wheels (i.e., face velocity, NTU, Cr*, and effectiveness).

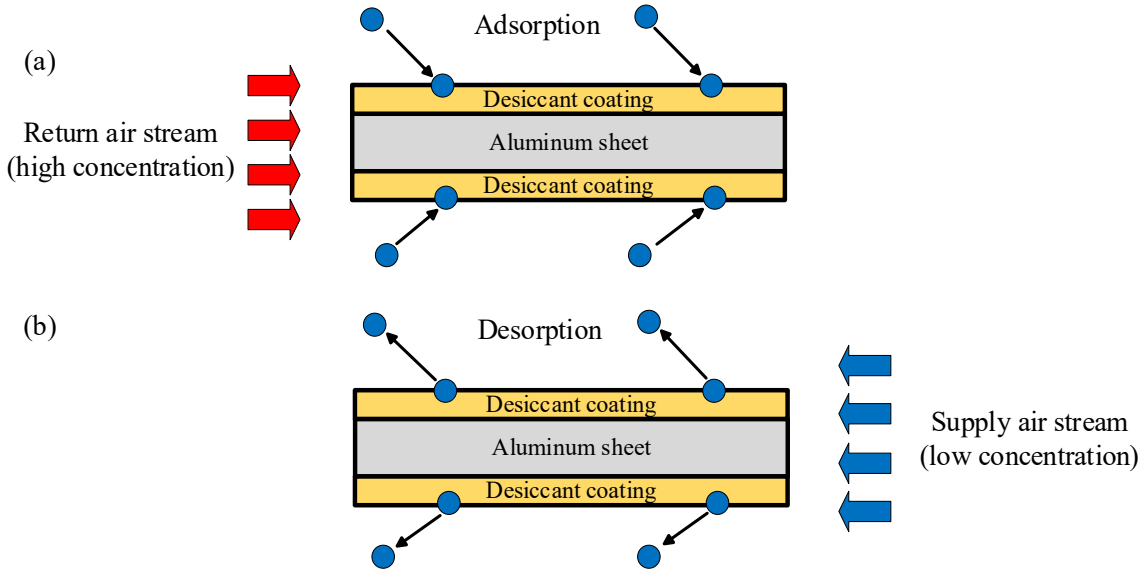

Figure 1.5. Schematic of adsorption/desorption mechanism, that would transfer contaminants from the exhaust air stream to the supply air stream by (a) adsorption of the gas in the desiccant coating from return airstream and (b) desorption from the desiccant to the supply airstream.

1.2.4 Absorption/evaporation

In addition to the mechanisms mentioned above, some gaseous contaminants in the return airstream get absorbed in the wheel and evaporate on the supply side. For example, when water vapor in the return airstream condenses to liquid water (or frost) within energy wheel channels, water soluble gaseous contaminants such as formaldehyde and methanol get absorbed in the liquid (or frozen) water. Gaseous contaminant absorption occurs because of attractive forces between gaseous contaminants and liquid (frozen) water. When the liquid water evaporates into the supply airstream, the absorbed contaminants may evaporate and transfer to the supply air.

1.2.5 Condensation/evaporation

The condensation of gaseous contaminants would occur if the concentration of the contaminant reached the saturation level. It may be possible for a contaminant to condense on the exhaust side of the wheel and evaporate on the supply side of the wheel.

CHAPTER 2

LITERATURE REVIEW

This chapter presents a summary of a literature review on the experimental studies in the area of gaseous contaminant transfer and their major findings. Laboratories hood exhaust may contain a variety of contaminants and volatile organic compounds (VOCs) depending on the nature of the work. The physio chemical properties and the possible sources of contaminants are prepared and tabulated in Table 2.1. It Several papers have reported the contaminant transfer rate of various contaminants, and most of them were focused on rotary-type energy exchangers. Gaseous contaminant transfer due to air leakage and carryover mechanisms has been studied and measured extensively in the literature using inert gases. The literature review showed that gaseous contaminant transfer rates vary between 0% to 75% with uncertainties between 1% to 30%. The available test data from the literature are summarized in Table 2.2.

Table 2.1. Physio chemical properties, threshold limit values (TLV) and the sources of gaseous contaminants.

Contaminant	Boiling point	Polarity	Solubility	TLV (ppm)	Sources
Acetaldehyde	20.2 °C	N/A	miscible	200	Incomplete combustion in fireplaces, wood-burning stoves, and environmental tobacco smoke, along with certain cooking processes (notably those which use cooking oil) (Government of Canada, 2017)
Acetic acid	118 °C	N/A	miscible	10	Burning of plastics or rubber, and exhaust fumes from vehicles, food and food products, fruit preservatives, papers (Public Health England, 2019).
Ammonia	-33.3 °C	N/A	miscible	50	Smoking, cooking, cleaning, concrete, and human emissions (M. Li et al., 2020).
Carbon dioxide	-78.4 °C	Nonpolar	16.1%	5000	Respiration and decomposition of living organisms, carbonate rocks, forest fires, volcanoes. Human activities, such as the burning of fossil fuels, production of cement (Brown et al., 1994a; NASA, 2016).

Hexane	69 °C	0.1	0.014%	500	Oil refineries, chemical plants, footwear manufacturing, petrol, paints, adhesives, rubber, cement, type-over correction fluids, non-mercury (low temperature) thermometers, alcohol preparations, aerosols in perfumes, paint thinners, general-purpose solvents, degreasing agents, and cleaners (Australian Government, 2022).
Isopropyl alcohol	82.5 °C	3.9	miscible	400	Cosmetics, skin and hair products, perfumes, pharmaceuticals, lacquers, dyes, cleaners, antifreezes, and other chemicals (New Jersey Department of Health, 2016)
Methanol	64.7 °C	5.1	miscible	200	Windshield washer fluid, gas line antifreeze, carburetor cleaner, copy machine fluid, perfumes, food warming fuel, and other types of fuels (Centers for Disease Control and Prevention, 2011).
Methyl isobutyl ketone	117 °C	4.2	1.7%	50	Solvent for gums, resins, paints, varnishes, lacquers(Williams, 2013).
Phenol	181.7 °C	N/A	8.3%	5	Natural decomposition of organic materials. A major part of phenol present in the environment, however, is of anthropogenic origin. Production and use of phenol and its products, especially phenolic resins and caprolactam, exhaust gases, residential wood burning, and cigarette smoke are potential sources (Brown et al., 1994a; Wolkoff, 1995b).
Sulfur hexafluoride (SF6)	-63.9 °C	Nonpolar	0.003%	1000	Non-reactive tracer gas
Xylene	138.4 °C	2.5	0.018%	100	Industrial sources, automobile exhaust, solvent, paints (Niaz et al., 2015)

The literature presented in this chapter discusses contaminant transfer mainly focused on three types of desiccant coated wheels: (a) silica gel, (b) molecular sieves, and (c) ion-exchange resins. It is known that both the silica gel and molecular sieves are porous adsorbents. They adsorb moisture onto their pores due to the humidity gradient between the airstream and the desiccant. Hence, considering the same principle, contaminants could also be adsorbed/desorbed because of the concentration gradient between the airstream and the desiccant. The ion-exchange resins are non-porous selective materials and the driving potential for moisture exchange is their swelling

behavior and volume change (Kodama, 2010), and its selectivity could be one of the reasons for the low transfer rate of contaminants.

The highest transfer rates were measured for phenol, toluene, nitrous oxide, ammonia, acetic acid, and formaldehyde (Table 2.2). A common chemical characteristic among these contaminants, except for nitrous oxide (a tracer, and a non-reacting gas) is their high-water solubility, which may be a possible reason for high contaminant transfer rates. The high value of EATR for nitrous oxide could be due to higher pressure on the exhaust side than the supply side of the energy wheel. The uncertainties in measured EATR varied between 1% and 30%, but most studies did not include a detailed uncertainty analysis. Furthermore, most studies did not determine if the experiments conserved mass of gaseous contaminants. It also identified that the exchanger design parameters (effectiveness and face velocity) have more significant effect on EATR than the operating conditions (relative humidity and temperature) for the case of energy wheels.

Table 2.2. Summary of the gaseous contaminant transfer rates and uncertainties measured on various energy exchangers.

Gaseous contaminants	Energy exchanger	Transfer rate	Uncertainty	Reference
1. Acetaldehyde	Energy wheel	17%	NR	(Bayer, 2011)
2. Ammonia	Energy wheel	10-46%	NR	(Okano et al., 2001b), (Kodama, 2010).
	Flat plate enthalpy exchanger	8-9%		(Nie et al., 2015)
3. Acetic acid	Energy wheel	7-36%	NR	(Okano et al., 2001b), (Bayer, 2011).
4. Methanol	Energy wheel	0-11%	NR	(Okano et al., 2001b), (Bayer, 2011).
5. Isopropyl alcohol	Energy wheel	0-4%	NR	(Okano et al., 2001b), (Bayer, 2011).
6. Methyl isobutyl ketone	Energy wheel	0-3%	NR	(Okano et al., 2001b), (Bayer, 2011).
7. Xylene	Energy wheel	0-30%	NR	(Okano et al., 2001b), (Bayer, 2011), (Roulet et al., 2002).
8. Carbon dioxide	Energy wheel	0.6-5%	NR	(Kodama, 2010), (Bayer, 2011), (Kassai, 2018).

	Flat plate type mass exchanger	1%		(Sparrow et al., 2001).
9. Propane or hexane	Energy wheel	0.2-7%	5%	(Kodama, 2010), (Bayer, 2011), (Fisk et al., 1985).
	Flat plate enthalpy exchanger	6-8%		(Fisk et al., 1985).
	Desiccant wheel	20%		(Wolfrum et al., 2008).
10. Phenol	Energy wheel	30-75%	NR	(Roulet et al., 2002).
11. Sulfur hexafluoride	Energy wheel	5-26%	1%	(Bayer, 2011), (Khoury et al., 1988), (Fisk et al., 1985), (Roulet et al., 2002).
	Flat plate enthalpy exchanger	5-8%		(Fisk et al., 1985)
12. Formaldehyde	Energy wheel	6-35%	3-29%	(Okano et al., 2001b), (Kodama, 2010), (Andersson et al., 1993), (Bayer, 2011), (Hult et al., 2014), (Fisk et al., 1985).
	Flat plate enthalpy exchanger	7-12%		(Fisk et al., 1985).
	RAMEE	5-6%		(Patel et al., 2014).
13. Nitrous oxide	Energy wheel	1-54%	3%	(Shang et al., 2001).
14. Acetone	Energy wheel	0	NR	(Okano et al., 2001b).
	Flat plate enthalpy exchanger	5-6		(Nie et al., 2015).
15. Toluene	RAMEE	2-3%	3-5%	(Patel et al., 2014).
	Desiccant wheel	70%		(Wolfrum et al., 2008).
	Flat plate enthalpy exchanger	7-8%		(Nie et al., 2015).
	Energy wheel	0-30%		(Okano et al., 2001b).
16. Inert tracer gas (For measuring air leakage and carryover)	Air-to-air heat/energy exchanger	----	3%	(ANSI/ASHRAE, 2020), CSA Standard C 439-18 (2018) (Canadian Standards Association, 2018).

RAMEE = Run-around membrane energy exchanger, NR = uncertainty not reported

An established test methodology for measuring contaminant transfer due to air leakage and carryover exists and is included in test standards ASHRAE 84-2020 (ANSI/ASHRAE, 2020) and CSA C439 (Canadian Standards Association, 2018). Contaminant transfer due to air leakage and carryover is quantified using exhaust air transfer ratio (EATR). Several researchers have measured contaminant transfer of non-inert gases in energy exchangers. While such measurements inherently include all transfer mechanisms (air leakage, carryover, and adsorption/desorption), no test methods exist in the literature to quantify the transfer due to phase change mechanisms. Detailed literature review findings and data are published as a manuscript and the same is attached as appendix B of this report.

CHAPTER 3

TEST FACILITY AND METHODOLOGY

This chapter discusses the development of a contaminant transfer test facility, test method and uncertainty analysis in detail. The proposed experimental method follows the guidelines provided in ASHRAE Standard 84 (ANSI/ASHRAE, 2020), and three additional criteria are introduced to quantify the gaseous contaminant transfer rate.

3.1 Energy wheel test facility

An experimental setup consisting of an energy wheel test rig, contaminant injection and sampling arrangements has been developed at the University of Saskatchewan. In contaminant transfer experiments, a known concentration of contaminant will be injected into the return airstream/Station 3 and the concentration will be measured from all the stations. The gaseous contaminant transfer will then be quantified using the measured concentration data. The facility consists of a test section connected to four air supply lines, arrangements for injecting contaminants into the test section, gas sampling ports and valves to take air samples for contaminant concentration measurements, as shown in Figure 3.2. Each of these sections is discussed in detail in the following sections.

3.1.1 Test section

The test section consists of an energy wheel fixed inside a cassette. Molecular sieve (MS) and silica gel (SG) coated energy wheels are used in the contaminant transfer experiments. These energy wheels have a 10-inch outer diameter and are 4 inch thick, as shown in Figure 3.1(a). The wheel is rotated by a motor-belt assembly, which is mounted on the cassette and is governed by a resistance speed controller. The cassette is connected to inlet and outlet diffusers as shown in Figure 3.1(b). The rotational speed of the wheel can be adjusted from 1-18 rpm. A rubber brush attached to the cassette, as shown in the Figure 3.1(a) is used to seal the airstreams, which minimizes leakage due to the difference in line pressures.

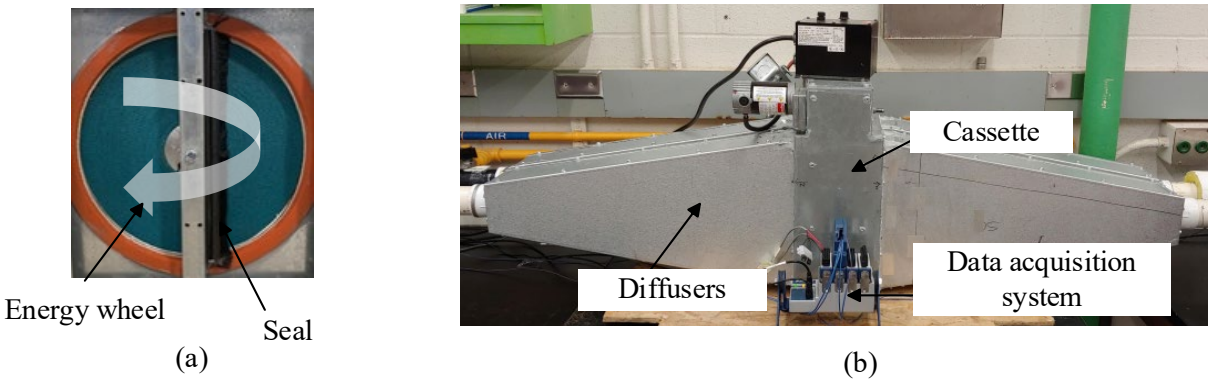

Figure 3.1. Photograph of (a) an energy wheel and (b) test section with inlet diffusers.

3.1.2 Air supply lines:

Two centrifugal fans are used in each air supply line to maintain the required flow rates and line pressures. These air supply lines are made of 2 inch" PVC pipes. The required flow rates and line pressures are achieved by controlling the rotational speed of the blower using a variable transformer. Orifice plates with differential pressure transducers are used to measure the flow rates. Honeycomb-type flow straighteners are installed upstream of the orifice plate to measure the flow rate accurately. The flow meters and straighteners are designed according to ISO standard 5167 (ISO, 2003a, 2003b). One of the air supply lines is connected to an environmental chamber where the temperature can be set from -40 to +20°C. PID-controlled tubular heaters are placed on the air supply lines to heat the air to required inlet conditions. The air supply lines can provide flow rates from 25-75 CFM, with corresponding face velocities ranging from 0.5-1.5 m/s. T-type thermocouples and capacitive humidity sensors are used to measure the temperature and humidity of airstreams at the inlets and outlets. The differential pressure transducers, thermocouples and humidity sensors were calibrated using a Druck pressure calibrator (Druck, n.d.), Drywell temperature calibrator (Hart Scientific, 2002) and Thunder scientific humidity generator (Thunder Scientific® Corporation, n.d.), and the obtained uncertainties are ±2%, ±0.2°C and ±2%, respectively.

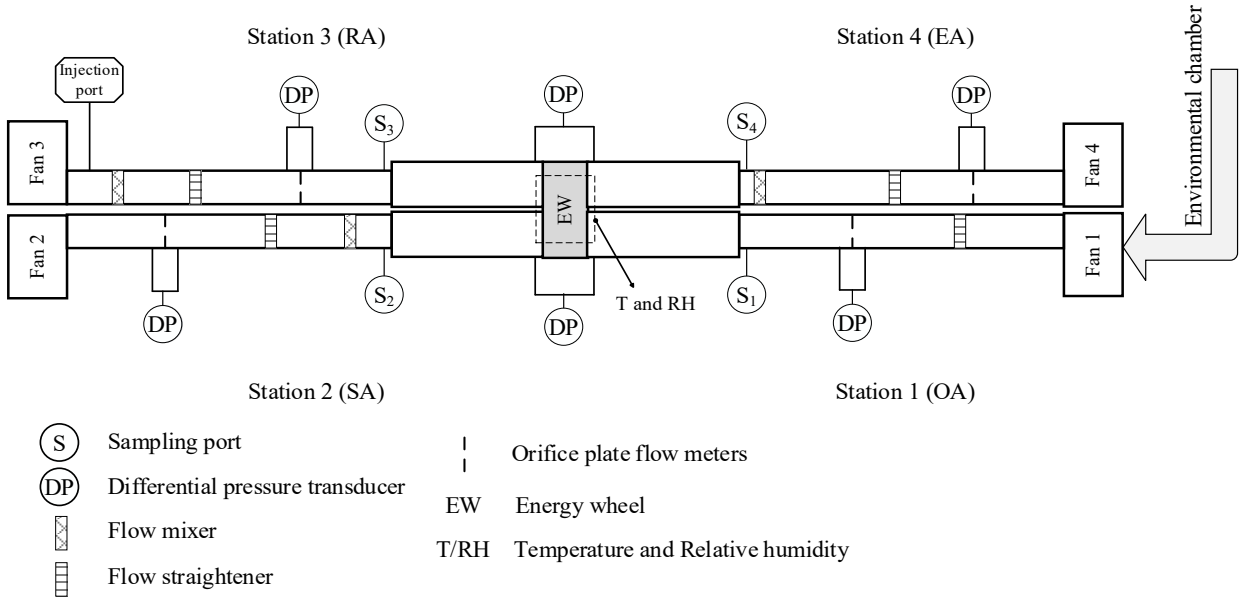

Figure 3.2. Schematic of contaminant transfer test facility

These air supply lines are connected to diverging (at the inlets) and converging ducts (at the outlets) having a cross-section of 10" x 2" to maintain a uniform flow at the test section. The thermocouples are arranged circumferentially at the inlet of the wheel to measure the temperature of the airstreams. The humidity sensors are placed along with the thermocouples to measure the air humidity. For air sampling, ¼" sampling ports are provided in each line, and the flow mixer is placed upstream of the sampling ports.

3.1.3 Contaminant injection methods

The gaseous contaminants are injected into the return airstream to evaluate their transfer to the supply air stream. The contaminant is injected at the turbulent region of the inlet (indicated as the injection port in Figure 3.2) to achieve a uniform mixing at the energy wheel inlet. Two techniques - compressed gas injection and liquid evaporation, are used to inject the contaminants, depending on their physical state at room conditions.

3.1.3.1 Compressed gas injection technique

In this method, a commercially available pressurized cylinder containing the gaseous contaminant is used as an external source to inject the contaminant. The flow rate of the contaminant is controlled using a rotameter to achieve the desired concentration in the return air stream. This technique is used for contaminants in gaseous state at room temperature (such as CO_2 and SF_6). The advantage of the gas injection technique is that it is simple to implement and control and can

achieve a steady concentration of contaminants in the RA. In this work, the transfer of SF_6 and CO_2 has been evaluated using the compressed gas injection technique. Figure 3.3 shows the schematic of gas injection method.

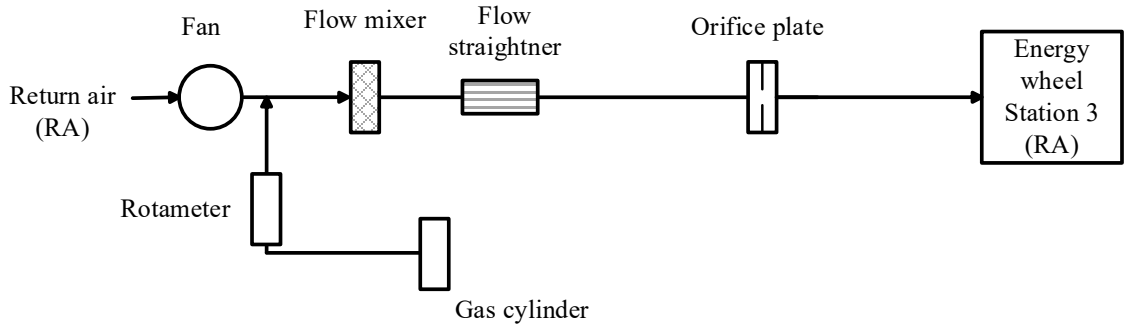

Figure 3.3. Schematic of compressed gas injection technique.

3.1.3.2 Liquid evaporation technique

In this technique, the liquid contaminant is injected into a compressed airstream with the help of a syringe pump (New Era Syringe pump 100). The airstream must be heated to a temperature near to the boiling point of the contaminant. The location of the syringe is adjusted so that the contaminant will be directed to the center of the high-velocity airstream. A tubular heater and a rotameter are used to heat and control the compressed airstream, respectively. The air containing the evaporated contaminant will be mixed with the return airstream and flows to the energy wheel inlet. Figure 3.4(a) and (b) show the schematic and photographs of the liquid evaporation technique.

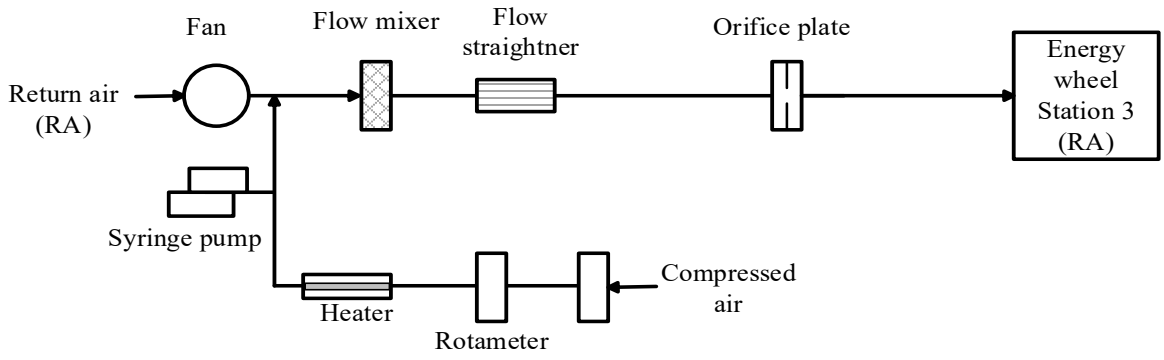

Figure 3.4 (a). Schematic of liquid evaporation technique.

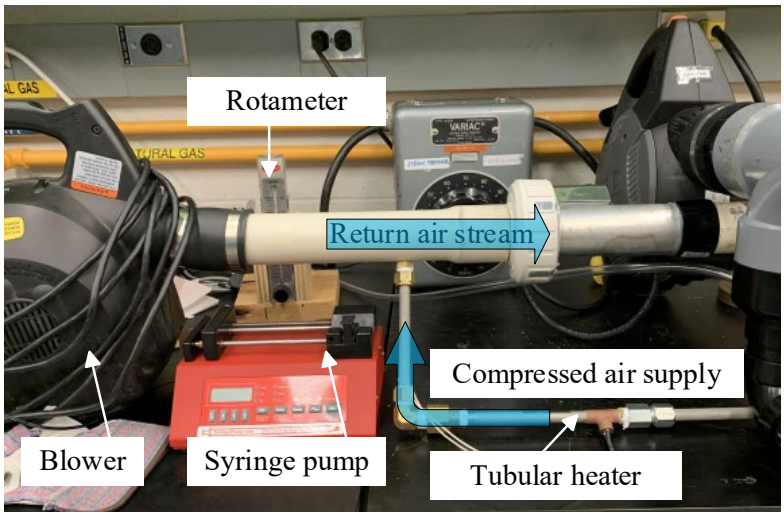

Figure 3.4 (b). Photograph of liquid evaporation technique.

3.1.4 Contaminant sampling

Figure 3.5 shows the gas sampling configuration to draw the air from different sampling locations to the gas analyzer to measure the concentration of tracer gas/contaminants. With the help of a vacuum pump (model: 1LAA-10M-1000X, GAST, USA), gas samples were collected from all the air supply lines via Teflon sampling tubes connected to sampling ports. The sampling lines and ports were designed according to the guidelines provided in ASHRAE Standard 84 (ANSI/ASHRAE, 2020). Since the gas analyzer can only measure the concentration of a single airstream at a time, computer-controlled solenoid valves were used to select the airstream to be sampled. Air streams were sampled in the order OA, SA, EA and RA to minimize the effect of sampling on the air flow rate, which may affect the energy/contaminant transfer in the wheel.

The Teflon tubes from each sampling port are connected to the main sampling tube after the solenoid valves. During the sampling process, the respective solenoid valve will be activated, and the airstream will be drawn to the gas analyzer with the help of the vacuum pump. A rotameter is used to control the flow rate to the sample cell and is set to 0.2 L/s (approximately 2% of the airflow rate in supply lines). After completing the measurements with one contaminant, the sample cell is flushed with nitrogen to remove any residual gas. The volume of the sample cell is 30 L and previously, it was found that flushing the cell three times would completely remove the traces of contaminants from the cell (Patel et al., 2014). The gas samples from the gas analyzer were exhausted to a fume hood through a separate exhaust duct. During the gas sampling process, the

instantaneous concentration values were monitored using Calcmet (associated software of the gas analyzer), and the average of these measurements was used for contaminant transfer calculation. More details about concentration measurement and instantaneous measurements are presented in section 4.3.1.

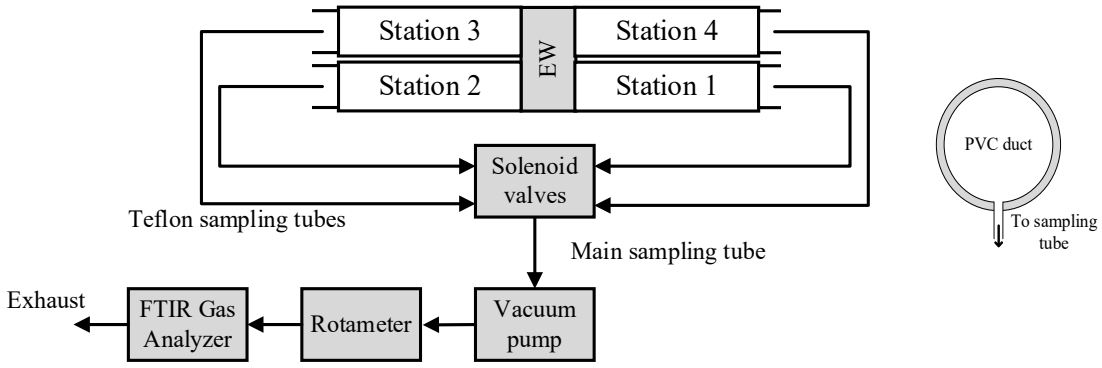

Figure 3.5. Contaminant sampling arrangement

3.1.5 Gas concentration measurement:

A Gasmet CR-100M FTIR gas analyzer (Gasmet Technologies Oy, 2006) has been used to measure the concentration of gaseous contaminants present in the airstream. The analyzer works on the principle of infrared (IR) spectroscopy, in which a beam of IR light passes through the sample gas and the gas molecules absorb specific frequencies corresponding to the frequencies of their molecular vibration. The quantitative analysis of the absorption spectrum is based on the principle of Beer-Lambert law (Eq. (3.1)).

$$\log(I_0/I) = \log(1/T) = A = abc \qquad (3.1)$$

Where, I_0 = intensity of infrared radiation entering the gas sample, I = intensity of infrared radiation After passing through the sample, T = transmittance, A = absorbance, a = absorptivity (m^2 /mol), b = optical path length (m), and c = sample concentration (ppm). If the optical path length is constant, Beer's law states that the absorbance is directly proportional to the concentration of the sample gas at a given wavelength. In the software associated with FTIR, Calcmet compares the sample with the reference gas spectra and provides the concentration measurement. An example sample spectrum of ambient air and SF_6 measured by the gas analyzer is shown in Figure 3.6, and the peaks corresponding to water vapor, CO_2 and SF_6 are indicated. The uncertainty in the gas analyzer is ±2% of the reference gas spectra of the respective chemical. The uncertainty in

concentration measurement can be minimized by adding reference spectra for a wide range of concentration values (Patel et al., 2014).

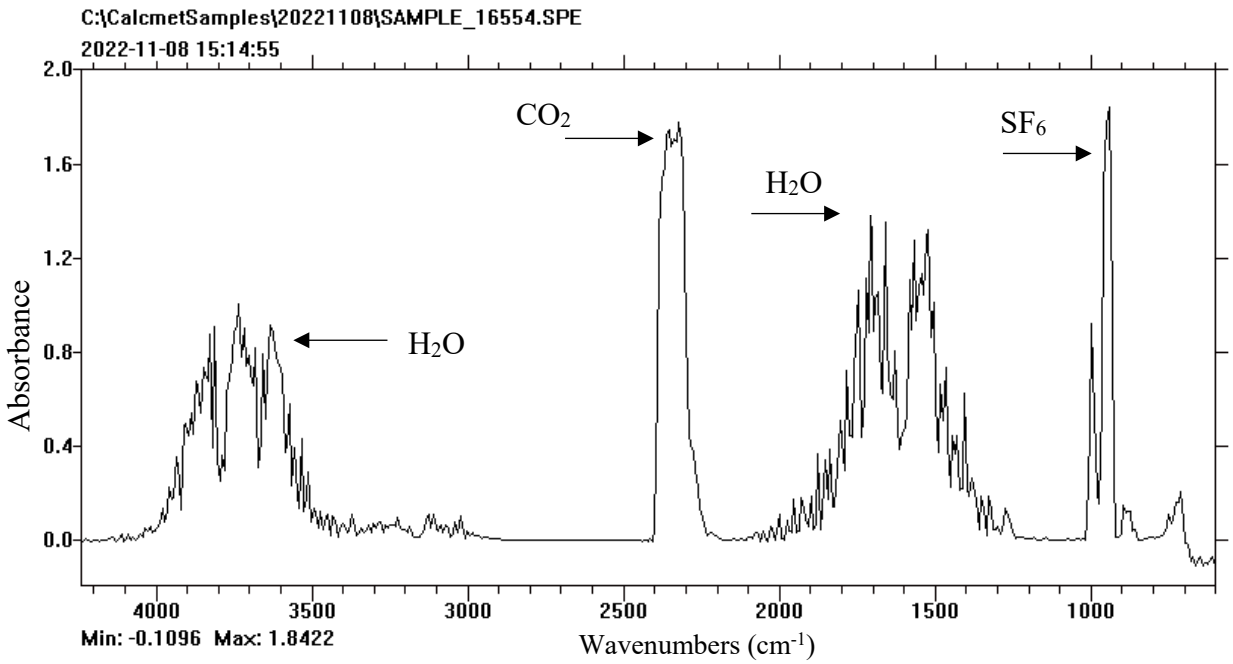

Figure 3.6. Sample FTIR spectrum for concentration measurement

3.2 Test method to evaluate gaseous contaminant transfer

3.2.1 Performance testing of energy wheels – ASHRAE Standard 84

The performance of energy wheels has been evaluated following the guidelines provided in ASHRAE standard 84 (ANSI/ASHRAE, 2020). The standard provides recommendations for instrumentation, test facility configuration, and reporting test parameters and data. The heat and moisture transfer performance of energy wheels are often quantified using sensible, latent, and total effectiveness as presented in Eq. (3.2). They are defined as the ratio of the transfer rate of heat/moisture/enthalpy to the maximum possible transfer rate of heat/moisture/enthalpy between the airstreams.

$$\varepsilon_{s,l,t} = \frac{C_2\,(X_1 - X_2)}{C_{\,minimum\,(2,3)}\,(X_1 - X_3)} \tag{3.2}$$

Where 1, 2 and 3 indicate Station 1, 2 and 3 and X represents temperature, humidity or enthalpy for sensible, latent, or total effectiveness, and C indicates the capacity rate of supply or exhaust air streams, respectively.

To evaluate the conservation of dry air mass flow rate, the experiment should satisfy the following inequality (Eq. (3.3)):

For mass flow rates:

$$\frac{|\dot{m}_1 - \dot{m}_2 + \dot{m}_3 - \dot{m}_4|}{m_{minimum\ (1,3)}} < 0.05 \tag{3.3}$$

The experiments should satisfy the heat, water vapor and enthalpy inequality given in Eq. (3.4).

For energy transfer:

$$\frac{\left|\dot{m}_1 c_{P,1} T_1 - \dot{m}_2 c_{P,2} T_2 + \dot{m}_3 c_{P,3} T_3 - \dot{m}_4 c_{P,4} T_4\right|}{C_{minimum\ (1,3)}\ |T_1 - T_3|} < 0.20 \tag{3.4a}$$

$$\frac{|\dot{m}_1 W_1 - \dot{m}_2 W_2 + \dot{m}_3 W_3 - \dot{m}_4 W_4|}{\dot{m}_{\ minimum\ (2,3)}\ |W_1 - W_3|} < 0.20 \tag{3.4b}$$

$$\frac{|\dot{m}_1 h_1 - \dot{m}_2 h_2 + \dot{m}_3 h_3 - \dot{m}_4 h_4|}{\dot{m}_{\ minimum\ (2,3)}\ |h_1 - h_3|} < 0.20 \tag{3.4c}$$

Where T, W and h are temperature, humidity ratio, and enthalpy at outdoor, supply, return and exhaust airstreams.

Exhaust air transfer ratio (EATR) is used to express the percentage of an inert tracer gas transferred from the return air stream to the supply airstream. It is defined as the ratio of the tracer gas concentration difference between the supply and the outdoor air streams, to the tracer gas concentration difference between the return and the outdoor air streams (ANSI/ASHRAE, 2020), and can be calculated using Eq. (3.5).

$$EATR = \frac{C_2 - C_1}{C_3 - C_1} \tag{3.5}$$

where C_1, C_2, and C_3 are the tracer gas concentration measured at stations 1, 2 and 3, respectively. It should be noted that EATR is a measure of bulk leakage of air within the energy exchanger and is not directly applicable to the measurement of other gaseous contaminants in the device as described in ASHRAE standard 84 (ANSI/ASHRAE, 2020). Experiments must satisfy the tracer gas inequality shown in Eq. (3.6).

Tracer gas inequality:

$$\frac{|\dot{m}_1 C_1 - \dot{m}_2 C_2 + \dot{m}_3 C_3 - \dot{m}_4 C_4|}{m_{minimum\ (1,3)}\ |C_1 - C_3|} < 0.15 \tag{3.6}$$

Where C_1, C_2, C_3, and C_4 are the concentration of tracer gas at outdoor, supply, return and exhaust airstreams.

Tracer gas measurement procedure: An inert tracer gas is injected into the turbulent region of the return air stream to measure the EATR. Then the air samples are drawn from each station, and the tracer gas concentration will be measured using calibrated gas analyzers. The air sampling lines must be short enough to avoid dilution and sample line transients. The maximum allowed uncertainty in ASHRAE standard 84 (ANSI/ASHRAE, 2020) for EATR is less than 3%. The requirements of sampling equipment and recommendations on the sampling grid are also provided in the test standards (ANSI/ASHRAE, 2020; Canadian Standards Association, 2018).

3.2.2 Test method for gaseous contaminant transfer

The ASHRAE Standard 84 (ANSI/ASHRAE, 2020) requires an inert tracer gas such as SF_6 and the same inlet conditions (temperature and relative humidity) for contaminant transfer experiments. These experiments measure contaminant transfer in terms of EATR by bulk airflow only. They do not include the transfer due to phase change mechanisms such as adsorption/desorption and transfer during extreme conditions such as condensation and frosting. Therefore, a methodology needs to be developed to consider these effects. The contaminant transfer in rotary energy wheels may depend on many factors, such as the nature of the contaminant, type of desiccant material, exchanger design considerations, and operating conditions. Hence, a new parameter, Exhaust Contaminant Transfer Ratio (ECTR) is proposed to quantify the transfer of gaseous contaminants in rotary wheels. The $ECTR_{pc}$ is the contribution of the phase change mechanisms in gaseous contaminant transfer in energy exchangers, and the ECTR is the total contaminant transfer. The $ECTR_{pc}$ is determined by subtracting the EATR measured with an inert tracer gas (SF_6 – according to ASHRAE standard 84 (ANSI/ASHRAE, 2020)) from the ECTR measured with a different non-inert gas (e.g., VOCs) as given in Eq. (3.7).

$$ECTR_{pc} = ECTR\ - EATR \tag{3.7}$$

In addition to ASHRAE Standard 84 (ANSI/ASHRAE, 2020) recommendations, the following parameters are introduced to assure the quality of test data in these experiments.

Steady-state criterion: Steady-state criterion or inlet inequality represents a steady-state injection of contaminants. It is recommended to maintain the concentration fluctuations (at the wheel inlet) less than 5% of the concentration difference between the outdoor and return airstreams, as shown in Eq. (3.8). A low value of inlet inequality indicates that the injection process is steady and does not vary with time.

$$\frac{\delta C}{C_1 - C_3} < 0.05 \tag{3.8}$$

Contaminant mass inequality: During contaminant transfer testing, the concentration measured from all the stations shall satisfy the following inequality equation:

$$\frac{|\dot{m}_1 C_1 - \dot{m}_2 C_2 + \dot{m}_3 C_3 - \dot{m}_4 C_4|}{m_{minimum\ (1,3)}\ |C_1 - C_3|} < 0.2 \tag{3.9}$$

Uncertainty in ECTR and ECTR$_{pc}$: It is recommended to report the ECTR and ECTR$_{pc}$ within ±3% and ±5% uncertainty limits, respectively.

$$U_{ECTR} < 3\% \tag{3.10}$$

$$U_{ECTR_{pc}} < 5\% \tag{3.11}$$

3.3 Uncertainty analysis

The uncertainty in EATR /ECTR can be determined by propagating the uncertainties in concentration measurements in Eq. (3.5) and can be written as Eq. (3.12) (ASME/ANSI, 1998).

$$U_{EATR\,/ECTR} = \sqrt{(U_{C_2}\frac{1}{(C_3 - C_1)})^2 + (U_{C_1}\frac{C_2 - C_3}{(C_3 - C_1)^2})^2 + (U_{C_3}\frac{C_1 - C_2}{(C_3 - C_1)^2})^2} \tag{3.12}$$

where U_{C_1}, U_{C_2} and U_{C_3} are uncertainty in tracer gas/contaminant concentration measurement in stations 1, 2 and 3, respectively. It should also be noted that the uncertainty in tracer gas/contaminant depends on the calibration curve available on gas analyzers. In the Gasmet CR-

100M FTIR gas analyzer, the uncertainty in concentration measurement is 2% of the full-scale concentration corresponding to the calibration curve.

The uncertainty in $ECTR_{pc}$ can be determined using Eq (3.13).

$$U_{ECTR_{pc}} = \sqrt{\left(U_{ECTR}\right)^2 + \left(U_{EATR}\right)^2} \tag{3.13}$$

CHAPTER 4

EVALUATION AND VALIDATION OF THE TEST METHOD

In this chapter, the evaluation of contaminant transfer test method for eleven gaseous contaminants in 3Å molecular sieve (MS) and silica gel (SG) coated wheels is presented. The criteria proposed in Chapter 3 to ensure quality data are also validated for all the experiments.

4.1 Energy wheel performance test data

Prior to the contaminant transfer experiments, the performance tests were conducted according to ASHRAE Standard 84 (ANSI/ASHRAE, 2020) and the results have been verified with the manufacturer's data. The sensible, latent, and total effectiveness of the energy wheel are determined using the temperature, humidity, and flow rate measurements. Experiments were performed at AHRI (Air-Conditioning Heating and Refrigeration Institute, 2013) winter test conditions and the effectiveness of the wheels were determined by after 90 minutes of continuous operation of the wheel. Within 60 minutes of operation, the inlet and outlet airstreams, as well as the wheel, had reached a steady state. For MS and SG wheels, the calculated sensible and latent effectiveness are 86 ± 5% and 78 ± 7%, at the nominal face velocity of 1 m/s [196 fpm]. The uncertainties in effectiveness values are acceptable as the maximum allowed uncertainties in ASHRAE Standard 84 (2020) [15] are ± 5% for sensible, and ± 7% for latent effectiveness.

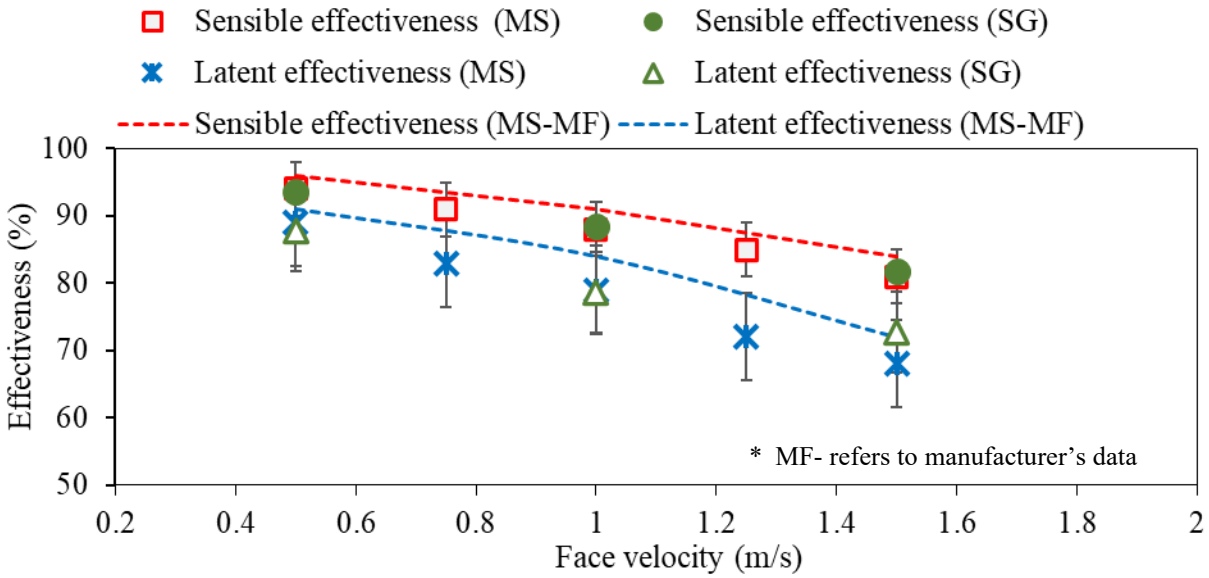

Figure 4.1. Sensible and latent effectiveness of molecular sieve (MS) and silica gel (SG) coated energy wheels for face velocities ranging from 0.5 to 4.5 m/s.

Figure 4.1 compares the effectiveness obtained from the experiments with MS and SG wheels. The manufacturer's data are available only for MS wheel and that are based on a simulation software, not actual experimental data, and no uncertainty limits are reported. However, the uncertainties can be assumed to be in the same order as experimental data from ASHRAE Standard 84 (2020) [15]. Further, the SG wheel is assembled at the University of Saskatchewan by obtaining matrix, hub, and other wheel parts from different manufacturers. As a result, there is no manufacturer data available for the SG wheel. For the MS wheel, the experimental and manufacturer's sensible and latent effectiveness data agree within ±5%, which under the experimental uncertainty limits. Slight leakages in the test facility and interaction of the wheels/airstreams with the surroundings could result in effectiveness variations. Considering these possibilities, it is confirmed that the test facility provides reliable results. The residence time of air in an energy wheel can be defined as the time it takes for air to flow through the exchangers. The residence time is calculated by dividing the thickness of the wheel by the speed of the air flow. With increasing velocity, the flow residence time decreases, resulting in a decrease in effectiveness, which agrees with the regenerator theory (Shah & Sekulic, 2004).

4.2 Summary of operating conditions

The proposed test method has been evaluated by conducting experiments at four set of operating parameters: (i) room conditions (isothermal and equal humidities), (ii) isothermal and unequal humidities, (iii) winter operating conditions and (iv) summer operating conditions, and two sets of design parameters (i) face velocities and (ii) pressure difference between supply and return air streams. The detailed operating conditions are tabulated along with the results and the summary of test conditions is presented in a psychrometric chart shown in Figure 4.2.

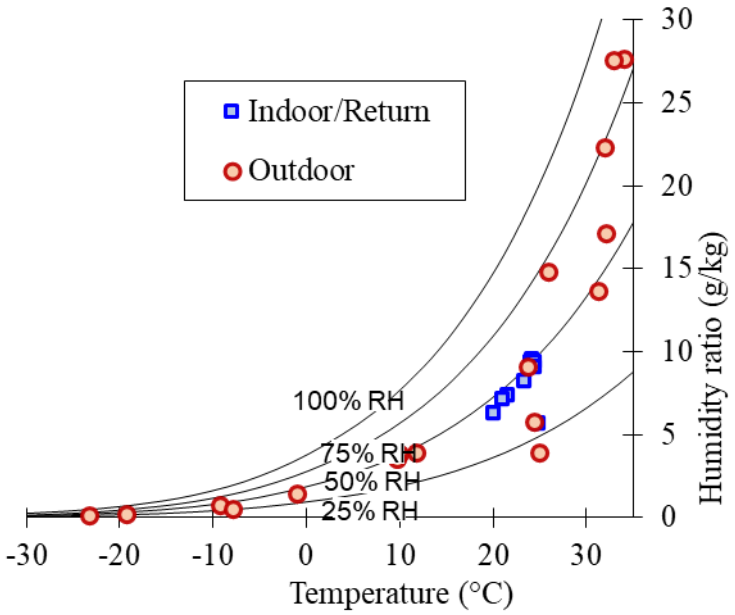

Figure 4.2. Psychrometric chart indicating the indoor (blue square) and outdoor (red circle) operating conditions used in contaminant transfer experiments.

4.3 Evaluation of the test method for different contaminants and desiccants

The test method was evaluated by conducting experiments at room conditions for MS and SG desiccant coated wheels. The exhaust contaminant transfer ratio (ECTR) and the EATR of both wheels (using SF_6) were measured. Then the transfer due to all the mechanisms except carryover and leakage (or transfer due to the phase change process) was quantified using Eq. (3.7). The supply line pressure was maintained at 30±10 Pa higher than the return side for all the experiments, which confirms no leakage from the return to the supply airstream and the obtained EATR is primarily due to the carryover. The EATR for MS and silica gel wheel were 1.7±3% and 6.8±3%, and the ECTR for all the gaseous contaminants are shown in Figure 4.3.

For the molecular sieve wheel, the highest transfer ratio is observed for ammonia (nearly 71%), and the lowest is for CO_2, about 3%. The silica gel wheel also follows a similar trend; however, the ECTR values are 80% and 9%, respectively. Since these tests were performed at room conditions, adsorption-desorption would be the mechanism causing a majority of transfer. Specifically, the contaminant concentration gradient between the desiccant surface and the return airstream causes the adsorption of the same into the desiccants. When the same desiccant surface is exposed to return airstreams (with minimum or zero concentration), the adsorbed contaminants are released into the airstream, resulting in cross-contamination. The contribution of mechanisms

other than carryover and leakage were quantified using $ECTR_{pc}$ and the results are presented in Figure 4.4.

Contaminants that are smaller in size, soluble in water, and polar have relatively high $ECTR_{pc}$. Ammonia is relatively small, highly polar, and soluble in water, having a very high transfer ratio on both wheels. The hydroxyl groups in silica gel and molecular sieve form hydrogen bonds with the polar contaminants and get adsorbed in the wheel. In general, contaminants with the highest polarity adsorb more than nonpolar, non-reactive contaminants such as CO_2, hexane, or xylene.

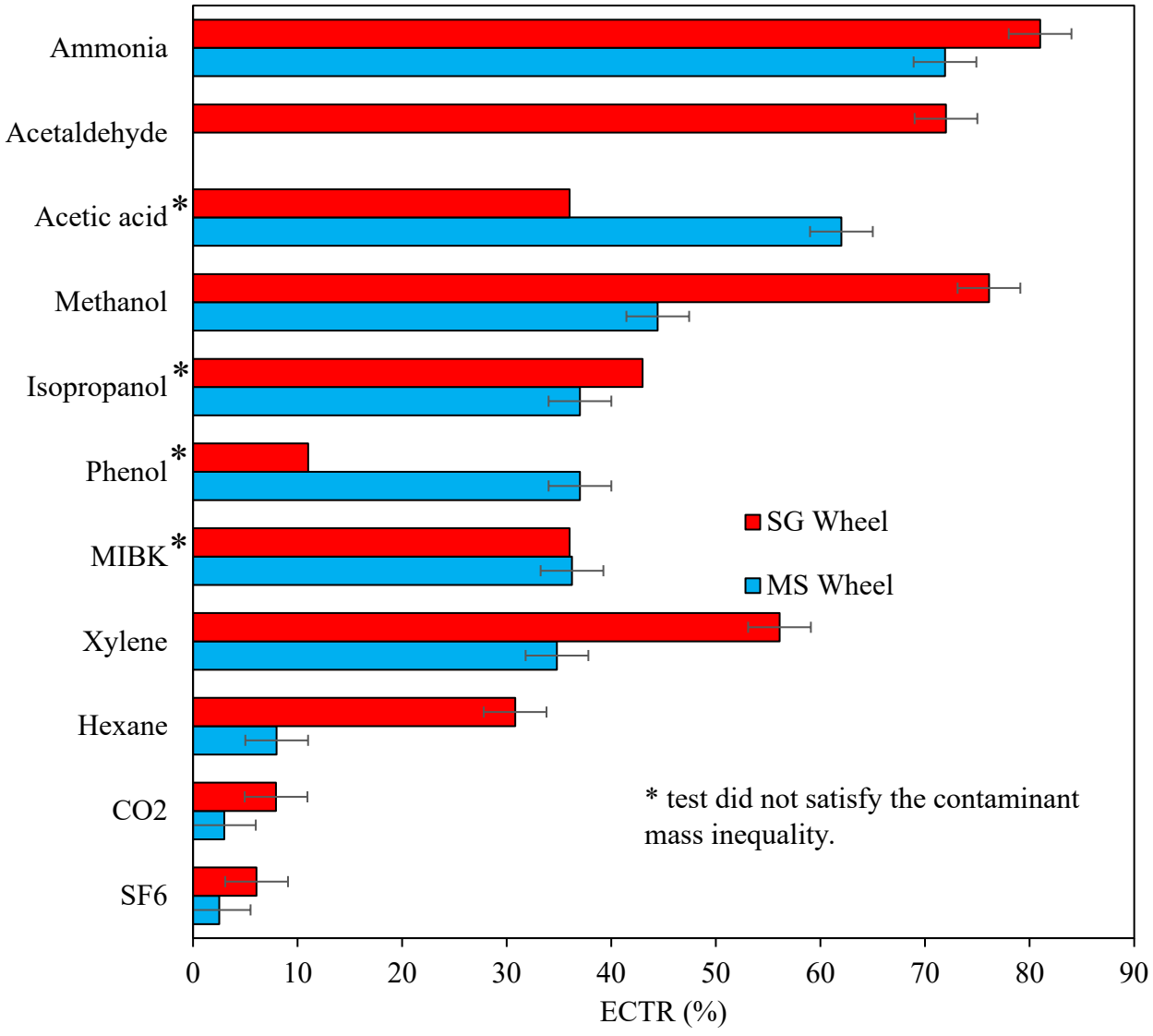

Figure 4.3. Exhaust contaminant transfer ratio (ECTR) of eleven different contaminants for molecular sieve and silica gel coated wheels at room conditions. Detailed operating conditions are listed in Table 4.1.

The molecular sieves can be fine-tuned to transfer water vapor selectively by varying their pore sizes; however, the contaminants with similar molecular sizes and which are polar get transferred along with the water vapor.

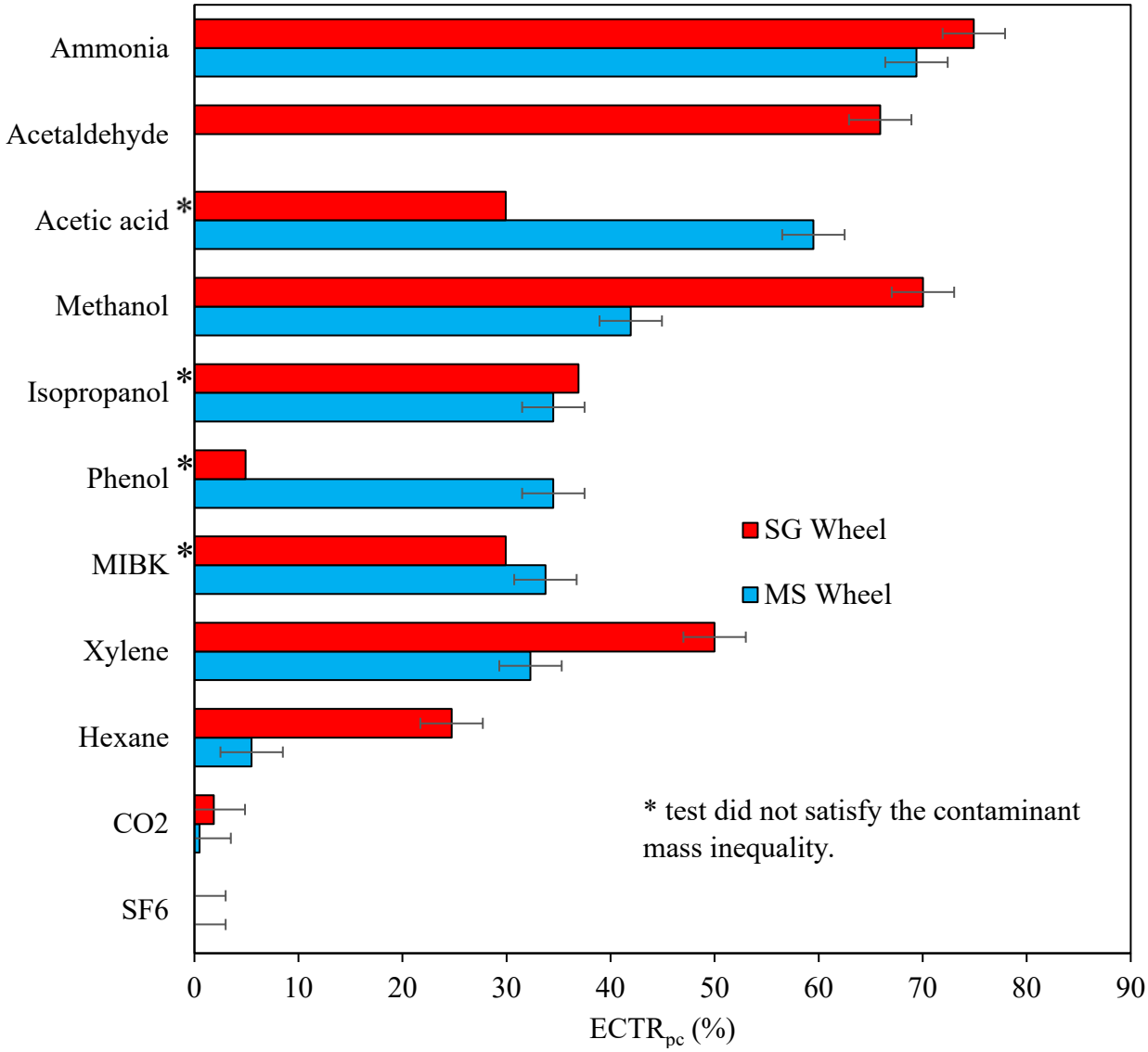

Figure 4.4. Contaminant transfer ratio due to phase change mechanisms (ECTR$_{pc}$) of eleven different contaminants for molecular sieve and silica gel coated wheels at room conditions. Detailed operating conditions are listed in Table 4.1.

For isopropanol, acetic acid, methyl isobutyl ketone and phenol, the experiments on the silica gel wheel have not met the contaminant mass inequality due to their accumulation in wheels. Though the ECTR of these contaminants are unknown, it can be inferred that they would have higher ECTR

than molecular sieve wheels. The mass inequality results for all the contaminants are discussed in section 4.9.

Table 4.1. Operating conditions of return and outdoor air streams for room temperature contaminant transfer tests in molecular sieve and silica gel wheels presented in Figures 4.3 and 4.4.

Parameter	Outdoor air	Return air
Face velocity	1 m/s [197 fpm]	1 m/s [197 fpm]
Temperature	25 ±0.5 °C [77±0.9 °F]	25±0.5 °C [77±0.9 °F]
Relative humidity	35±3 %	35±3 %
Pressure difference between supply and return air streams (P_{supply}-$P_{exhaust}$)	30±10 Pa	
Rotational speed of energy wheel	18 rpm	
Outdoor air correction factor	1.1	

4.3.1 Concentration measurements

The contaminant concentrations are measured at the inlet and outlets of the energy wheel using a Fourier Transform Infrared gas analyzer (Gasmet), and the data analyzed using the software Calcmet (Gasmet Technologies Oy, 2006). The FTIR sample cell has a volume of 30 L; previously, we found that the cell should be flushed three times to get accurate measurements. With a pumping rate of 30 L/min, the sample was pumped to the cell for 3 minutes. Measurements were taken for the next 5 minutes and the average of measured data from 5-8 minutes is used to determine the contaminant concentration. It should also be noted that the FTIR cannot sample multiple airstreams simultaneously. More details about concentration measurement procedures and sampling arrangements were discussed in Chapter 3, Section 3.1.4.

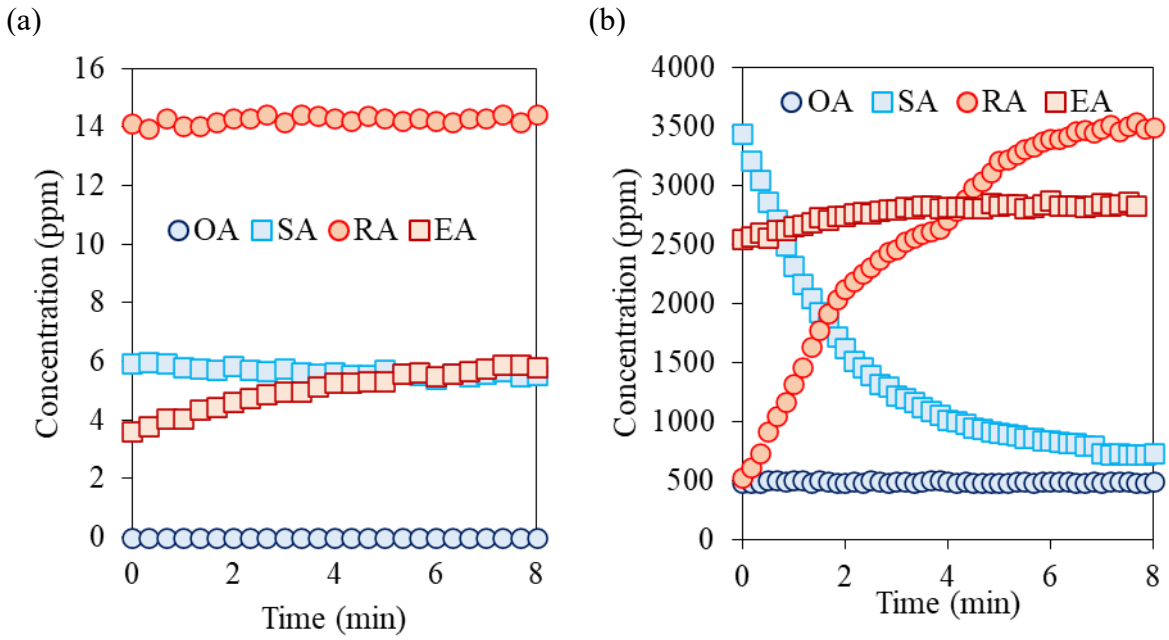

Figure 4.5. Concentration of (a) xylene and (b) carbon dioxide measured from outdoor, supply, return and exhaust airstreams for silica gel wheel as a function of time. Detailed operating conditions are listed in Table 4.1.

Figure 4.5 shows representative concentration data for xylene and CO_2. The xylene was injected into the test section using the liquid evaporation technique, and CO_2 was injected using the gas injection method. Since the uncertainty in concentration measurements in the FTIR is 2% of the available concentration reference spectra, the injection concentration is maintained close to the reference spectra. For xylene, the injected concentration was about 14.5 ppm and for CO_2, it was approximately 3500 ppm. The instantaneous concentration data also confirms the uniformity of contaminant concentration at the wheel inlets and outlets.

4.4 Evaluation of the test method for different face velocities

The proposed test method was evaluated by quantifying the ECTR at different face velocities from 0.5 m/s to 1.5 m/s. The other operating conditions including temperature, flow rate, and pressure drop were kept constant in these tests. The detailed operating conditions are listed in Table 4.2. The transfer of contaminants or ECTR increases as the face velocity decreases, as shown in Figure 4.6. The trend is similar to that of latent effectiveness. i.e., at lower face velocities, the number of transfer units would be high and result in high moisture transfer or latent effectiveness.

Table 4.2. Operating conditions of return and outdoor air streams for studying the effect of face velocity on gaseous contaminant transfer in the molecular sieve wheel presented in Figure 4.6.

Parameter	Outdoor air	Return air
Face velocity	0.25 -1.5 m/s [5-295 fpm]	0.25 -1.5 m/s [5-295 fpm]
Temperature	25 ±0.5 °C [77±0.9 °F]	25±0.5 °C [77±0.9 °F]
Relative humidity	20±2 %	20±2 %
Pressure difference between supply and return air streams (P_{supply}-$P_{exhaust}$)	30±10 Pa	
Rotational speed of energy wheel	18 rpm	
Outdoor air correction factor	1.1	

The highest ECTR is observed for ammonia, and it increased from 50% to 90% when the face velocity reduced from 1.5 to 0.5 m/s. The transfer of acetic acid and methanol is similar and it varied from 40% to 80%. The ECTR of isopropanol, MIBK, and xylene were similar, ranging from 30 to 60%. As the velocity/flow rate decrease, the flow residence time (or contact time) of gaseous contaminants increases and desiccants can adsorb more quantity. For hexane, CO_2 and SF_6, which are non-reactive and nonpolar, the transfer rates varied from 1 to 6%.

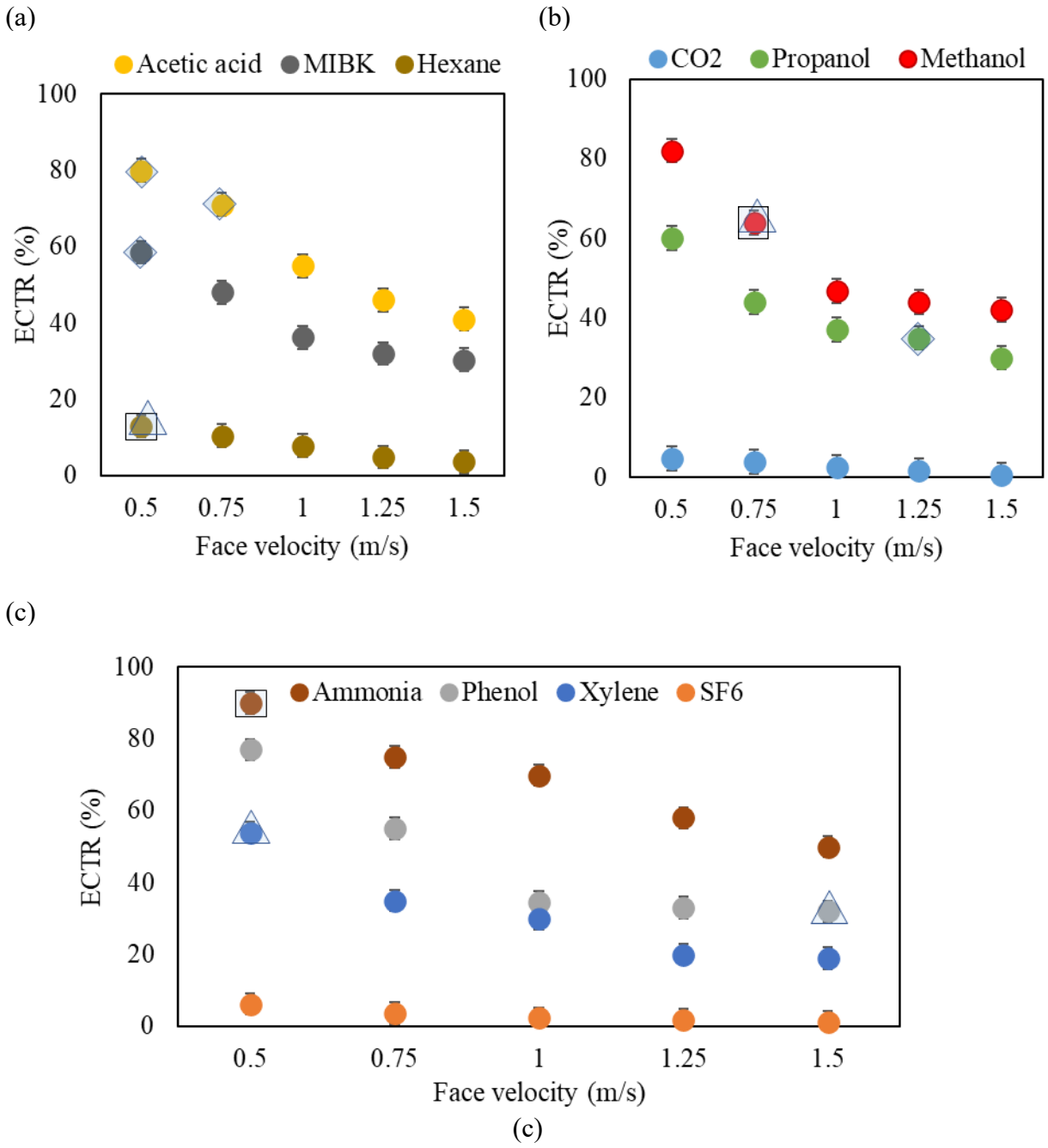

Figure 4.6. The contaminant transfer results (ECTR) for face velocities ranging from 0.5 m/s to 1.5 m/s in the molecular sieve wheel. Detailed operating conditions are listed in Table 4.2. The test points highlighted did not meet the recommended steady state concentration inlet inequality of less than ±5% (□), contaminant mass inequality of less than ±20% (Δ) and uncertainty limits of less than ±3% (◇).

4.5 Evaluation of the test method for pressure difference between supply and return airstreams

The proposed test method was evaluated by conducting experiments at the same inlet air conditions but at different line pressures. The ECTR results for ten contaminants are evaluated for different ΔP (supply-return) ranging from -50 to +50 Pa and are shown in Figure 4.7. When the supply line pressure is higher than the return line ($P_{supply}>P_{return}$), contaminant transfer is not changed. The results are nearly the same for various pressure difference values within the experimental uncertainties. When the return line pressure is higher than the supply line (i.e, $P_{supply} <P_{return}$), the transfer rate increases with the pressure difference. The highest ECTR is observed in the experiments when the return line is maintained at higher pressure than the supply line (P_{return}-P_{supply} = 50 Pa). When the supply line pressure is lower than the return line pressure, the leakage from the return to supply airline increases, which results in high transfer.

Table 4.3. Operating conditions of return and outdoor air streams for studying the effect of the pressure difference between supply and return air streams on gaseous contaminant transfer in the molecular sieve wheel presented in Figure 4.7.

Parameter	Outdoor air	Return air
Face velocity	1 m/s [197 fpm]	1 m/s [197 fpm]
Temperature	25 ±0.5 °C [77±0.9 °F]	25±0.5 °C [77±0.9 °F]
Relative humidity	20±2 %	20±2 %
Pressure difference between supply and return air streams (P_{supply}-$P_{exhaust}$)	-50, -25, 0, 25, 50 Pa (±10 Pa)	
Rotational speed of energy wheel	18 rpm	
Outdoor air correction factor	1.1	

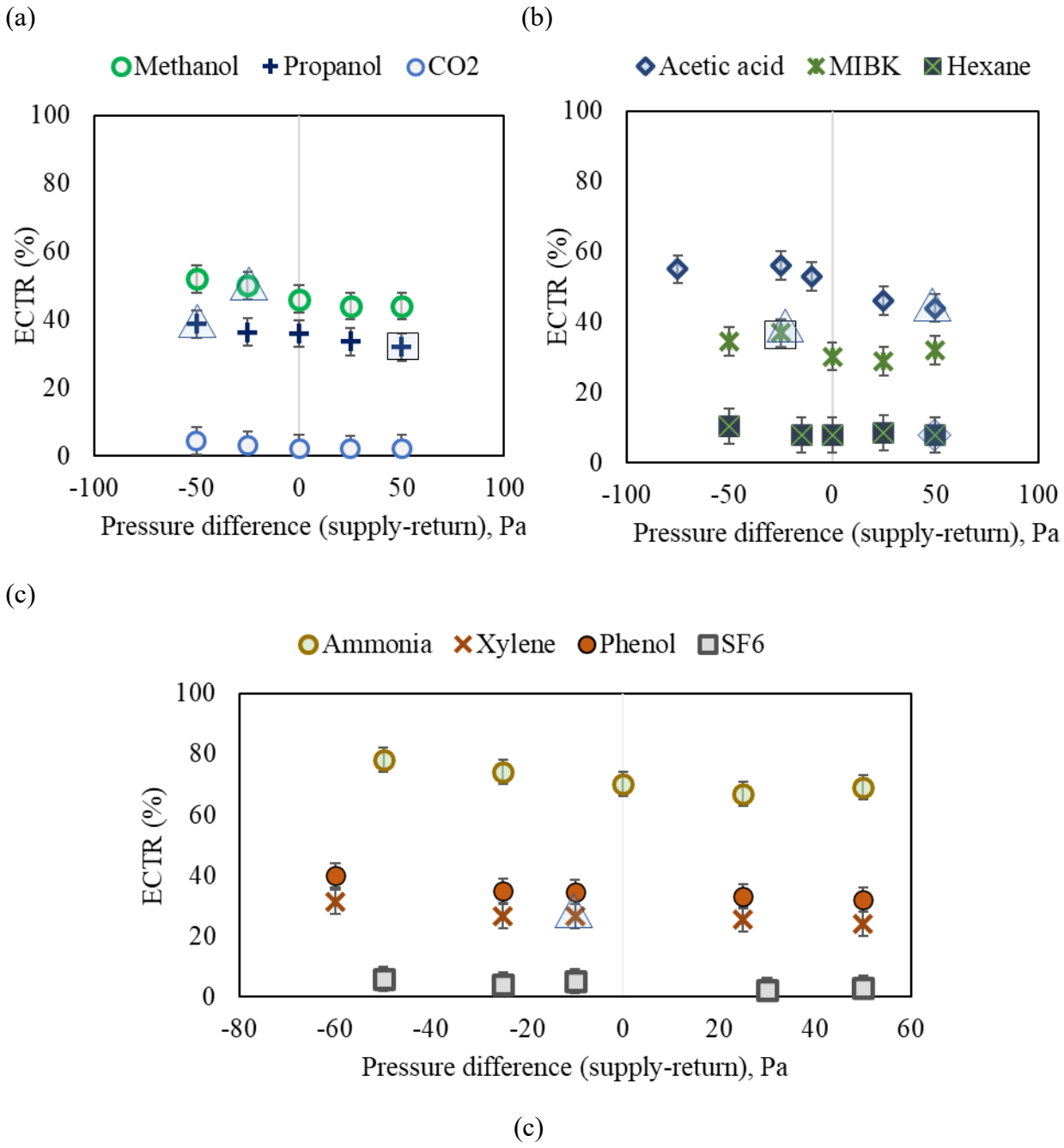

Figure 4.7. The exhaust contaminant transfer ratio (ECTR) for pressure difference between supply and return airstreams from -50 Pa to +50 pa in the molecular sieve wheel. Detailed operating conditions are listed in Table 4.3. The test points highlighted did not meet the recommended steady state concentration inlet inequality of less than ±5% (□), contaminant mass inequality of less than ±20% (Δ) and uncertainty limits of less than ±3% (◇).

For all the contaminants, the increase in ECTR for a 50 Pa pressure difference is about ≈5-7%. Since these experiments were performed at the same rotational speeds and face velocity, the

contribution of leakage in ECTR is similar in all contaminants, irrespective of their physical or chemical characteristics, which is plotted in Figure 4.9. Since these experiments were not performed at the exact same pressure differences as that of SF_6, the $ECTR_{pc}$ can not be evaluated by subtracting the ECTR from $EATR_{SF6}$. Therefore, a trend line is fitted on SF_6 data to determine the increase in EATR as a function of pressure difference between supply and exhaust airstreams, as shown in Figure 4.8. The generated EATR values from the curve fit is used to determine the $ECTR_{pc}$ for all the contaminants and the results are shown in Figure 4.9. For instance, change in ECTR for methanol and xylene are similar in magnitude (≈5%) within the test uncertainty limits.

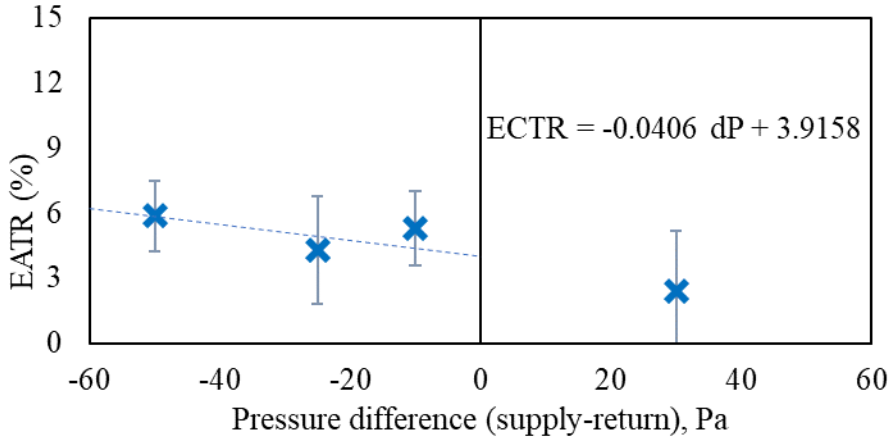

Figure 4.8. ECTR as a function of pressure difference between supply and return airstreams for SF_6.

(a) (b)

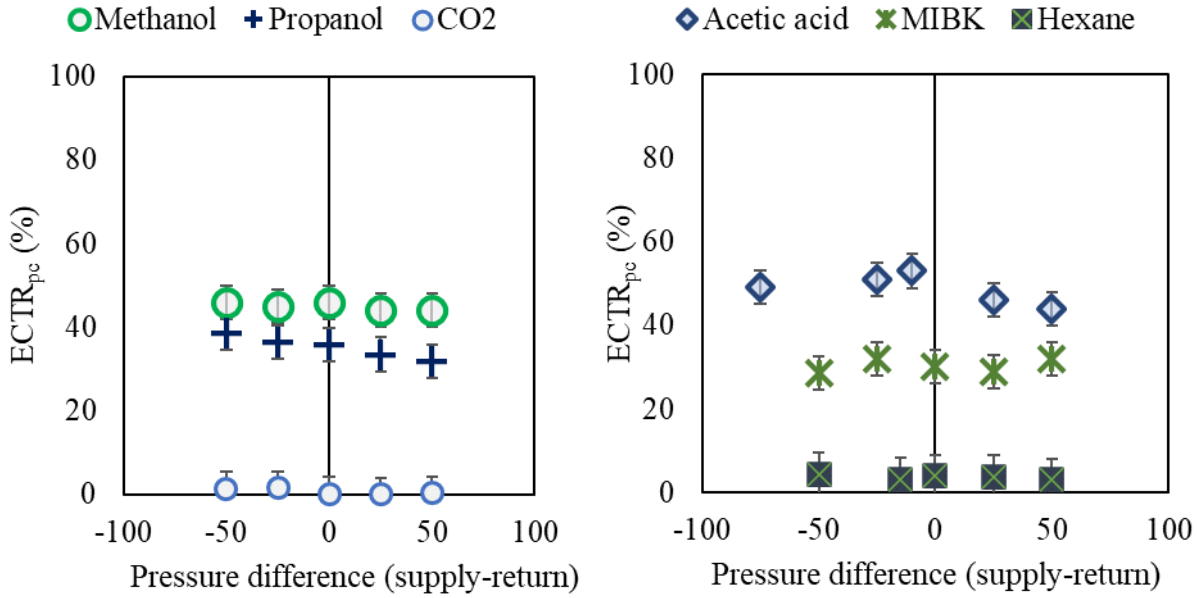

(c)

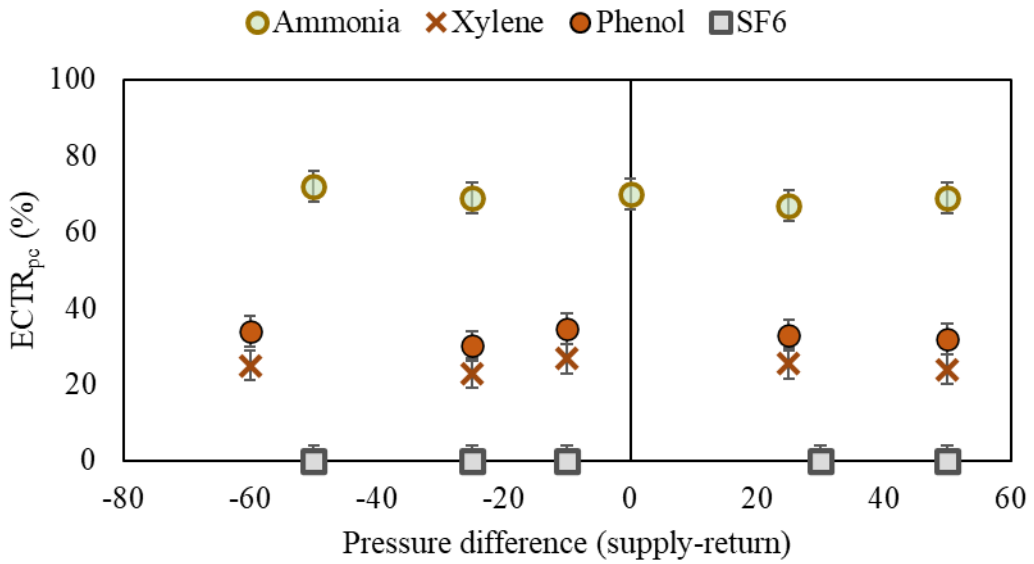

(c)

Figure 4.9. Contaminant transfer due to phase change mechanisms ($ECTR_{pc}$) for pressure difference between supply and return airstreams from -50 Pa to +50 pa in the molecular sieve wheel. Detailed operating conditions are listed in Table 4.3.

4.6 Evaluation of the test method for different outdoor air temperatures

The effect of outdoor air temperature on contaminant transfer rate is studied by varying outdoor air temperature from -23 °C to 31 °C. The detailed test conditions are reported in Table 4.4. There is no noticeable difference in ECTR observed with the temperature change. Each of these tests lasts for an hour after the wheel reaches a steady state and the results are presented in Figure 4.10.

Table 4.4. Operating conditions of return and outdoor air streams for studying the effect of air temperature on gaseous contaminant transfer in molecular sieve wheel presented in Figure 4.10.

Parameter	Outdoor air	Return air
Face velocity	1 m/s [197 fpm]	1 m/s [197 fpm]
Temperature	-23 to 31 (±0.5) °C [-9 to 88 (±0.9) °F]	25±0.5 °C [77±0.9 °F]
Relative humidity	44±2 %	45±2 %
Pressure difference between supply and return air streams (P_{supply}-$P_{exhaust}$)	30±10 Pa	
Rotational speed of energy wheel	18 rpm	
Outdoor air correction factor	1.1	

The highest transfer rate is observed for ammonia, followed by acetic acid and methanol. The transfer rate for isopropanol, phenol, methyl isobutyl ketone and xylene are similar, ranging

between 30-40%. The hexane, carbon dioxide and SF_6 have the lowest ECTR, between 2-7%. The uncertainties in ECTR are varied from 2-3% for these experiments.

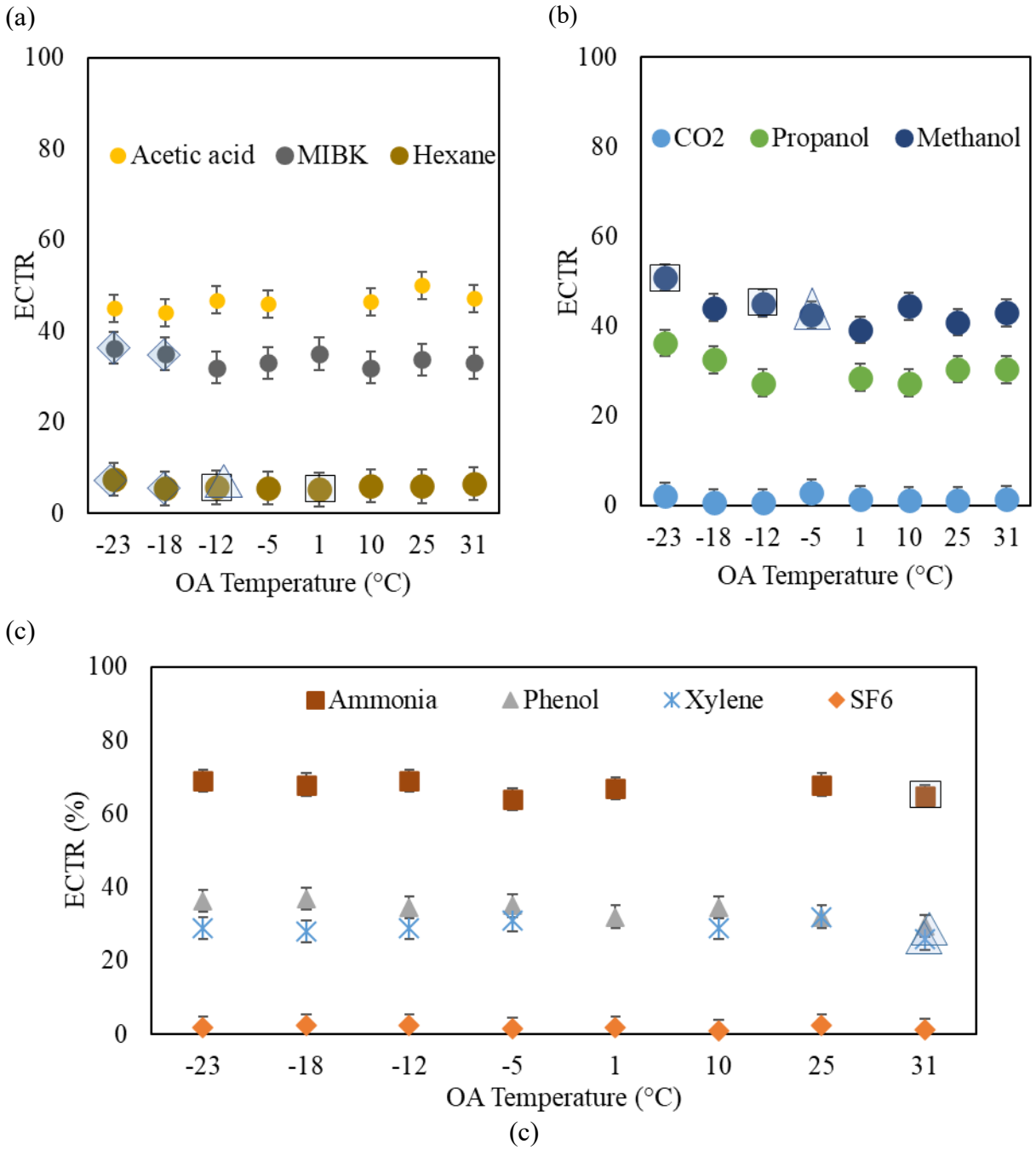

Figure 4.10. The contaminant transfer results (ECTR) for outdoor air temperatures ranging from -23°C to 31°C in molecular sieve wheel. Detailed operating conditions are listed in Table 4.4. The test points highlighted did not meet the recommended steady state concentration inlet inequality of less than ±5% (□), contaminant mass inequality of less than ±20% (Δ) and uncertainty limits of less than ±3% (◇).

Even though the variations in ECTR values are within the uncertainty limits, some contaminants show an increasing trend at low temperatures. For example, the propanol and methanol show an increment in ECTR from -12 °C to -23 °C, and there is a possibility of frosting at cold operating

conditions. Long-duration tests were performed to evaluate the effect of frosting on contaminant transfer and the results are discussed in Section 4.7.

4.7 Frosting experiments

The effect of frosting on the contaminant transfer is studied by conducting experiments on the molecular sieve wheel using methanol and carbon dioxide. The detailed test conditions are summarized in Table 4.5.

Table 4.5. Operating conditions of return and outdoor air streams for studying the effect of frosting on gaseous contaminant transfer in molecular sieve wheel presented in Figures 4.11 and 4.12.

Parameter	Outdoor air	Return air
Face velocity	1 m/s [197 fpm]	1 m/s [197 fpm]
Temperature	-21 ±0.5 °C [-6±0.9 °F]	26±0.5 °C [79±0.9 °F]
Relative humidity	35±2 %	50±2 %
Pressure difference between supply and return air streams (P_{supply}-$P_{exhaust}$)	30±10 Pa	
Rotational speed of energy wheel	18 rpm	
Outdoor air correction factor	1.	

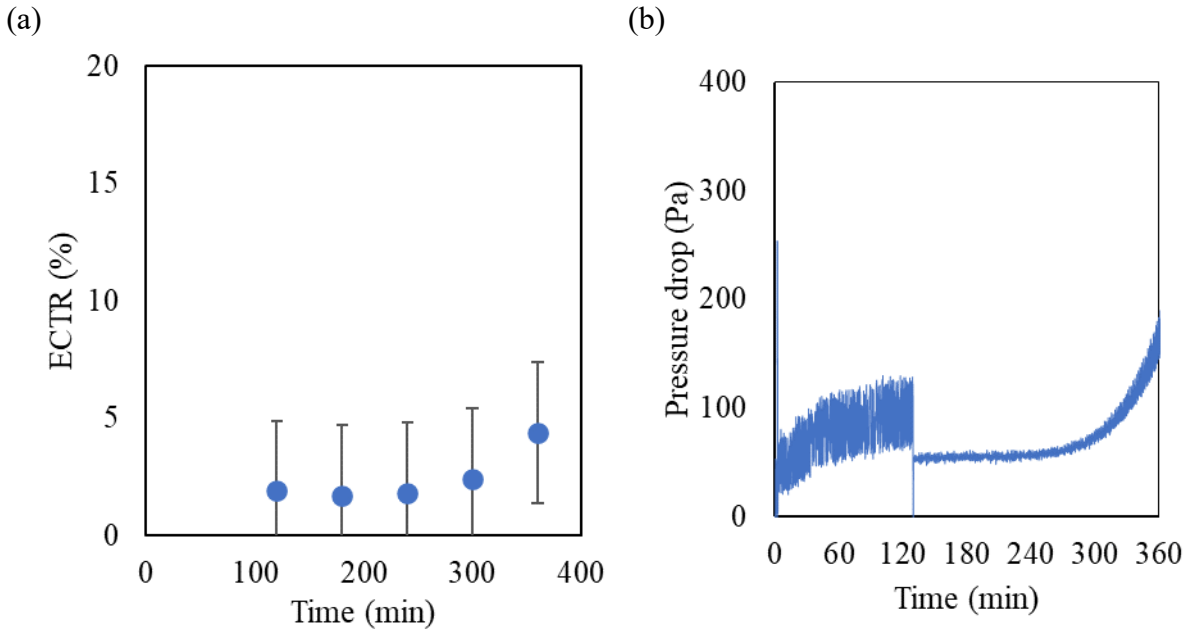

Figure 4.11. (a) The contaminant transfer results (ECTR) for CO_2 under frosting conditions in the molecular sieve wheel, (b) the pressure drop measured across the exhaust side of the wheel as a function of time (P_{return}-$P_{exhaust}$). Detailed test conditions are reported in Table 4.5.

(a) (b)

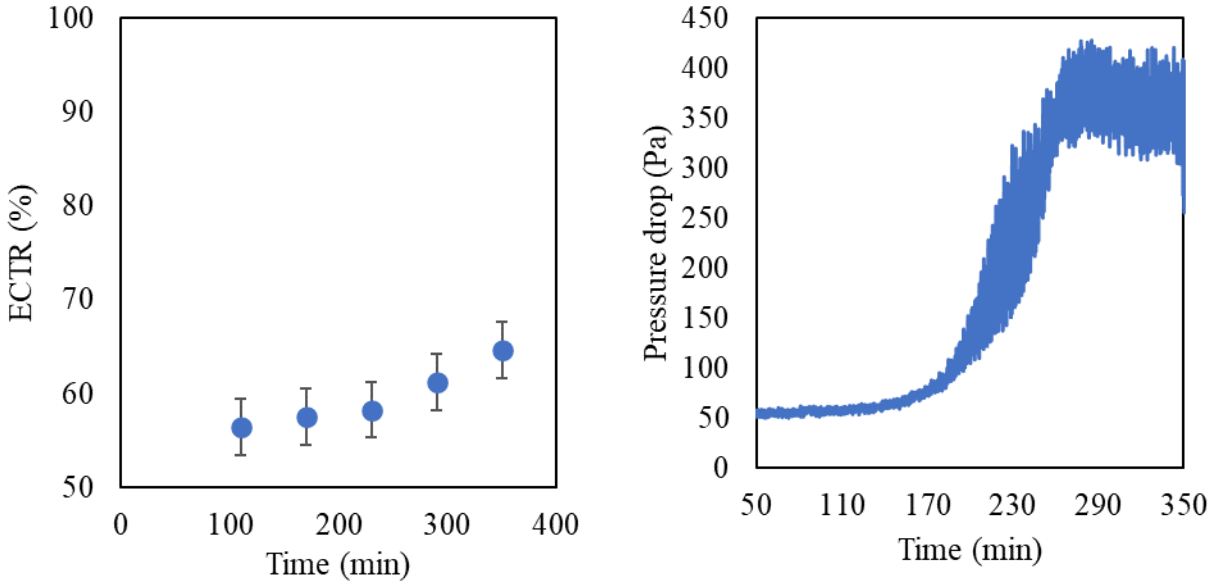

Figure 4.12. (a) The contaminant transfer results (ECTR) for methanol under frosting conditions in the molecular sieve wheel, (b) the pressure drop measured across the exhaust side of the wheel as a function of time (P_{return}-$P_{exhaust}$). Detailed test conditions are reported in Table 4.5.

Figures 4.11 and 4.12 shows the ECTR and pressure drop across the molecular sieve wheel during the frost tests. Each experiment takes approximately 3-4 hours to identify the frost. The ECTR is measured every hour during the experiment and their values compared as presented in Figure 4.11 (a) and Figure 4.12 (a). The pressure drop across the wheel measured on the exhaust side started increasing after 3 hours of continuous operation, which is an indication of frosting (Rafati Nasr et al., 2016). For both gases, the cross contamination or ECTR increased once the frosting started. The ECTR increased from 2% to 4% for CO_2 and 57% to 63% for methanol. It should also be noted that the pressure in the supply side is maintained higher than that of in the return airside to avoid the transfer due to the air leakage. Based on the results, it is confirmed that frosting increases the cross contamination in total energy recovery wheels. The increase in pressure drop above the uncertainty limit of pressure measuring instrumentation could be an indication of frosting in energy wheels.

4.8 Evaluation of the test method for different humidities

The proposed test method was evaluated by conducting three sets of experiments. These are (i) outdoor humidity varied from 50-85% for summer operating conditions, (ii) return humidity varied from 20% to 30% for summer operating conditions and (iii) outdoor humidity varied from 30 % to 70% at room conditions. The detailed test conditions are presented in Tables 4.6, 4.7 and 4.8.

4.8.1 Outdoor air humidity

In these experiments, the outdoor humidity varies from 50% to 85% with a constant return air humidity of 50%. These experiments are conducted in the molecular sieve wheel. The detailed test conditions are presented in Table 4.6. The observed ECTR is nearly the same for all the humidity conditions for most of the contaminants, as presented in Figure 4.13. A slight increase in ECTR was observed for phenol, ammonia, and xylene, but the changes were within the experimental uncertainty limits. Therefore, it is concluded that the outdoor air humidity does not significantly influence the ECTR.

Table 4.6. Operating conditions of return and outdoor air streams for studying the effect of outdoor air humidity on gaseous contaminant transfer in the molecular sieve wheel presented in Figure 4.13.

Parameter	Outdoor air	Return air
Face velocity	1 m/s [197 fpm]	1 m/s [197 fpm]
Temperature	31 ±0.5 °C [88±0.9 °F]	25±0.5 °C [77±0.9 °F]
Relative humidity	50-82 (±5 %)	45±2 %
Pressure difference between supply and return air streams (P_{supply}-$P_{exhaust}$)	30±10 Pa	
Rotational speed of energy wheel	18 rpm	
Outdoor air correction factor	1.27	

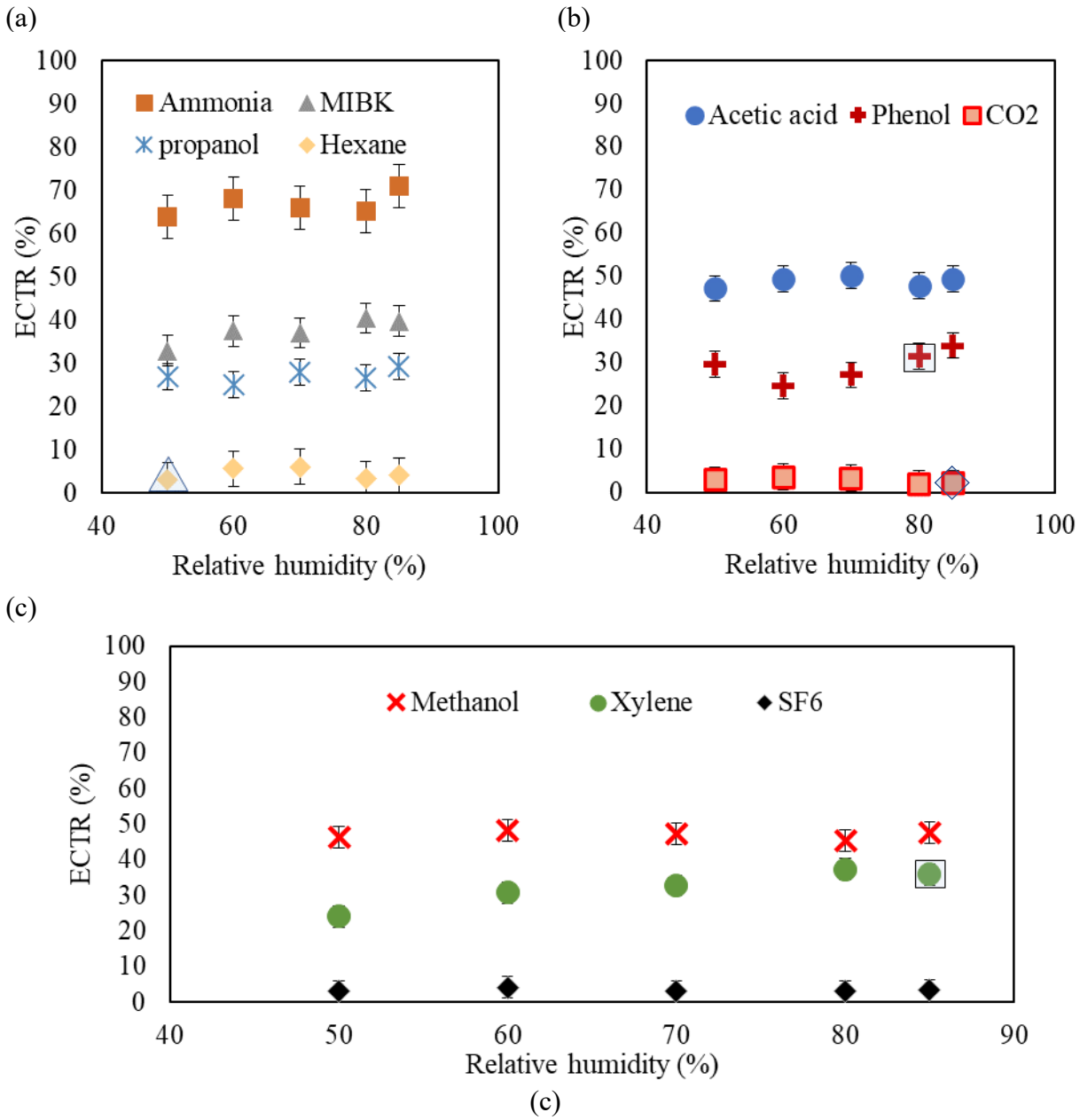

Figure 4.13. The contaminant transfer results (ECTR) for outdoor air humidities ranging from 50% to 85% in the molecular sieve wheel. Detailed test conditions are presented in Table 4.6. The test points highlighted did not meet the recommended steady state concentration inlet inequality of less than ±5% (□), contaminant mass inequality of less than ±20% (Δ) and uncertainty limits of less than ±3% (◇).

4.8.2 Return air humidity

Figure 4.14 shows the variation in ECTR when the return humidities were maintained at 20% and 30%. In these tests, outdoor air conditions were maintained at AHRI summer and winter operating conditions (Air-Conditioning Heating and Refrigeration Institute, 2013). The detailed test

conditions are reported in Table 4.7. Figure 4.14 (a), (b) and (c) shows the test data for all the contaminants during summer and winter test conditions.

Table 4.7. Operating conditions of return and outdoor air streams for studying the effect of return air humidity on gaseous contaminant transfer in the molecular sieve wheel presented in Figure 4.14.

Parameter	Outdoor air	Return air
Face velocity	1 m/s [197 fpm]	1 m/s [197 fpm]
Temperature	31 ±0.5 °C [77±0.9 °F] 1±0.5°C [34±0.9 °F]	25±0.5 °C [77±0.9 °F]
Relative humidity	45±5%	20±2 %, 30±2 %
Pressure difference between supply and return air streams (P_{supply}-$P_{exhaust}$)	30±10 Pa	
Rotational speed of energy wheel	18 rpm	
Outdoor air correction factor	1.1	

Irrespective of return air humidities, the ECTR obtained for all the contaminants during summer and winter tests are nearly the same within the experimental uncertainties. The summer test data for methanol and MIBK shows a slight increment in ECTR; however, the changes are within the experimental uncertainties, and since there are no changes observed for winter tests, it can be confirmed that the return air humidity conditions do not have any effect on contaminant transfer or ECTR.

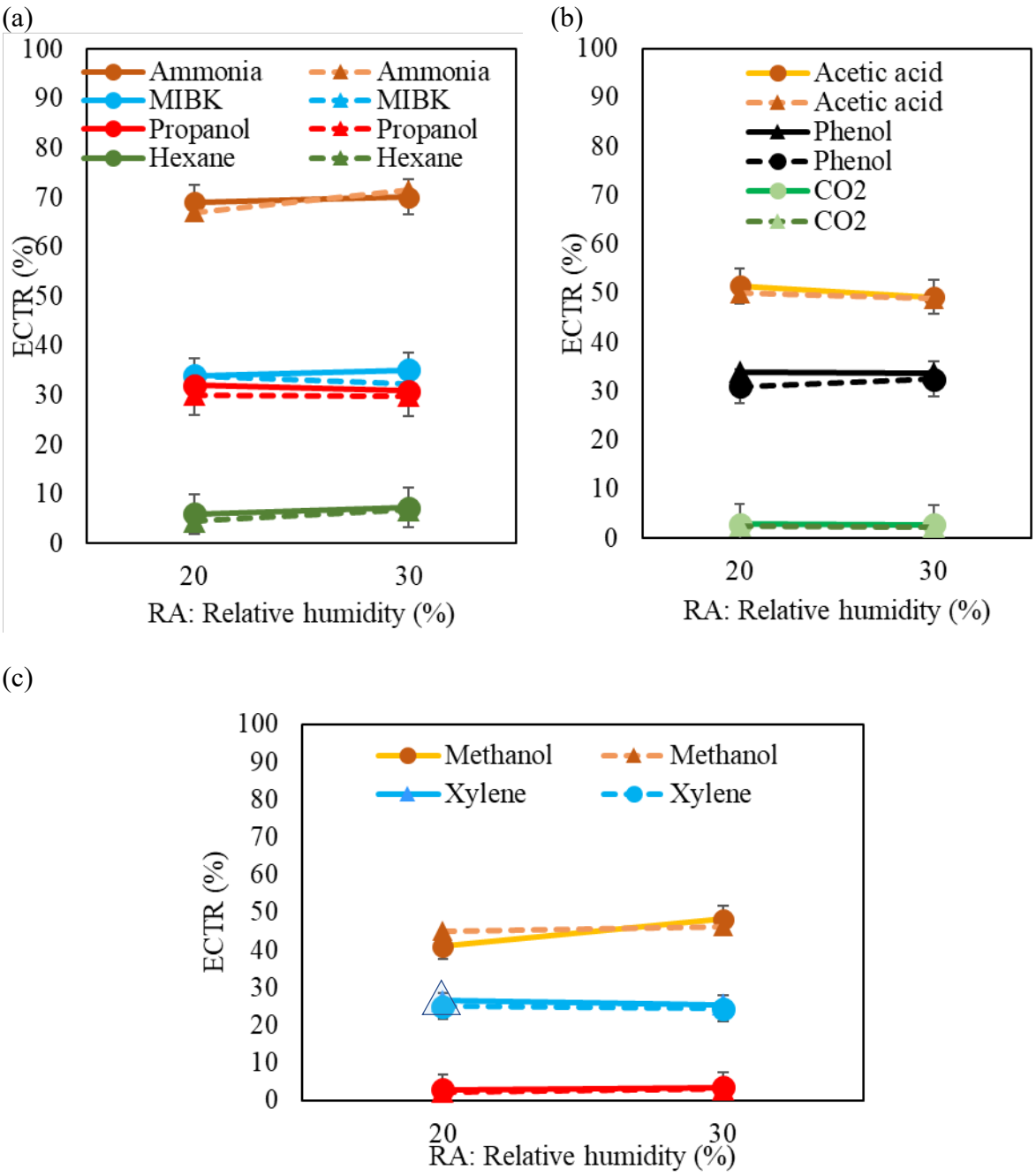

Figure 4.14. The contaminant transfer results (ECTR) for return air humidities 20% and 30% for winter (solid lines) and summer (dotted lines) operating conditions in the molecular sieve wheel. Detailed test conditions are reported in Table 4.7. The test points highlighted did not meet the recommended steady state concentration inlet inequality of less than ±5% (□), contaminant mass inequality of less than ±20% (Δ) and uncertainty limits of less than ±3% (◇).

4.8.3 Return air humidity at room conditions

The effect of return air humidity was investigated by conducting experiments at three different return humidities at room temperature conditions. The detailed test conditions are summarized in Table 4.8. Methanol and carbon dioxide are the contaminants used in these tests.

Table 4.8. Operating conditions of return and outdoor air streams for studying the effect of return air humidity on gaseous contaminant transfer in the molecular sieve wheel presented in Figure 4.15.

Parameter	Outdoor air	Return air
Face velocity	1 m/s [197 fpm]	1 m/s [197 fpm]
Temperature	25 ±0.5 °C [77±0.9 °F]	25±3 °C [77±0.9 °F]
Relative humidity	50±3%	30±5%, 70±5% 12±3%, 43±4%
Pressure difference between supply and return air streams (P_{supply}-$P_{exhaust}$)	30±10 Pa	
Rotational speed of energy wheel	18 rpm	
Outdoor air correction factor	1.1	

Figure 4.15 shows the ECTR data of methanol for MS and SG wheels and CO_2 data for MS wheel. The obtained transfer results are nearly the same and have not changed with the humidity.

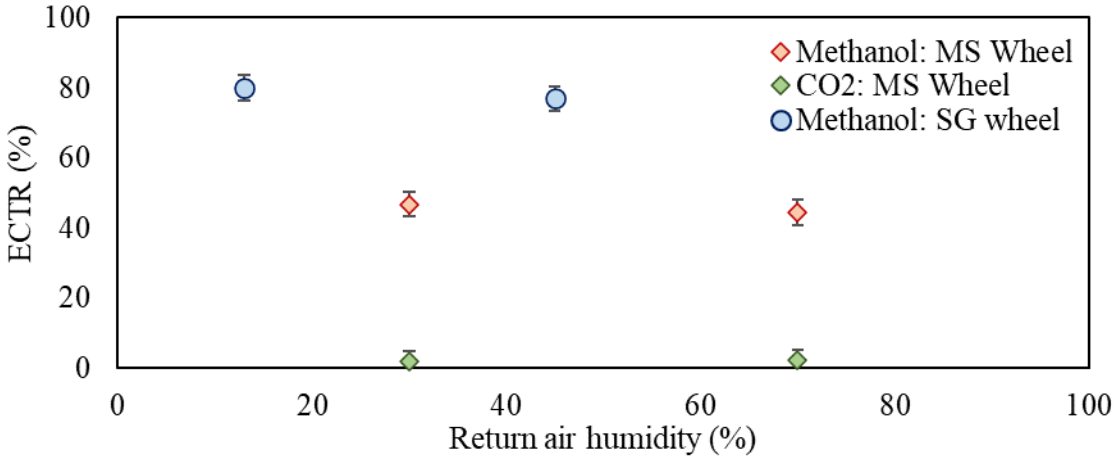

Figure 4.15. The contaminant transfer results (ECTR) of methanol and CO2 for return air humidities 30% and 70% for room temperature conditions in the molecular sieve wheel. Detailed test conditions are summarized in Table 4.8.

In MS wheel, the ECTR increased from 1.8% to 2.3% for CO_2, and decreased from 47% to 45% for methanol when the return humidity varied from 30% to 70%. When the humidity increased from 12% to 45%, the ECTR of methanol decreased from 80% to 77% in SG wheel. However,

these variations are within the uncertainty limits (±3%). Based on the experimental observations, it is concluded that the changes in humidity in the return and outdoor airstreams does not have any impact on the contaminant transfer rate or ECTR.

4.9 Validation of test method

4.9.1 Steady state inlet inequality

A very low inlet inequality value confirms that the contaminant injection is steady and does not vary with time. Since the gas analyzer allows to take real-time measurements, the inequalities can be reported as a function of time. Figure 4.16 shows the contaminant inequality data for xylene and carbon dioxide. For xylene, the steady state inequality was less than 5% from the beginning, whereas it took about 5 minutes to get a steady state CO_2 measurement at the return side inlet.

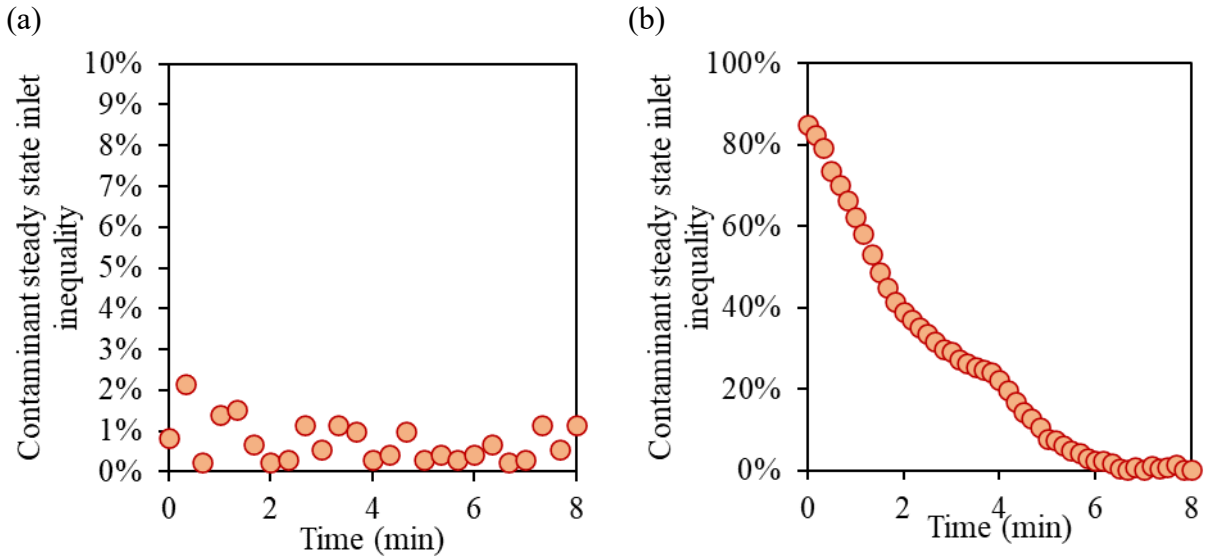

Figure 4.16. Concentration inlet inequality measured at the return airstream for (a) xylene and (b) carbon dioxide for silica gel wheel as a function of time. Detailed operating conditions are listed in Table 4.1.

The contaminant steady state inequality data of all the experiments are summarized and plotted in Figure 4.16. Among the tested contaminants, isopropanol and hexane are having the highest average steady state inequality of 3.5% and 3.3%, respectively. Considering all the data, the average contaminant inlet inequality is found to be 2.8%. Considering the distribution of contaminant inlet steady state inequality, it is confirmed that the proposed 5% limit is achievable and acceptable for the contaminant transfer tests.

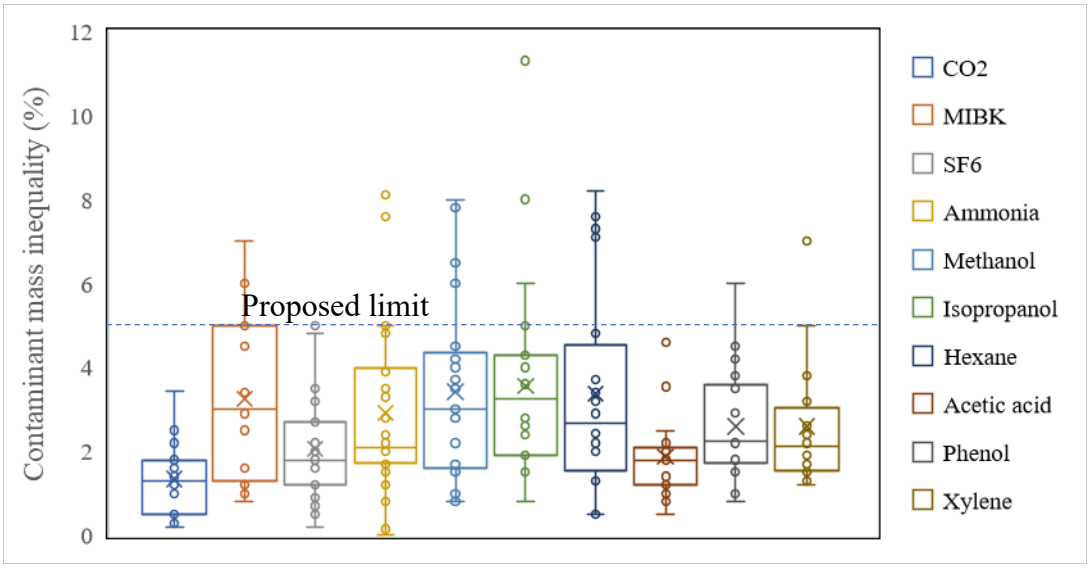

Figure 4.17. Comparison of contaminant steady state inlet inequality data (Eq. 3.8) for different contaminants. The horizontal line in the box plot refers to the median value of steady state inequality, and the circle symbols are outliers. The top and bottom of the boxes indicate 75th and 25th percentiles. The top and bottom bars indicate the minimum and maximum values of steady state inlet inequality. The data include both silica gel and molecular sieve wheels tests.

4.9.2 Contaminant mass inequality

It is essential to verify the contaminant mass inequality in every experiment to assure the quality of test data. High inequality in contaminant mass could be due to leakage in air ducts, non-uniform contaminant injection, sampling loss, or accumulation of contaminant in energy wheels or ducts. The contaminant mass inequality in these experiments is reported in Table 4.9. Generally, the contaminants injected using compressed gas injection tend to have very low mass inequality, which could be due to the fact that they exist in gaseous form and do not need to be heated or evaporated like the liquid evaporation technique. Most of the contaminants were able to achieve an inequality of less than 20%, which confirms the validity of these data.

Table 4.9. Contaminant mass inequality data of eleven contaminants in the silica gel and molecular sieve wheels presented in Figure 4.3.

Contaminant	Contaminant mass inequality (%)	
	Silica gel wheel	Molecular sieve wheel
1. Acetaldehyde	±6	--
2. Acetic acid	±56	±13
3. Ammonia	±12	±14
4. Carbon dioxide	±5	±12
5. Hexane	±8	±10
6. Isopropyl alcohol	±47	±19
7. Methanol	±9	±11
8. Methyl isobutyl ketone	±56	±5
9. Phenol	±77	±20
10. Sulfur Hexafluoride (SF6)	±7	±3
11. Xylene	±20	±9

In the case of the silica gel wheel, the inequality obtained for acetic acid, isopropyl alcohol, phenol and methyl isobutyl ketone is higher than 20%. Since all these contaminants are polar and water-soluble, and these experiments satisfy the dry air mass balance (<5%), the possible reason for the high inequality could be the accumulation of these contaminants in the silica gel wheel. All these gases were tested for 7-8 hours continuously to verify the transfer without changing the test conditions. It is found that as the ECTR increases, the contaminant mass inequality decreases with time. However, these tests were stopped after 6-8 hours because of the practical limitations of continuing more than that. Figure 4.18 and Figure 4.19 show the representative results of ECTR measured with ammonia and acetic acid, along with their mass inequality as a function of time. The graphs show that the test with acetic acid did not attain a steady state within 8 hours of injection, and possibly the transfer would be higher than the reported results. These experiments must be continued for long duration to reach a steady state and then the measured data could be used to determine the contaminant transfer ratio. The true value of contaminant transfer ratio cannot be determined without satisfying the contaminant mass balance. Previous literature on the adsorption of chemicals by silica gel and solvent recovery using desiccants confirm that silica gel can store significant amounts of certain chemicals, which can be recovered via various regeneration methods.

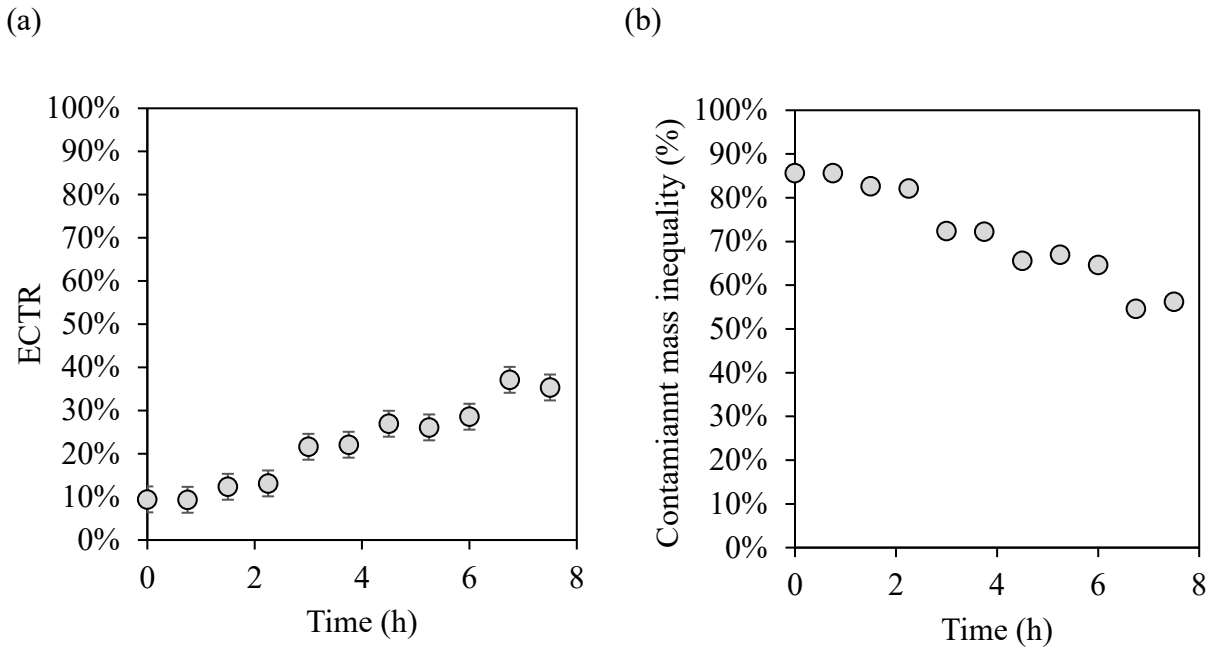

Figure 4.18. (a) Exhaust contaminant transfer ratio (ECTR) and (b) mass inequality data for acetic acid in silica gel wheel. Detailed operating conditions are listed in Table 4.1.

In the case of ammonia, the ECTR varied from 24% to 81% in 4 hours and reached a mass inequality of 12%, which is acceptable. Therefore, it is crucial to report the mass inequality in contaminant transfer experiments to understand the transfer process in wheels.

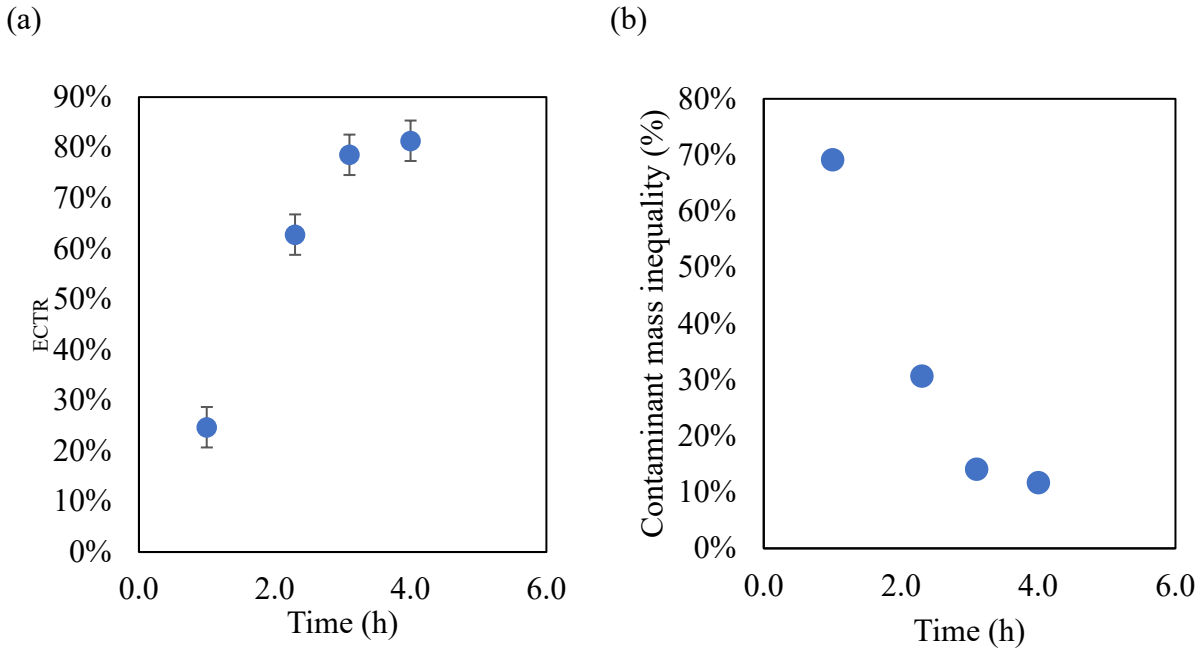

Figure 4.19. Exhaust contaminant transfer ratio (ECTR) and mass inequality for ammonia in silica gel wheel as a function of time. Detailed operating conditions are listed in Table 4.1.

The contaminant mass inequality of all the experiments is summarized and plotted in Figure 4.20. In this analysis, the test data of acetic acid, isopropyl alcohol, phenol and methyl isobutyl ketone (MIBK) in silica gel wheel were not considered since they did not meet the inequality criterion (presented in Eq. (3.9)). Among the tested contaminants, phenol and hexane are having the highest average mass inequality of 17% and 15%, respectively. Considering all the inequality results, the average contaminant mass inequality is found to be 11.8% with a standard deviation of 6%. It is also observed that the phenol is consistently having high values of mass inequality (nearly 20%) for all the experiments, and it could be due to its high boiling point (181.7°C). Considering the distribution of contaminant mass inequality, it is confirmed that the proposed 20% limit is achievable and acceptable for the contaminant transfer tests. The experiments should satisfy 20% of contaminant mass inequality limit to report the ECTR measurements accurately.

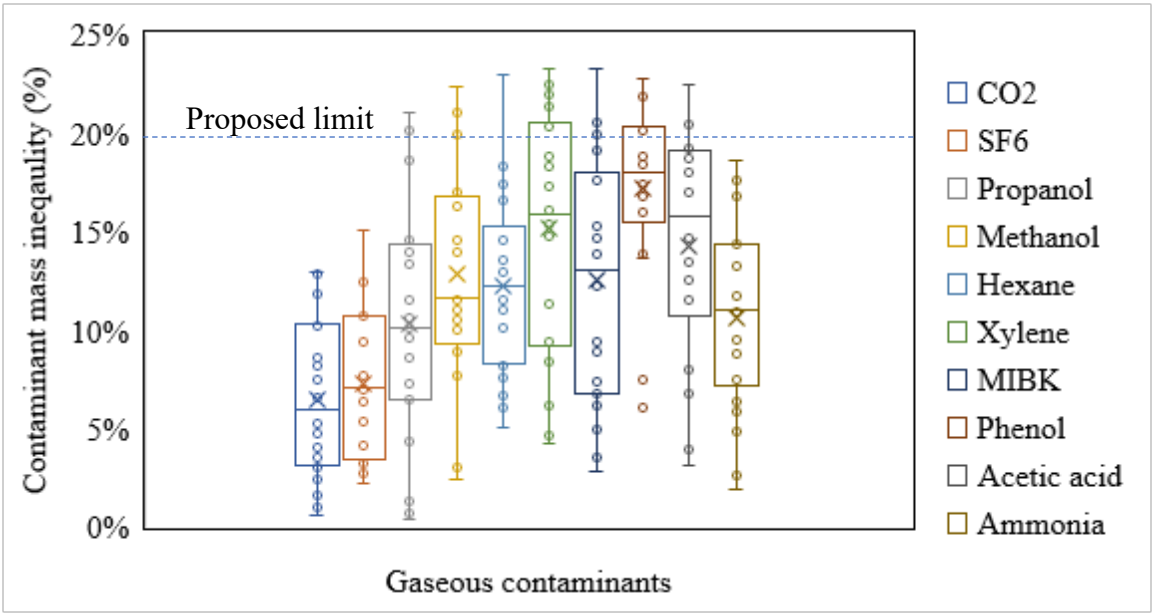

Figure 4.20. Comparison of contaminant mass inequality data (Eq. 3.9) for different contaminants. The horizontal line in the box plot refers to the median mass inequality, and the circle symbols are outliers. The top and bottom of the boxes indicate 75th and 25th percentiles. The top and bottom bars indicate the minimum and maximum values of contaminant mass inequality. The data include both silica gel and molecular sieve wheels tests.

4.9.3 Uncertainty analysis

The uncertainty in ECTR and $ECTR_{pc}$ is calculated using Eqs. (3.12) an (3.13). In FTIR analyzers, the uncertainty in concentration measurements depends on the availability of reference spectra and

it can be minimized by operating the experiments (or maintaining the concentrations) close to the reference spectra values. The uncertainties in ECTR and $ECTR_{pc}$ are reported in Table 4.10.

Figure 4.21 shows the uncertainty in ECTR for all the experiments performed in molecular sieve and silica gel coated wheels. As mentioned in the previous section, this analysis also excluded the data of acetic acid, isopropyl alcohol, phenol and methyl isobutyl ketone (MIBK) in silica gel wheel since they did not meet the inequality criterion. Most of the experiments satisfied the required limit of 3% and a few tests exceeded the limit, mainly due to the selection of operating conditions. In FTIR, the uncertainty depends on the calibration curves/ reference spectra of the contaminants. Therefore, by injecting the contaminants at a concentration close to the calibration curve, we could minimize the uncertainty in ECTR results. In this project, considering all the tests, the average uncertainty in ECTR is 2% with a standard deviation of 0.65%. The maximum and minimum uncertainties are obtained for propanol (4.2%) and for CO2 (0.6%). Considering the distribution of uncertainty results, it is confirmed that the proposed 3% limit is achievable and acceptable for the contaminant transfer tests.

In a few experiments, the steady state inequality, the mass balance of contaminants, and the uncertainty limits were exceeded; however, we used these data to develop this test method.

Table 4.10. Uncertainty in ECTR and $ECTR_{pc}$ of eleven gaseous contaminants for silica gel and molecular sieve wheels. Corresponding operating conditions are listed in Table 4.1.

Contaminant	Uncertainty (%)			
	Silica gel wheel		Molecular sieve wheel	
	ECTR	$ECTR_{pc}$	ECTR	$ECTR_{pc}$
1. Acetaldehyde	±4	±5	--	--
2. Acetic acid	±4	±5	±3	±4
3. Ammonia	±5	±6	±5	±6
4. Carbon dioxide	±2	±3	±2	±3
5. Hexane	±5	±6	±5	±6
6. Isopropyl alcohol	±3	±4	±2	±3
7. Methanol	±2	±3	±2	±3
8. Methyl isobutyl ketone	±4	±5	±3	±4
9. Phenol	±4	±5	±4	±5
10. Sulfur Hexafluoride (SF6)	±2	--	±2	--
11. Xylene	±3	±4	±2	±4

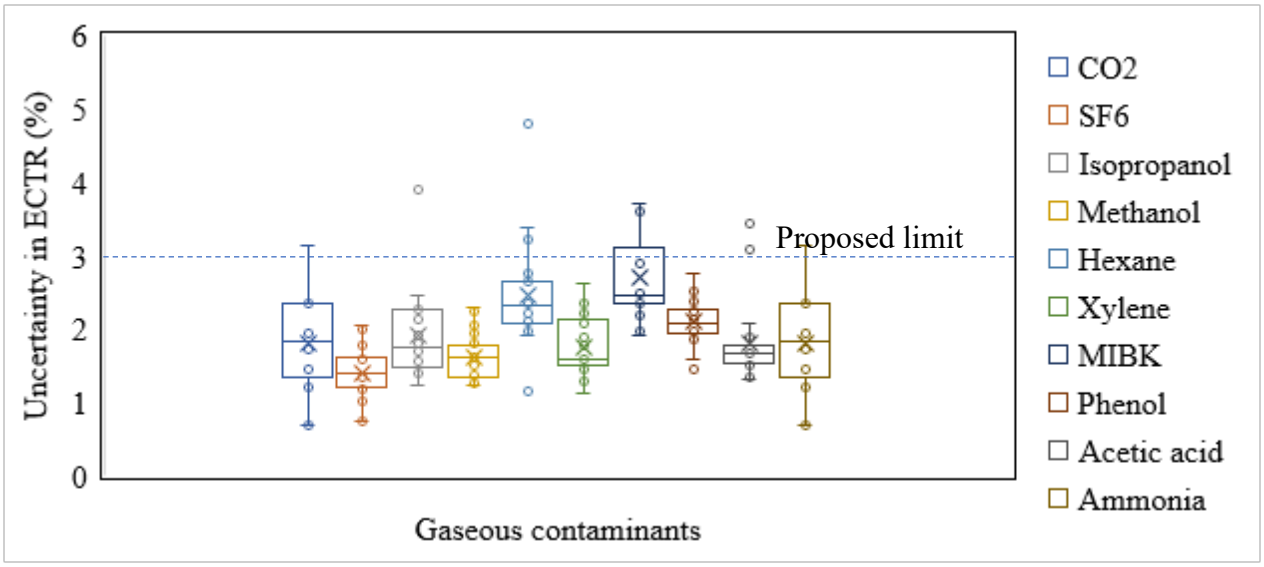

Figure 4.21. Comparison of uncertainty in ECTR data (Eq. 3.10) for different contaminants. The horizontal line in the box plot refers to the median uncertainty, and the circle symbols are outliers. The top and bottom of the boxes indicate 75th and 25th percentiles. The top and bottom bars indicate the minimum and maximum uncertainties. The data include both silica gel and molecular sieve wheel tests.

CHAPTER 5

FINAL TEST METHOD

Based on the literature review in Chapter 2, proposed test method in Chapter 3, and the evaluation and validation of the test method in Chapter 4, this chapter presents the final test method for contaminant transfer in energy wheels. The final recommended test method relies on ASHRAE Standard 84-2020 (ANSI/ASHRAE, 2020) and adds additional parameters and criteria to accurately quantify gaseous contaminant transfer in energy wheels. The final test method proposed in this report uses the same test facility and uncertainty methods as ASHRAE Standard 84-2020 and those are not reported here. Rather, new definitions, requirements, test parameters and uncertainty criteria that are needed to quantify gaseous contaminant transfer and ensure quality test data are specified. The final test method is presented in this chapter using the sections used in ASHRAE Standard 84-2020.

5.1 Purpose

In the final test method for gaseous contaminant transfer, the purpose section of ASHRAE Standard 84 needs to be expanded to include exhaust contaminant transfer ratio (ECTR) in addition to the effectiveness and other performance parameters (EATR, RER, OACF, and ΔP). The purpose of the contaminant transfer test method is to:

a. establish a uniform method of test for obtaining the gaseous contaminant transfer in energy wheels, and
b. specify the test conditions, data required, uncertainty analysis to be performed, calculations to be used, and reporting procedures for evaluating contaminant transfer in an energy wheel

5.2 Scope

The scope of ASHRAE Standard 84-2020 includes regenerators (energy wheels and fixed-bed regenerators), exchangers with intermediate energy transfer medium arranged in a closed loop circuit (heat pipes, thermosiphons and run-around loops) and recuperators. The final test method for gaseous contaminant transfer could be applied to all the exchangers in scope of ASHRAE Standard 84 but has only been validated for rotary energy wheels.

5.3 Definitions

The final gaseous contaminant transfer test method needs two definitions in addition to the definitions in ASHRAE Standard 84. The new definitions are presented below.

- ***Exhaust contaminant transfer ratio (ECTR):*** The exhaust contaminant transfer ratio is defined as the difference in the concentration of gaseous contaminants between the supply air outlet and the supply air inlet, divided by the concentration difference of gaseous contaminants between the exhaust air inlet and the supply air inlet, expressed as a percentage.
- ***Exhaust contaminant transfer ratio due to phase change mechanisms ($ECTR_{pc}$):*** The contribution of phase change mechanisms: adsorption, absorption, frosting/condensation to contaminant transfer. $ECTR_{pc}$ can be determined by subtracting the exhaust air transfer ratio (EATR) measured using an inert tracer gas (like SF_6) from the ECTR measured for the gaseous contaminant of interest.

The existing definitions in ASHRAE Standard 84 that are the most relevant to the final gaseous contaminant transfer test method are copied from ASHRAE Standard 84 below.

- ***adjustable purge:*** in a rotary regenerator, a segment, whose angle or area is adjustable, that directs outdoor air through a portion of the wheel medium into the exhaust air outlet to limit carryover of exhaust air.
- ***air leakage:*** air transferred from the exhaust to the supply airstream due to pressure differentials.
- ***carryover:*** in regenerators, the amount of exhaust air that is moved to the supply from the exhaust by the mechanical operation of the exchanger.
- ***exhaust air transfer:*** the air quantity transferred from the exhaust to the supply.
- ***exhaust air transfer ratio (EATR):*** the tracer gas concentration difference between the supply air outlet and the supply air inlet, divided by the tracer gas concentration difference between the exhaust air inlet and the supply air inlet, expressed as a percentage.
- ***outdoor air correction factor (OACF):*** a factor defined as the entering supply airflow divided by the leaving supply airflow.
- ***rotary heat wheel:*** an exchanger with porous discs, fabricated from materials with heat retention capacity, that are regenerated by collocated supply and exhaust airstreams.

- ***uncertainty:*** an expression of the ability of an instrument to indicate or record the true value of a measured quantity.

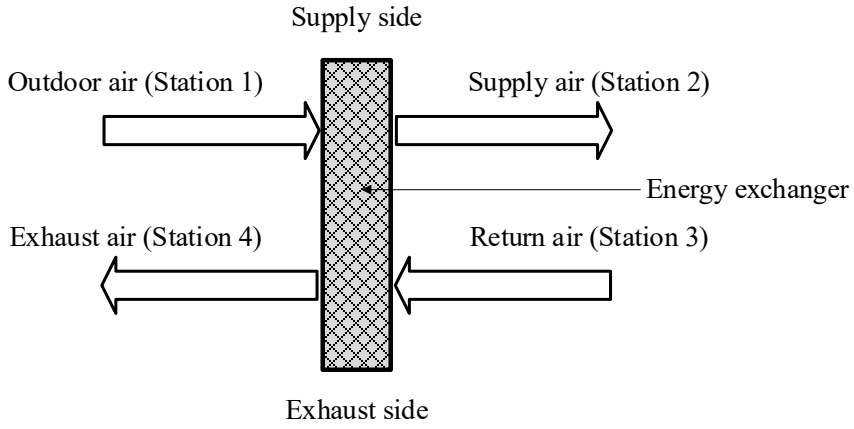

Figure 5.1. Schematic of an energy wheel test facility showing four measurement stations corresponding to outdoor air (Station 1), supply air (Station 2), return air (Station 3) and exhaust air (Station 4).

5.4 Requirements for performance testing

5.4.1 Performance metrices

In addition to the performance metrics specified in ASHRAE Standard 84, the following metrics are needed to quantify gaseous contaminant transfer in energy wheels:

(a) Exhaust contaminant transfer ratio (ECTR) and

(b) Phase change contaminant transfer ratio ($ECTR_{pc}$)

Determination of the ECTR of an energy wheel is given by the equation (5.1)

$$ECTR = \frac{C_2 - C_1}{C_3 - C_1} \tag{5.1}$$

Determination of the $ECTR_{pc}$ of an energy wheel is given by the equation (5.2)

$$ECTR_{pc} = ECTR_{total} - EATR_{SF_6} \tag{5.2}$$

ASHRAE Standard 84 contains the following metrics: (a) effectiveness and net effectiveness, (b) recovery efficiency ratio and net recovery efficiency ratio, (c) pressure drop, (d) outdoor air correction factor (OACF), and (e) exhaust air transfer ratio (EATR). EATR is the important performance metric for measuring gaseous contaminant transfer and the equation from ASHRAE Standard 84 is given below.

Determination of the EATR of an energy wheel is given by the equation (5.3)

$$EATR = \frac{C_2 - C_1}{C_3 - C_1} \tag{5.3}$$

where C_1, C_2, and C_3 are the gas concentrations at Stations 1, 2, and 3, respectively, as shown in Figure 5.1.

5.4.2 Apparatus

As in ASHRAE Standard 84, the test apparatus for gaseous contaminant transfer requires four measurement stations. In addition to measuring the temperature, humidity and dry air mass flow rate at each station as required in ASHRAE Standard 84, the test apparatus requires concentration to be measured at each station as summarized below.

a. Station 1—Supply Inlet: Temperature 1, Humidity 1, Dry-Air Mass Flow Rate 1, Concentration 1.

b. Station 2—Supply Outlet: Temperature 2, Humidity 2, Dry-Air Mass Flow Rate 2, Concentration 2.

c. Station 3—Exhaust Inlet: Temperature 3, Humidity 3, Dry-Air Mass Flow Rate 3, Concentration 3.

d. Station 4—Exhaust Outlet: Temperature 4, Humidity 4, Dry-Air Mass Flow Rate 4, Concentration 4.

The pretest uncertainty analysis, test duct leakage requirements, equipment installation, and instrument calibration methods are same as ASHRAE Standard 84 (ANSI/ASHRAE, 2020) and are not reported here.

5.5 Operating conditions, inequality checks, and conditions for rejection of test data

The criteria related to temperature, humidity, energy and moisture balances in ASHRAE Standard 84 would apply to the new test method for gaseous contaminant transfer in general. However, these criteria are not applicable where testing is done under isothermal and equal humidity conditions, The criteria that are needed to ensure quality data for contaminant transfer testing are provided below.

For contaminant mass inequality:

$$\frac{|\dot{m}_1 C_1 - \dot{m}_2 C_2 + \dot{m}_3 C_3 - \dot{m}_4 C_4|}{m_{minimum\ (1,3)}\ |C_1 - C_3|} < 0.2 \tag{5.4}$$

For inlet contaminant concentration inequality:

$$\frac{|\delta C_3|}{|C_1 - C_3|} < 0.05 \tag{5.5}$$

Where C_1 and C_3 are the contaminant concentrations in outdoor and return airstreams and δC is the maximum deviation of any concentration measurement from its time-averaged mean value. For most contaminant transfer experiments, the value of C_1 will be zero as the outdoor air typically doesn't have any VOCs. However, measuring the C_1 is critical as it involves in the ECTR calculations.

The Standard 84-2020 suggests an inequality of 0.15 for tracer gas testing. However, the gaseous contaminant transfer experiments are challenging due to the volatility of the contaminants and the difficulties in maintaining a steady state concentration at the Station 3 or return air inlet. Out of 325 tests, the average contaminant mass inequality obtained was about 12% with a standard deviation of 6%. Therefore, contaminant mass inequality of 0.2 would be acceptable and achievable in contaminant transfer tests.

During testing to determine the ECTR and EATR, the readings should satisfy the airflow mass inequality requirement (Eq. (5.6)) as presented ASHRAE Standard 84.

$$\frac{|\dot{m}_1 - \dot{m}_2 + \dot{m}_3 - \dot{m}_4|}{m_{minimum\ (1,3)}} < 0.05 \tag{5.6}$$

5.6 Pre and post test uncertainty analysis

In the new test method, the uncertainties in the exhaust contaminant transfer ratios should be below the values specified below to ensure quality data.

$$U(ECTR_{total}) < 3\% \tag{5.7}$$

$$U(ECTR_{pc}) < 5\% \tag{5.8}$$

5.7 Instruments and methods of measurement

The tracer gas concentration measurement method provided in ASHRAE Standard 84 would apply to the new test method for measuring the contaminant concentration from each station and the method is described below.

> **Concentration measurement: "***To measure the contaminant transfer from the exhaust to the supply side of an exchanger, the gaseous contaminant is injected into a turbulent region of the exhaust inlet. Air samples are then drawn from each of Stations 1 to 4. The sampling equipment required is as follows: (a) multipoint equal-length sampling grids or a single sampling tube with a mixing device 10 diameters or more upstream of measuring Stations 1, 2, 3, and 4 and (b) a means of collecting and transporting air samples from each station to a calibrated gas analyzer. The gas should be injected and mixed into the airstream before the exhaust inlet (Station 3) fan. The uniformity of this gas in the exhaust inlet duct should be checked. Samples should be drawn from these streams by a laboratory-approved sampling procedure. Sample lines should be short enough that dilution of the sample does not occur due to long sample lines and that the sample line transients do not affect the final recorded samples***"** (ANSI/ASHRAE, 2020).

5.8 Recommended tests to characterise contaminant transfer in a specific wheel

To quantify the ECTR for a specific wheel, all contaminants of interest should be measured at room operating conditions. In these tests, it is recommended that the air at the Stations 1 and 3 be isothermal and equal humidity conditions and the dry-air mass flow rates at, Station 2, and Station 3 can be equal.

A longer test at frosting conditions is required if the wheel is intended to be used in a cold climate where frosting is expected to occur. An increase in pressure drop on the exhaust side can be considered as an indication of frosting.

CHAPTER 6

CONCLUSIONS

The main aim of this research was to develop a test method to evaluate the cross-contamination of gaseous contaminants within total energy recovery wheels. Methods exist (e.g., ASHRAE Standard 84 (ANSI/ASHRAE, 2020)) to quantify the energy performance of energy wheels in terms of effectiveness and cross-contamination due to bulk airflow (such as carryover and leakage) in terms of exhaust air transfer ratio (EATR). However, gaseous contaminant transfer occurs due to other mechanisms (such as adsorption, absorption, condensation, and frosting) in addition to carryover and leakage. Therefore, in this report, an experimental method is proposed to quantify the total cross-contamination of gaseous contaminants including all transfer mechanisms.

6.1 Literature review on test methodologies and research data on gaseous contaminant transfer

The first objective of this project was to review the available test methods and data on the transfer of gaseous contaminants in energy wheels. There are nearly 25 published manuscripts/reports available in the literature, and the main conclusions from the review are:

- Several researchers have measured the transfer of gaseous contaminants in energy exchangers. While such measurements inherently include all transfer mechanisms (air leakage, carryover, and adsorption/desorption), no test method exists in the literature to quantify the transfer specifically due to phase change mechanisms.
- Gaseous contaminant transfer rates vary between 0% and 75%. Higher transfer rates were measured for phenol, toluene, nitrous oxide, ammonia, acetic acid, and formaldehyde.
- The uncertainties in measured ECTR varied between 1% and 30%, but most studies did not include a detailed uncertainty analysis. Furthermore, these studies did not determine whether the experiments conserved the mass of gaseous contaminants.
- The energy wheel design parameters (effectiveness and face velocity) have a more significant effect on ECTR than the operating conditions (relative humidity and temperature).

6.2 Development of test method

The second objective of this project was to develop a test methodology to quantify the gaseous contaminant transfer in energy wheels. The new test method and the test facility were built based on ASHRAE Standard 84. The recommendations of ASHRAE Standard 84 were followed in the commissioning and performance evaluation of the energy wheels. In the proposed test method, a new parameter called Exhaust Contaminant Transfer Ratio (ECTR) is introduced and defined as the difference in the concentration of gaseous contaminants between the supply air outlet and the supply air inlet, divided by the concentration difference of gaseous contaminants between the exhaust air inlet and the supply air inlet, expressed as a percentage (Eq. (6.1)).

$$ECTR = \frac{C_2 - C_1}{C_3 - C_1} \tag{6.1}$$

where C_1, C_2, and C_3 are the gas concentrations at outdoor (Station 1), supply (Station 2) and return (Station 3) airstreams, respectively. The gaseous contaminant transfer due to phase change mechanisms is quantified by subtracting the measured Exhaust Contaminant Transfer Ratio (ECTR) from the Exhaust Air Transfer Ratio (EATR) measured with an inert tracer gas like SF_6, as shown in Eq. (6.2)

$$ECTR = EATR + ECTR_{pc} \tag{6.2}$$

The ECTR includes transfer due to all mechanisms and $ECTR_{pc}$ quantifies transfer due to sorption and condensation/evaporation, while the EATR only includes transfer due to bulk air flow. The maximum limits for steady-state concentration inequality, contaminant mass inequality and uncertainty limit for ECTR are proposed for contaminant transfer experiments.

6.3 Evaluation and validation of test method

Wheels coated with 3Å Molecular sieve and silica gel desiccants are used to evaluate the proposed test methodology. The test method worked well for all 325 tests conducted during RP 1780 which included different wheel designs (two types of desiccant materials, face velocities, pressure differences) and operating conditions (temperature, relative humidity). The test method is validated by conducting experiments at various design parameters and operating conditions, and the gaseous contaminant transfer is evaluated using the proposed method. The major findings are listed below.

- The test method was verified for different contaminants and desiccant materials. It is found that gaseous contaminant transfer in total energy recovery wheels depends on the contaminant properties and the desiccant material used in the wheel.
- For the molecular sieve wheel, the highest transfer ratio or ECTR is observed for ammonia, followed by acetic acid, methanol, phenol, methyl isobutyl ketone, isopropanol, p-xylene, hexane and carbon dioxide. The highest and lowest ECTR (for ammonia and carbon dioxide) are 70% and 3%, respectively.
- In the case of silica gel wheels, similar to the molecular sieve wheel, ammonia and carbon dioxide have the highest and lowest transfer rates of 81% and 6%, respectively. However, the mass inequalities for several contaminants in the silica gel wheel (phenol, acetic acid, methanol and isopropanol) were outside the proposed bounds and the imbalance was believed to be due to accumulation of contaminants inside the wheel. Therefore, transfer ratios or ECTR were not quantified accurately for these contaminants. In general, the silica gel wheel tends to have high transfer rates for all the contaminants compared to the molecular sieve wheels at the same operating conditions.
- Experiments have shown that the contaminants that are small, water soluble /polar, tend to have greater transfer rates.
- The test method and criteria were shown to work well for wheels with both silica gel and molecular sieve desiccants, and most experiments meet the mass and concentration inequality recommendations.
- Face velocity is an important design parameter in rotary wheels, since the effectiveness changes with the face velocity/flow rate (for a given wheel). The proposed method was verified for six different face velocities ranging from 0.25 m/s [50 fpm] to 1.5 m/s [295 fpm]. Similar to the water vapor transfer or latent effectiveness, the contaminant transfer rate also decreases with an increase in face velocity. As the velocity/flow rate is increased, the contact time or flow residence time of the airstream inside the exchanger decreases, resulting in low transfer rates. For instance, the transfer ratio decreased from 90% to 50% for the case of ammonia when the face velocity increased from 0.25 m/s to 1.5 m/s.
- The test method was verified for different pressures in the air supply lines by varying the pressure difference between supply and return lines (P_{supply} - P_{return}) between -50 Pa and +50 Pa. When the supply line pressure is higher than the return line ($P_{supply} > P_{return}$), the

magnitude of the pressure difference doesn't affect the transfer. The results are nearly the same within the experimental uncertainties. When the return line pressure is higher ($P_{supply} < P_{return}$), the transfer increases as the pressure difference increases. The higher transfer observed when ($P_{supply} < P_{return}$) is due to increased air leakage as it is similar for all the contaminants and tracer gas.

The proposed test method is verified by conducting experiments at different operating conditions. The molecular sieve wheel is used to determine the effect of temperature, humidity, face velocity and pressure difference between supply and return air streams on gaseous contaminant transfer, and the major findings are summarized below.

- The proposed method has been verified for a wide range of outdoor air temperatures from -23 °C [-10 °F] to 32 °C [90 °F] and the results showed that outdoor air temperature does not have any significant impact on the contaminant transfer rates for all the contaminants, when there is no frosting on the wheel.
- Long duration tests at cold conditions revealed that there is an increase in the contaminant transfer ratio because of frosting. These tests were conducted using carbon dioxide and methanol in the molecular sieve wheel. It should also be noted that the contaminant mass inequality criteria did not show the short duration tests at cold conditions to be invalid, but the ECTR increases with time and therefore longer tests are required during frosting conditions.
- The method has been verified for outdoor and return air humidities by testing at indoor humidity ranging from 3.7 g/kg [26 gr/lb] to 13.1 g/kg [91 gr/lb] and outdoor humidity ranging from 0.1 g/kg [0.7 gr/lb] to 25.9 g/kg [181 gr/lb]. From the three sets of data, it is concluded that humidity does not have any significant impact on the contaminant transfer rates for all the contaminants.

6.4 Final test method

After evaluation and validation, the final test method for contaminant transfer is presented in this report. The method follows ASHRAE Standard 84-2020 with an additional parameter, Exhaust Contaminant Transfer Ratio (ECTR) to quantify the gaseous contaminant transfer and additional criteria to ensure acceptable data, as presented below.

For contaminant mass inequality:

$$\frac{|\dot{m}_1 C_1 - \dot{m}_2 C_2 + \dot{m}_3 C_3 - \dot{m}_4 C_4|}{m_{minimum\ (1,3)}\ |C_1 - C_3|} < 0.2 \tag{6.3}$$

For inlet contaminant concentration inequality:

$$\frac{|\delta C_3|}{|C_1 - C_3|} < 0.05 \tag{6.4}$$

Where C_1 and C_3 are the contaminant concentrations in outdoor and return airstreams and δC is the maximum deviation of any concentration measurement from its time-averaged mean value.

The proposed maximum uncertainties in the exhaust contaminant transfer ratio to ensure quality data are specified below.

$$U(ECTR_{total}) < 3\% \tag{6.5}$$

$$U\left(ECTR_{pc}\right) < 5\% \tag{6.6}$$

Finally, the following test conditions are recommended to quantify the gaseous contaminant transfer (cross contamination of gaseous contaminant) in total energy recovery wheels in terms of ECTR.

- Test all the contaminants at room conditions (same inlet temperatures and humidities).
- Long test at frosting conditions where the ΔP_{wheel} on the exhaust side can be used to indicate frosting.

REFERENCES

Air-Conditioning Heating and Refrigeration Institute. (2013). *Performance Rating of Air-to-Air Exchangers for Energy Recovery Ventilation Equipment*. AHRI.

Andersson, B., Andersson, K., Sundell, J., & Zingmark, P. -A. (1993). Mass transfer of contaminants in rotary enthalpy exchangers. *Indoor Air*, *3*(2), 143–148. https://doi.org/10.1111/j.1600-0668.1993.t01-1-00009.x

ANSI/ASHRAE. (2020). *Standard 84, Method of testing air-to-air heat/energy exchangers*.

ASME/ANSI. (1998). *Performance Test Code 19.1 Test Uncertainty: Instruments and Apparatus*.

Australian Government. (2022). *National Pollutant Inventory*. https://www.dcceew.gov.au/environment/protection/npi/substances

Bayer, C. W. (2011). *Total energy recovery wheel contaminant transfer study report*.

Brown, S. K. (1999). Chamber Assessment of Formaldehyde and VOC Emissions from Wood-Based Panels. *Indoor Air*, *9*(3), 209–215. https://doi.org/10.1111/j.1600-0668.1999.t01-1-00008.x

Brown, S. K., Sim, M. R., Abramson, M. J., & Gray, C. N. (1994a). Concentrations of volatile organic compounds in indoor air - a review. *Indoor Air*, *4*(2), 123–134. https://doi.org/10.1111/j.1600-0668.1994.t01-2-00007.x

Brown, S. K., Sim, M. R., Abramson, M. J., & Gray, C. N. (1994b). Concentrations of Volatile Organic Compounds in Indoor Air - A Review. *Indoor Air*, *4*(2), 123–134. https://doi.org/10.1111/j.1600-0668.1994.t01-2-00007.x

Canadian Standards Association. (2018). Standard laboratory methods of test for rating the performance of heat/energy-recovery ventilators. In *Canadian Standards Association*. CSA Group.

Centers for Disease Control and Prevention. (2011). *Methanol: Systemic Agent*. https://www.cdc.gov/niosh/topics/methyl-alcohol/

Druck, G. (n.d.). *DPI 605 Precision Portable Pressure Calibrator*. Retrieved October 20, 2019, from http://www.testequipmentdepot.com/druck/pressure-calibrators/dpi605.htm

Fisk, W., Pedersen, B., Hekmat, D., Chant, R., & Kaboli, H. (1985). Formaldehyde and tracer gas transfer between airstreams in enthalpy-type Air-to-air heat exchangers. *ASHRAE Transactions*, *91*(Part 1B), 173–186.

Gasmet Technologies Oy. (2006). *In-Lab Series Instruction & Operating Manual for the Gasmet CR-100M FT-IR gas analyzer model*. Gasmet Technologies Oy.

Government of Canada. (2017). *Residential indoor air quality guideline: acetaldehyde*. Healthy Living. https://www.canada.ca/en/services/health/publications/healthy-living.html

Harčárová, K., Vilčeková, S., & Balintova, M. (2020). Building materials as potential emission sources of VOC in the indoor environment of buildings. *Key Engineering Materials*, *838*, 74–80. https://doi.org/10.4028/www.scientific.net/KEM.838.74

Hart Scientific. (2002). *9105 / 9107 Dry-well Calibrator User's Guide*.

Hult, E. L., Willem, H., & Sherman, M. H. (2014). Formaldehyde transfer in residential energy recovery ventilators. In *Building and Environment* (Vol. 75, pp. 92–97). https://doi.org/10.1016/j.buildenv.2014.01.004

ISO. (2003a). International Standard: ISO 5167-1 Measurement of fluid flow by means of pressure differential devices inserted in circular cross-section conduits running full--Part 1: General principles and requirements. In *ISO*.

ISO. (2003b). International Standard: ISO 5167-2, Measurement of fluid flow by means of pressure differential devices inserted in circular cross section conduits running full--part 2 Orifice plates. In *ISO*.

Justo Alonso, M., Liu, P., Mathisen, H. M., Ge, G., & Simonson, C. (2015). Review of heat/energy recovery exchangers for use in ZEBs in cold climate countries. In *Building and Environment* (Vol. 84, pp. 228–237). https://doi.org/10.1016/j.buildenv.2014.11.014

Kassai, M. (2018). Experimental investigation of carbon dioxide cross-contamination in sorption energy recovery wheel in ventilation system. *Building Services Engineering Research and Technology*, *39*(4), 463–474. https://doi.org/10.1177/0143624417744733

Khoury, G. A., Chang, S. N., Lessley, D. A., Abdelghani, A. A., & Anderson, A. C. (1988). An investigation of reentrainment of chemical fume hood exhaust air in a heat recovery unit. *American Industrial Hygiene Association Journal*, *49*(2), 61–65. https://doi.org/10.1080/15298668891379396

Kodama, A. (2010). Cross-contamination test of an enthalpy wheel loading a strong acidic cation ion-exchange resin or 3A zeolite as a desiccant material. *Journal of Chemical Engineering of Japan*, *43*(10), 901–905. https://doi.org/10.1252/jcej.10we148

Krishnan, E. N., Soltan, J., & Simonson, C. J. (2022). *Evaluation of gaseous contaminant transfer in rotary energy wheels*.

Li, M., Weschler, C. J., Bekö, G., Wargocki, P., Lucic, G., & Williams, J. (2020). Human Ammonia Emission Rates under Various Indoor Environmental Conditions. *Environmental Science & Technology*, *54*(9), 5419–5428. https://doi.org/10.1021/acs.est.0c00094

Li, Y., Cheng, P., & Jia, W. (2022). Poor ventilation worsens short-range airborne transmission of respiratory infection. *Indoor Air*, *32*(1). https://doi.org/10.1111/ina.12946

Liu, P., Mathisen, H. M., Skaten, M., & Justo Alonso, M. (2022). Use of membrane energy exchanger in ventilation: Odour sensory measurement. *Building and Environment*, *222*(May), 109430. https://doi.org/10.1016/j.buildenv.2022.109430

NASA. (2016). *Cllinate science investigations*. http://www.ces.fau.edu/nasa/module-4/

New Jersey Department of Health. (2016). *Hazardous substance fact sheet*.

Niaz, K., Bahadar, H., Maqbool, F., & Abdollahi, M. (2015). A review of environmental and occupational exposure to xylene and its health concerns. *EXCLI Journal*, *14*, 1167–1186. https://doi.org/10.17179/excli2015-623

Nie, J., Yang, J., Fang, L., & Kong, X. (2015). Experimental evaluation of enthalpy efficiency and gas-phase contaminant transfer in an enthalpy recovery unit with polymer membrane foils. *Science and Technology for the Built Environment*, *21*(2), 150–159. https://doi.org/10.1080/10789669.2014.967165

Okano, H., Hirose, T., & Jin, W. L. (2008). Comparison of odor transfer characteristics of total heat exchangers between ion exchange resin and porous adsorbent as desiccant. *AIChE Annual Meeting, Conference Proceedings*, 1–8.

Okano, H., Tanaka, H., Hirose, T., Funato, H., Ishihara, S., & Chirarattananon, S. (2001a). A novel total heat exchanger with little odor transfer using ion exchange resin as a desiccant. *ASHRAE Transactions*, *107 Part 2*, 66–71.

Okano, H., Tanaka, H., Hirose, T., Funato, H., Ishihara, S., & Chirarattananon, S. (2001b). A novel total heat exchanger with little odor transfer using ion exchange resin as a desiccant. In *ASHRAE Transactions: Vol. 107 Part 2* (pp. 66–71).

Patel, H., Ge, G., Abdel-Salam, M. R. H., Abdel-Salam, A. H., Besant, R. W., & Simonson, C. J. (2014). Contaminant transfer in run-around membrane energy exchangers. *Energy and Buildings*, *70*, 94–105. https://doi.org/10.1016/j.enbuild.2013.11.013

Public Health England. (2019). *Acetic acid: general information*. Acetic Acid: Health Effects and Incident Management. https://www.gov.uk/government/publications/acetic-acid-properties-uses-and-incident-management

Rafati Nasr, M., Fathieh, F., Kadylak, D., Huizing, R., Besant, R. W., & Simonson, C. J. (2016). Experimental methods for detecting frosting in crossflow air-to-air energy exchangers. *Experimental Thermal and Fluid Science*, *77*, 100–115. https://doi.org/https://doi.org/10.1016/j.expthermflusci.2016.04.009

Roulet, C. A., Pibiri, M. C., Knutti, R., Pfeiffer, A., & Weber, A. (2002). Effect of chemical composition on VOC transfer through rotating heat exchangers. *Energy and Buildings*, *34*(8), 799–807. https://doi.org/10.1016/S0378-7788(02)00098-1

Shang, W., & Besant, R. W. (2008). Theoretical and experimental methods for the sensible effectiveness of Air-to-Air energy recovery wheels. *HVAC and R Research*, *14*(3), 373–396. https://doi.org/10.1080/10789669.2008.10391015

Shang, W., Wawryk, M., & Besant, R. W. (2001). Air crossover in rotary wheels used for air-to-air heat and moisture recovery. *ASHRAE Transactions*, 72–84.

Sparrow, E. M., Abraham, J. P., Martin, G. P., & Tong, J. C. Y. (2001). An experimental investigation of a mass exchanger for transferring water vapor and inhibiting the transfer of other gases. *International Journal of Heat and Mass Transfer*, *44*(22), 4313–4321. https://doi.org/10.1016/S0017-9310(01)00044-8

Teichman, K. Y. (1994). Indoor Air Quality: Exploring Policy Options to Reduce Human Exposures. *Indoor Air*, *4*(3), 202–211. https://doi.org/10.1111/j.1600-0668.1994.t01-1-00009.x

Thunder Scientific® Corporation. (n.d.). *Model 1200 Mini "Two-Pressure" Humidity Generator.* Retrieved October 20, 2019, from https://www.thunderscientific.com/humidity_equipment/model_1200.html

Torabi, M. (2021). *A test methodology for measuring gaseous contaminant transfer in energy wheels* [MSc thesis, University of Saskatchewan, Saskatoon]. https://harvest.usask.ca/handle/10388/13747

Williams, M. (2013). The Merck Index: An Encyclopedia of Chemicals, Drugs, and Biologicals, 15th Edition Edited by M.J.O'Neil, Royal Society of Chemistry, Cambridge, UK ISBN 9781849736701; 2708 pages. April 2013, $150 with 1-year free access to The Merck Index Online. *Drug Development Research*, *74*(5), 339–339. https://doi.org/10.1002/ddr.21085

Wolfrum, E. J., Peterson, D., & Kozubal, E. (2008). The volatile organic compound (VOC) removal performance of Desiccant-Based dehumidification systems: Testing at Sub-ppm VOC concentrations. *HVAC & R Research*, *14*(1), 129–140. https://doi.org/10.1080/10789669.2008.10390998

Wolkoff, P. (1995a). Volatile Organic Compounds Sources, Measurements, Emissions, and the Impact on Indoor Air Quality. *Indoor Air*, *5*(S3), 5–73. https://doi.org/10.1111/j.1600-0668.1995.tb00017.x

Wolkoff, P. (1995b). Volatile Organic Compounds Sources, Measurements, Emissions, and the Impact on Indoor Air Quality. *Indoor Air*, *5*(S3), 5–73. https://doi.org/10.1111/j.1600-0668.1995.tb00017.x

Yurdakul, S., Civan, M., Özden, Ö., Gaga, E., Döğeroğlu, T., & Tuncel, G. (2017). Spatial variation of VOCs and inorganic pollutants in a university building. *Atmospheric Pollution Research*, *8*(1), 1–12. https://doi.org/10.1016/j.apr.2016.07.001

APPENDIX A

In this appendix, test data and the detailed operating conditions from all the gaseous contaminant transfer experiments are summarized and presented in Tables A.1 to A.23. The results summarized in Tables A.1 to A.10 are from the molecular sieve wheel and from A.11 to A.21 are from silica gel wheel. It should also be noted that long-duration tests were required for silica gel wheels. The data presented in Tables A.15 to A.21 were measured (hourly) during long-duration tests of respective contaminants. The results presented in Tables A.22 and A.23 are from the frost tests. In these tests, the contaminant concentrations were measured in every hour and reported the respective ECTR values. The indoor and outdoor operating conditions at which these experiments were conducted is also consolidated and presented in Figure A.1. The outdoor air conditions were varied from cold and dry (-23°C, 0.11 g/kg) to hot and humid (34°C, 27.60 g/kg).

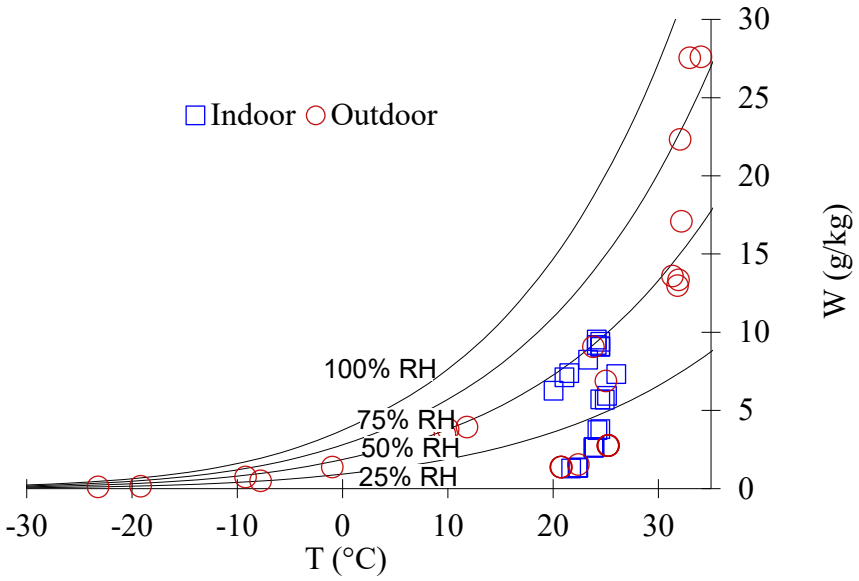

Figure A.1. Psychrometric chart indicating the indoor (blue square) and outdoor (red circle) operating conditions used in contaminant transfer experiments.

In the test data (Appendix A Tables A.1 to A. 23), asterisk (*) symbol on outdoor air temperature (OA) column indicates that the test did not meet the recommended contaminant mass inequality limit.

Table A.1. Temperature, humidity, flow rate, pressure difference (between supply and return side) and concentration data for carbon dioxide tests in molecular sieve coated energy wheel.

Temperature (°C)				Relative humidity (%)				Mass flow rate (g/s)				Concentration (ppm)				Pressure (Pa)
OA	SA	RA	EA	OA	SA	RA	EA	OA	SA	RA	EA	OA	SA	RA	EA	P_s-P_r
25.0	26.1	26.0	25.5	35.0	35.0	35.0	34.0	27.6	23.1	26.3	30.2	461.0	488.0	1631.0	1592.0	32
-23.3	15.2	21.5	-7.9	24.7	54.0	46.2	77.9	30.1	24.3	27.1	32.1	478.0	496.0	1667.0	1351.0	29
-19.2	15.0	21.1	-5.5	22.5	51.8	45.8	66.3	30.7	24.7	27.1	33.1	519.0	548.0	2815.0	2321.0	21
-9.2	19.4	23.3	2.6	44.1	46.7	46.2	57.4	29.2	23.5	27.4	33.2	519.2	559.0	2801.0	2354.1	38
-7.8	16.7	20.0	1.9	25.6	41.6	43.0	43.1	0.0	0.0	0.0	0.0	518.5	557.5	2849.9	2473.5	30
23.8	24.4	24.9	23.8	49.4	33.2	29.1	41.1	27.3	22.1	27.6	32.5	478.0	496.0	1667.0	1351.0	34
31.3	25.7	24.1	29.0	47.4	48.6	50.8	45.0	26.0	21.7	27.5	32.3	507.0	562.0	2444.0	2120.0	32
32.2	26.1	24.5	29.7	56.4	56.0	49.0	58.2	26.6	21.8	27.3	33.3	486.0	561.0	2638.0	2325.0	31
32.0	26.8	24.5	30.7	73.6	54.8	47.3	62.1	26.3	21.9	26.5	31.4	471.0	500.0	1360.0	1154.0	35
34.0	26.2	24.1	30.6	80.8	65.1	49.0	81.1	26.9	21.9	26.5	32.3	477.3	557.1	4506.0	4053.0	34
33.0	26.8	24.5	30.7	85.5	61.8	47.6	76.3	27.1	22.3	27.6	32.5	491.0	578.0	4506.0	4000.0	27
25.2	24.1	23.9	24.6	13.9	14.4	14.4	13.9	27.7	25.1	27.3	29.4	501.0	565.0	1915.0	1770.0	-50
25.2	24.2	23.9	24.6	14.0	14.5	14.5	14.0	26.7	23.1	26.0	29.2	496.0	552.0	1936.0	1751.0	-25
25.2	24.1	23.8	24.6	14.0	14.6	14.5	13.9	27.1	23.1	27.0	31.2	500.0	532.0	1925.0	1660.0	0
25.2	24.1	23.8	24.6	13.9	14.4	14.4	13.8	27.5	22.8	27.1	32.5	501.0	545.0	1945.0	1760.0	25
25.2	24.1	23.8	24.6	13.9	14.4	14.4	13.9	27.4	21.4	27.5	32.5	500.0	528.0	1887.0	1612.0	50
20.8	22.6	22.4	21.8	9.2	8.0	8.0	8.2	39.4	33.6	39.7	47.1	491.0	500.0	1690.0	1410.0	32
20.7	22.5	22.4	21.8	9.2	8.0	8.1	8.2	34.4	29.2	35.1	41.2	488.0	508.0	1680.0	1375.0	36
20.7	22.5	22.3	21.8	9.2	8.0	8.0	8.2	20.2	16.1	20.2	25.0	502.0	531.0	1695.0	1395.0	35
22.4	22.3	21.7	21.6	9.2	8.0	8.0	8.2	14.5	9.9	14.9	19.8	471.0	546.0	2050.0	1690.0	34
11.8	18.2	24.2	16.4	46.0	29.2	20.0	36.0	26.7	22.2	26.9	31.6	501.0	542.0	2100.0	1947.0	38
31.8	26.8	24.5	30.7	44.0	34.1	20.0	35.0	27.1	22.5	27.3	32.2	509.0	539.0	2108.0	1928.0	32
9.7	19.2	25.1	31.9	47.0	28.7	30.0	34.9	26.7	22.2	26.9	31.6	511.0	549.0	2135.0	1830.0	38
31.9	26.8	24.5	30.7	45.0	33.5	30.0	40.9	27.1	22.5	27.3	32.2	503.0	543.0	2112.0	1695.0	30

	Room operating conditions test		Effect of return air humidity		Effect of pressure difference (Ps_{supply}-P_{return})
	Effect of outdoor air temperature		Effect of outdoor air humidity		Effect of mass flow rate/face velocity

Table A.2. Temperature, humidity, flow rate, pressure difference (between supply and return side) and concentration data for sulfur hexafluoride tests in molecular sieve coated energy wheel.

Temperature (°C)				Relative humidity (%)				Mass flow rate (g/s)				Concentration (ppm)				Pressure (Pa)
OA	SA	RA	EA	OA	SA	RA	EA	OA	SA	RA	EA	OA	SA	RA	EA	Ps-Pr
25.0	26.1	26.0	25.5	35.0	35.0	35.0	34.0	27.6	23.1	26.3	30.2	0.0	0.4	24.8	20.7	32
-23.3	15.2	21.5	-7.9	24.7	54.0	46.2	77.9	30.1	24.3	27.1	32.1	0.0	0.3	29.5	21.5	29
-19.2	15.0	21.1	-5.5	22.5	51.8	45.8	66.3	30.7	24.7	27.1	33.1	0.0	0.6	24.0	20.0	21
-9.2	19.4	23.3	2.6	44.1	46.7	46.2	57.4	29.2	23.5	27.4	33.2	0.0	0.4	27.5	20.8	38
-7.8	16.7	20.0	1.9	25.6	41.6	43.0	43.1	0.0	0.0	0.0	0.0	0.0	0.4	29.1	23.1	30
23.8	24.4	24.9	23.8	49.4	33.2	29.1	41.1	27.3	22.1	27.6	32.5	0.0	0.5	27.8	22.5	34
31.3	25.7	24.1	29.0	47.4	48.6	50.8	45.0	26.0	21.7	27.5	32.3	0.0	0.2	22.5	21.0	32
32.2	26.1	24.5	29.7	56.4	56.0	49.0	58.2	26.6	21.8	27.3	33.3	0.0	0.8	25.1	17.6	31
32.0	26.8	24.5	30.7	73.6	54.8	47.3	62.1	26.3	21.9	26.5	31.4	0.0	0.9	53.1	37.5	35
34.0	26.2	24.1	30.6	80.8	65.1	49.0	81.1	26.9	21.9	26.5	32.3	0.0	1.0	32.5	--	34
33.0	26.8	24.5	30.7	85.5	61.8	47.6	76.3	27.1	22.3	27.6	32.5	0.0	1.6	53.2	--	27
25.2	24.1	23.9	24.6	13.9	14.4	14.4	13.9	27.7	25.1	27.3	29.4	0.0	1.9	33.8	28.9	-70
25.2	24.2	23.9	24.6	14.0	14.5	14.5	14.0	26.7	23.1	26.0	29.2	0.0	1.7	33.9	27.5	-65
25.2	24.1	23.8	24.6	14.0	14.6	14.5	13.9	27.1	23.1	27.0	31.2	0.0	1.7	32.1	24.9	-15
25.2	24.1	23.8	24.6	13.9	14.4	14.4	13.8	27.5	22.8	27.1	32.5	0.0	1.2	39.2	30.9	25
25.2	24.1	23.8	24.6	13.9	14.4	14.4	13.9	26.9	22.2	27.1	33.2	0.0	1.0	33.1	25.5	55
26.9	24.6	24.5	25.3	11.0	12.1	12.1	11.3	39.2	33.3	40.5	47.2	0.0	0.5	20.1	18.2	32
20.7	22.5	22.4	21.8	9.2	8.0	8.1	8.2	34.4	29.2	35.1	41.2	0.0	0.5	27.4	22.2	36
20.7	22.5	22.3	21.8	9.2	8.0	8.0	8.2	20.2	16.1	20.2	25.0	0.0	1.0	27.8	20.0	35
21.7	22.5	21.8	22.6	14.1	13.5	13.9	13.2	13.1	8.6	13.4	18.4	0.0	3.0	47.5	39.1	34
11.8	18.2	24.2	16.4	46.0	29.2	20.0	36.0	26.7	22.2	26.9	31.6	0.0	0.8	27.8	25.0	38
31.8	26.8	24.5	30.7	44.0	34.1	20.0	35.0	27.1	22.5	27.3	32.2	0.0	0.9	27.4	24.2	32
9.7	19.2	25.1	31.9	47.0	28.7	30.0	34.9	26.7	22.2	26.9	31.6	0.0	0.7	29.2	22.8	38
31.9	26.8	24.5	30.7	45.0	33.5	30.0	40.9	27.1	22.5	27.3	32.2	0.0	0.8	28.6	21.1	30

Table A.3. Temperature, humidity, flow rate, pressure difference (between supply and return side) and concentration data for isopropanol tests in molecular sieve coated energy wheel.

Temperature (°C)				Relative humidity (%)				Mass flow rate (g/s)				Concentration (ppm)				Pressure (Pa)
OA	SA	RA	EA	OA	SA	RA	EA	OA	SA	RA	EA	OA	SA	RA	EA	P_s-P_r
24.8*	25.9	26.2	25.3	36.0	37.9	38.6	37.1	27.2	23.0	26.8	30.9	0.0	6.4	21.2	17.6	32
-22.7	15.3	21.3	-7.4	24.6	53.8	47.3	66.7	30.2	24.3	26.9	33.2	0.0	8.0	22.0	14.9	29
-17.5	14.8	23.9	-4.1	29.0	55.1	48.2	67.5	30.1	24.1	26.9	32.1	0.0	7.898	24.3	13.7	21
-8.0	20.4	24.1	3.2	49.2	51.2	50.5	59.5	29.7	23.9	28.4	34.1	0.0	5.788	21.2	14.9	38
-5.8	18.0	21.5	2.3	22.3	39.8	44.0	45.1	29.5	25.1	29.8	35.4	0.0	5.802	21.2	13.5	30
24.1	24.6	25.1	23.9	50.0	33.0	32.0	43.1	27.9	22.7	27.8	33.2	0.0	6.199	21.8	14.1	34
31.3	25.7	24.1	29.0	47.4	48.6	50.8	45.0	26.0	21.7	27.5	32.3	0.0	5.979	21.9	16.5	32
32.6	26.7	24.5	29.9	53.5	54.2	46.0	56.5	26.9	22.2	27.3	33.4	0.0	9.300	34.5	19.3	31
32.0	26.8	24.5	30.7	73.6	54.8	47.3	62.1	26.3	21.9	26.5	31.4	0.0	10.90	28.6	17.6	35
34.0	26.2	24.1	30.6	80.8	65.1	49.0	81.1	26.9	21.9	26.5	32.3	0.0	10.9	35.9	--	34
33.0	26.8	24.5	30.7	85.5	61.8	47.6	76.3	27.1	22.3	27.6	32.5	0.0	12.1	36.9	--	27
25.2*	24.1	23.9	24.6	13.9	14.4	14.4	13.9	27.7	25.1	27.3	29.4	0.0	12.2	31.0	14.2	-52
25.2	24.2	23.9	24.6	14.0	14.5	14.5	14.0	26.7	23.1	26.0	29.2	0.0	12.1	33.2	14.3	-28
25.2	24.1	23.8	24.6	14.0	14.6	14.5	13.9	27.1	23.1	27.0	31.2	0.0	11.5	32.2	15.8	2
25.2	24.1	23.8	24.6	13.9	14.4	14.4	13.8	27.5	22.8	27.1	32.5	0.0	10.3	30.8	14.1	26
25.2	24.1	23.8	24.6	13.9	14.4	14.4	13.9	26.9	22.2	27.1	33.2	0.0	6.7	21.9	11.5	52
28.1	26.4	26.4	26.7	7.4	7.8	7.8	7.5	39.3	33.6	39.9	46.8	0.0	9.5	31.5	17.6	45
25.3	24.6	24.7	24.7	8.3	8.3	8.2	8.1	34.5	29.4	35.0	41.0	0.0	4.9	13.8	8.2	50
24.6	25.5	25.3	25.0	15.8	14.6	14.5	15.0	20.9	16.1	20.4	25.2	0.0	14.8	34.3	15.5	48
23.5	24.9	24.8	24.5	11.3	10.3	10.4	10.5	14.6	8.3	12.6	19.1	0.0	19.1	32.2	12.4	34
10.5	17.8	25.1	17.1	51.0	36.0	19.0	38.0	25.7	21.5	26.8	31.3	0.0	10.9	35.5	20.1	38
30.8*	25.5	24.9	30.4	47.0	36.0	21.0	37.0	26.5	22.2	27.1	32.2	0.0	10.5	34.5	16.5	32
10.0	19.9	25.2	30.9	49.0	28.8	21.1	35.6	25.5	21.6	25.4	30.5	0.0	11.2	39.3	21.5	38
31.1	26.2	24.8	31.5	47.0	36.5	29.5	40.5	26.8	23.5	26.9	31.9	0.0	9.9	32.2	18.1	30

Table A.4. Temperature, humidity, flow rate, pressure difference (between supply and return side) and concentration data for methanol tests in molecular sieve coated energy wheel.

Temperature (°C)				Relative humidity (%)				Mass flow rate (g/s)				Concentration (ppm)				Pressure (Pa)
OA	SA	RA	EA	OA	SA	RA	EA	OA	SA	RA	EA	OA	SA	RA	EA	Ps-Pr
24.8	25.9	26.2	25.3	36.0	37.9	38.6	37.1	27.2	23.0	26.8	30.9	0.0	18.8	46	21.2	32
-22.7	15.3	21.3	-7.4	24.6	53.8	47.3	66.7	30.2	24.3	26.9	33.2	0.0	16.0	31.5	12.5	29
-17.5	14.8	23.9	-4.1	29.0	55.1	48.2	67.5	30.1	24.1	26.9	32.1	0.0	13.5	30.6	13.2	21
-8.0	20.4	24.1	3.2	49.2	51.2	50.5	59.5	29.7	23.9	28.4	34.1	0.0	12.2	27	16.2	38
-5.8*	18.0	21.5	2.3	22.3	39.8	44.0	45.1	29.5	25.1	29.8	35.4	0.0	15.0	35.32	12.5	30
24.1	24.6	25.1	23.9	50.0	33.0	32.0	43.1	27.9	22.7	27.8	33.2	0.0	13.5	34.4	14.9	34
30.7	25.3	23.4	29.2	42.9	44.2	43.0	43.3	26.7	21.9	25.5	30.5	0.0	15.4	34.7	16.2	32
32.6	26.7	24.5	29.9	53.5	54.2	46.0	56.5	26.9	22.2	27.3	33.4	0.0	22.5	48.5	21.2	34
32.0	26.8	24.5	30.7	73.6	54.8	47.3	62.1	26.3	21.9	26.5	31.4	0.0	21.4	44.5	18.5	36
34.0	26.2	24.1	30.6	80.8	65.1	49.0	81.1	26.9	21.9	26.5	32.3	0.0	22.1	46.9	--	32
33.0	26.8	24.5	30.7	85.5	61.8	47.6	76.3	27.1	22.3	27.6	32.5	0.0	22.4	47.2	--	39
25.2	24.1	23.9	24.6	13.9	14.4	14.4	13.9	27.7	25.1	27.3	29.4	0.0	12.2	31.0	14.2	-52
25.2*	24.2	23.9	24.6	14.0	14.5	14.5	14.0	26.7	23.1	26.0	29.2	0.0	12.1	33.2	14.3	-28
25.2	24.1	23.8	24.6	14.0	14.6	14.5	13.9	27.1	23.1	27.0	31.2	0.0	11.5	32.2	15.8	1
25.2	24.1	23.8	24.6	13.9	14.4	14.4	13.8	27.5	22.8	27.1	32.5	0.0	10.3	30.8	14.1	26
25.2	24.1	23.8	24.6	13.9	14.4	14.4	13.9	26.9	22.2	27.1	33.2	0.0	6.7	21.9	11.5	52
28.1	26.4	26.4	26.7	7.4	7.8	7.8	7.5	39.3	33.6	39.9	46.8	0.0	13.3	31.5	14.4	45
25.3*	24.6	24.7	24.7	8.3	8.3	8.2	8.1	34.5	29.4	35.0	41.0	0.0	17.5	39.4	14.5	50
24.6	25.5	25.3	25.0	15.8	14.6	14.5	15.0	20.9	16.1	20.4	25.2	0.0	31.3	48.8	16.8	48
23.5	24.9	24.8	24.5	11.3	10.3	10.4	10.5	14.6	8.3	12.6	19.1	0.0	46.4	56.5	22.1	34
10.5	17.8	25.1	17.1	51.0	36.0	19.0	38.0	25.7	21.5	26.8	31.3	0.0	18.2	44.2	21.1	38
30.8	25.5	24.9	30.4	47.0	36.0	21.0	37.0	26.5	22.2	27.1	32.2	0.0	19.8	43.9	22.2	32
10.0	19.9	25.2	30.9	49.0	28.8	21.1	35.6	25.5	21.6	25.4	30.5	0.0	19.6	42.5	17.4	38
31.1	26.2	24.8	31.5	47.0	36.5	29.5	40.5	26.8	23.5	26.9	31.9	0.0	21.4	46.1	16.5	30

Table A.5. Temperature, humidity, flow rate, pressure difference (between supply and return side) and concentration data for n-hexane tests in molecular sieve coated energy wheel.

Temperature (°C)				Relative humidity (%)				Mass flow rate (g/s)				Concentration (ppm)				Pressure (Pa)
OA	SA	RA	EA	OA	SA	RA	EA	OA	SA	RA	EA	OA	SA	RA	EA	Ps-Pr
24.8	25.9	26.2	25.3	36.0	37.9	38.6	37.1	27.2	23.0	26.8	30.9	0.0	0.8	12.2	8.9	32
-22.7	15.3	21.3	-7.4	24.6	53.8	47.3	66.7	30.2	24.3	26.9	33.2	0.0	0.9	12.6	10.3	29
-17.5	14.8	23.9	-4.1	29.0	55.1	48.2	67.5	30.1	24.1	26.9	32.1	0.0	0.6	11.9	10.8	21
-8.0*	20.4	24.1	3.2	49.2	51.2	50.5	59.5	29.7	23.9	28.4	34.1	0.0	0.9	16.5	15.5	38
-5.8	18.0	21.5	2.3	22.3	39.8	44.0	45.1	29.5	25.1	29.8	35.4	0.0	1.2	21.2	18.2	30
24.1	24.6	25.1	23.9	50.0	33.0	32.0	43.1	27.9	22.7	27.8	33.2	0.0	1.2	20.5	13.2	34
30.7	25.3	23.4	29.2	42.9	44.2	43.0	43.3	26.7	21.9	25.5	30.5	0.0	2.1	34.7	25.3	32
32.6	26.7	24.5	29.9	53.5	54.2	46.0	56.5	26.9	22.2	27.3	33.4	0.0	0.6	19.5	13.2	34
32.0	26.8	24.5	30.7	73.6	54.8	47.3	62.1	26.3	21.9	26.5	31.4	0.0	1.0	18.3	12.7	36
34.0	26.2	24.1	30.6	80.8	65.1	49.0	81.1	26.9	21.9	26.5	32.3	0.0	1.1	18.2	--	32
33.0	26.8	24.5	30.7	85.5	61.8	47.6	76.3	27.1	22.3	27.6	32.5	0.0	0.8	19.5	--	39
25.2	24.1	23.9	24.6	13.9	14.4	14.4	13.9	27.7	25.1	27.3	29.4	0.0	1.6	15.5	13.9	-50
25.2	24.2	23.9	24.6	14.0	14.5	14.5	14.0	26.7	23.1	26.0	29.2	0.0	1.3	16.9	14.7	-15
25.2	24.1	23.8	24.6	14.0	14.6	14.5	13.9	27.1	23.1	27.0	31.2	0.0	1.4	17.5	12.5	0
25.2	24.1	23.8	24.6	13.9	14.4	14.4	13.8	27.5	22.8	27.1	32.5	0.0	1.3	14.8	13.5	25
25.2	24.1	23.8	24.6	13.9	14.4	14.4	13.9	26.9	22.2	27.1	33.2	0.0	0.7	8.5	7.1	50
26.1	24.4	24.5	24.6	10.8	11.5	11.4	11.1	39.0	32.8	38.3	45.4	0.0	0.5	15.2	13.2	54
24.4	23.6	23.6	23.7	11.6	11.8	11.7	11.5	33.5	28.2	33.4	39.2	0.0	0.9	18.5	16.5	50
21.9	22.7	22.5	22.2	13.2	12.3	12.3	12.5	21.4	16.5	21.2	26.3	0.0	1.9	17.9	15.6	41
21.5*	22.8	22.7	22.3	13.3	12.1	12.1	12.4	13.8	6.8	13.6	19.8	0.0	2.7	21.2	18.5	34
10.5	17.8	25.1	17.1	51.0	36.0	19.0	38.0	25.7	21.5	26.8	31.3	0.0	1.1	17.5	12.4	38
30.8	25.5	24.9	30.4	47.0	36.0	21.0	37.0	26.5	22.2	27.1	32.2	0.0	1.2	18.2	11.9	32
10.0	19.9	25.2	30.9	49.0	28.8	21.1	35.6	25.5	21.6	25.4	30.5	0.0	1.3	19.2	13.3	38
31.1	26.2	24.8	31.5	47.0	36.5	29.5	40.5	26.8	23.5	26.9	31.9	0.0	1.1	17.3	12.6	30

Table A.6. Temperature, humidity, flow rate, pressure difference (between supply and return side) and concentration data for p-xylene tests in molecular sieve coated energy wheel.

Temperature (°C)				Relative humidity (%)				Mass flow rate (g/s)				Concentration (ppm)				Pressure (Pa)
OA	SA	RA	EA	OA	SA	RA	EA	OA	SA	RA	EA	OA	SA	RA	EA	Ps-Pr
23.9	23.8	24.3	24.1	37.2	36.9	38.1	38.2	29.9	25.9	29.6	34.3	0.0	3.8	14.6	8.3	32
-23.3	15.3	21.5	-7.9	25.1	53.9	46.0	78.5	30.3	24.3	26.8	33.3	0.0	3.7	12.9	6.8	35
-17.8	16.6	21.6	-3.5	26.0	45.5	45.4	52.7	30.2	24.5	26.8	33.1	0.0	2.7	9.6	5.3	31
-12.4	19.3	22.9	1.4	24.3	37.9	44.1	41.1	30.0	24.3	26.7	32.3	0.0	3.1	10.7	5.2	29
-5.3	21.1	25.7	7.1	19.7	22.7	23.5	22.2	29.6	24.2	26.4	32.1	0.0	4.4	14.2	7.6	36
24.1*	24.6	25.1	23.9	50.0	33.0	32.0	43.1	27.9	22.7	27.8	33.2	0.0	4.0	12.5	5.3	31
30.7	25.3	23.4	29.2	42.9	44.2	43.0	43.3	26.7	21.9	25.5	30.5	0.0	2.8	10.8	6.9	39
32.6	26.7	24.5	29.9	53.5	54.2	46.0	56.5	26.9	22.2	27.3	33.4	0.0	3.6	14.8	7.1	34
32.0	26.8	24.5	30.7	60.0	54.8	47.3	62.1	26.3	21.9	26.5	31.4	0.0	5.0	16.2	7.4	36
34.0	26.2	24.1	30.6	71.2	65.1	49.0	81.1	26.9	21.9	26.5	32.3	0.0	4.9	15.1	--	32
33.0	26.8	24.5	30.7	85.5	61.8	47.6	76.3	27.1	22.3	27.6	32.5	0.0	4.0	11.2	--	35
24.0	24.0	24.0	23.9	15.8	15.7	15.3	15.5	26.7	25.2	27.2	28.6	0.0	4.8	15.5	8.2	-50
24.0	24.0	24.0	23.9	15.8	15.7	15.3	15.5	26.6	24.6	27.3	30.1	0.0	4.4	16.9	9.1	-27
24.0*	24.0	24.0	23.9	15.8	15.7	15.3	15.5	27.1	23.9	26.9	30.8	0.0	4.7	17.5	8.4	-10
24.0	24.0	24.0	23.9	15.8	15.7	15.3	15.5	27.0	24.2	26.7	30.9	0.0	3.8	14.8	7.2	23
24.0	24.0	24.0	23.9	15.8	15.7	15.3	15.5	26.8	20.8	25.7	31.3	0.0	2.1	8.5	4.3	52
25.0	24.3	24.4	24.3	17.2	16.0	15.3	16.5	38.5	33.6	39.1	45.6	0.0	1.7	9.1	6.2	45
23.9	23.8	23.7	23.6	14.3	14.1	14.0	14.0	32.3	25.3	32.2	39.3	0.0	2.0	9.8	5.3	50
21.7	23.0	22.9	22.2	16.4	15.0	14.9	15.5	20.6	15.7	20.3	25.2	0.0	6.3	17.9	8.2	48
21.1*	22.1	22.5	21.5	17.2	16.1	15.3	16.5	14.5	9.3	15.3	20.0	0.0	14.2	26.2	9.6	34
10.4	18.1	24.8	17.0	50.0	37.0	21.0	38.0	25.7	21.5	26.8	31.3	0.0	3.7	14.8	8.2	21
30.1	24.9	25.2	29.7	49.1	36.9	20.0	36.5	26.5	22.2	27.1	32.2	0.0	3.1	12.6	6.9	29
9.8*	20.1	25.5	15.6	52.0	31.1	20.8	35.5	25.5	21.6	25.4	30.5	0.0	3.5	13.9	6.5	28
32.2	26.7	24.8	31.5	48.0	327.0	30.2	41.1	26.8	23.5	26.9	31.9	0.0	3.6	14.5	8.2	34

Table A.7. Temperature, humidity, flow rate, pressure difference (between supply and return side) and concentration data for methyl isobutyl ketone (MIBK) tests in molecular sieve coated energy wheel.

Temperature (°C)				Relative humidity (%)				Mass flow rate (g/s)				Concentration (ppm)				Pressure (Pa)
OA	SA	RA	EA	OA	SA	RA	EA	OA	SA	RA	EA	OA	SA	RA	EA	Ps-Pr
23.9	23.8	24.3	24.1	37.2	36.9	38.1	38.2	29.9	25.9	29.6	34.3	0.0	3.9	15.3	9.2	32
-23.3	15.3	21.5	-7.9	25.1	53.9	46.0	78.5	30.3	24.3	26.8	33.3	0.0	3.8	10.4	7.2	35
-17.8	16.6	21.6	-3.5	26.0	45.5	45.4	52.7	30.2	24.5	26.8	33.1	0.0	3.5	9.9	6.2	31
-12.4	19.3	22.9	1.4	24.3	37.9	44.1	41.1	30.0	24.3	26.7	32.3	0.0	3.3	10.2	7.2	29
-5.3	21.1	25.7	7.1	19.7	22.7	23.5	22.2	29.6	24.2	26.4	32.1	0.0	3.6	10.8	6.8	36
24.1	24.6	25.1	23.9	50.0	33.0	32.0	43.1	27.9	22.7	27.8	33.2	0.0	4.8	14.2	10.1	31
30.7	25.3	23.4	29.2	42.9	44.2	43.0	43.3	26.7	21.9	25.5	30.5	0.0	5.1	15.4	7.5	39
32.6*	26.7	24.5	29.9	53.5	54.2	46.0	56.5	26.9	22.2	27.3	33.4	0.0	5.2	15.8	6.5	34
32.0	26.8	24.5	30.7	60.0	54.8	47.3	62.1	26.3	21.9	26.5	31.4	0.0	6.5	17.5	8.2	36
34.0	26.2	24.1	30.6	71.2	65.1	49.0	81.1	26.9	21.9	26.5	32.3	0.0	5.5	14.7	--	32
33.0	26.8	24.5	30.7	85.5	61.8	47.6	76.3	27.1	22.3	27.6	32.5	0.0	6.0	15.1	--	35
24.0	24.0	24.0	23.9	15.8	15.7	15.3	15.5	26.7	25.2	27.2	28.6	0.0	4.8	15.5	9.1	-50
24.0*	24.0	24.0	23.9	15.8	15.7	15.3	15.5	26.6	24.6	27.3	30.1	0.0	4.4	16.9	8.6	-27
24.0	24.0	24.0	23.9	15.8	15.7	15.3	15.5	27.1	23.9	26.9	30.8	0.0	4.7	17.5	12.2	-10
24.0	24.0	24.0	23.9	15.8	15.7	15.3	15.5	27.0	24.2	26.7	30.9	0.0	3.8	14.8	7.2	23
24.0	24.0	24.0	23.9	15.8	15.7	15.3	15.5	26.8	20.8	25.7	31.3	0.0	2.1	8.5	5.1	52
28.1	26.4	26.4	26.7	7.4	7.8	7.8	7.5	39.3	33.6	39.9	46.8	0.0	3.1	10.1	5.1	45
25.3	24.6	24.7	24.7	8.3	8.3	8.2	8.1	34.5	29.4	35.0	41.0	0.0	4.1	12.9	7.2	50
24.6	25.5	25.3	25.0	15.8	14.6	14.5	15.0	20.9	16.1	20.4	25.2	0.0	6.8	14.2	5.5	48
23.5	24.9	24.8	24.5	11.3	10.3	10.4	10.5	14.6	8.3	12.6	19.1	0.0	9.7	16.6	7.1	34
10.4	18.1	24.8	17.0	50.0	37.0	21.0	38.0	25.7	21.5	26.8	31.3	0.0	6.0	17.2	8.1	21
30.1	24.9	25.2	29.7	49.1	36.9	30.0	36.5	26.5	22.2	27.1	32.2	0.0	5.8	16.9	11.1	29
9.8	20.1	25.5	15.6	52.0	31.1	20.8	35.5	25.5	21.6	25.4	30.5	0.0	4.9	15.3	9.6	28
32.2	26.7	24.8	31.5	48.0	327.0	30.2	41.1	26.8	23.5	26.9	31.9	0.0	5.4	16.4	7.1	34

Table A.8. Temperature, humidity, flow rate, pressure difference (between supply and return side) and concentration data for phenol tests in molecular sieve coated energy wheel.

Temperature (°C)				Relative humidity (%)				Mass flow rate (g/s)				Concentration (ppm)				Pressure (Pa)
OA	SA	RA	EA	OA	SA	RA	EA	OA	SA	RA	EA	OA	SA	RA	EA	Ps-Pr
23.9*	23.8	24.3	24.1	37.2	36.9	38.1	38.2	29.9	25.9	29.6	34.3	0.0	6.2	19.5	8.3	32
-23.3	15.3	21.5	-7.9	25.1	53.9	46.0	78.5	30.3	24.3	26.8	33.3	0.0	3.8	10.5	4.2	35
-17.8	16.6	21.6	-3.5	26.0	45.5	45.4	52.7	30.2	24.5	26.8	33.1	0.0	5.6	20.1	9.1	31
-12.4	19.3	22.9	1.4	24.3	37.9	44.1	41.1	30.0	24.3	26.7	32.3	0.0	7.2	20.8	8.9	29
-5.3	21.1	25.7	7.1	19.7	22.7	23.5	22.2	29.6	24.2	26.4	32.1	0.0	6.6	21.2	8.9	36
24.1	24.6	25.1	23.9	50.0	33.0	32.0	43.1	27.9	22.7	27.8	33.2	0.0	7.2	22.5	12.5	31
31.3*	25.7	24.1	29.0	47.4	48.6	50.8	45.0	26.0	21.7	27.5	32.3	0.0	6.4	21.8	10.4	39
32.6	26.7	24.5	29.9	53.5	54.2	46.0	56.5	26.9	22.2	27.3	33.4	0.0	6.0	20.2	9.2	34
32.0	26.8	24.5	30.7	60.0	54.8	47.3	62.1	26.3	21.9	26.5	31.4	0.0	4.0	16.2	8.5	36
34.0	26.2	24.1	30.6	71.2	65.1	49.0	81.1	26.9	21.9	26.5	32.3	0.0	5.8	21.2	--	32
33.0	26.8	24.5	30.7	85.5	61.8	47.6	76.3	27.1	22.3	27.6	32.5	0.0	7.7	22.5	--	35.3
24.0	24.0	24.0	23.9	15.8	15.7	15.3	15.5	26.7	25.2	27.2	28.6	0.0	7.4	18.6	7.6	-50
24.0	24.0	24.0	23.9	15.8	15.7	15.3	15.5	26.6	24.6	27.3	30.1	0.0	6.3	17.9	8.1	-27
24.0	24.0	24.0	23.9	15.8	15.7	15.3	15.5	27.1	23.9	26.9	30.8	0.0	6.6	19.2	8.7	-10
24.0	24.0	24.0	23.9	15.8	15.7	15.3	15.5	27.0	24.2	26.7	30.9	0.0	7.1	21.6	10.1	23
24.0	24.0	24.0	23.9	15.8	15.7	15.3	15.5	26.8	20.8	25.7	31.3	0.0	6.3	19.8	9.8	52
25.0*	24.3	24.4	24.3	17.2	16.0	15.3	16.5	38.5	33.6	39.1	45.6	0.0	3.1	9.8	5.6	45
23.9	23.8	23.7	23.6	14.3	14.1	14.0	14.0	32.3	25.3	32.2	39.3	0.0	5	15.3	7.5	50
21.7	23.0	22.9	22.2	16.4	15.0	14.9	15.5	20.6	15.7	20.3	25.2	0.0	10	18.2	5.6	48
21.1	22.1	22.5	21.5	17.2	16.1	15.3	16.5	14.5	9.3	15.3	20.0	0.0	10.1	13.1	2.2	34
10.4	18.1	24.8	17.0	50.0	37.0	21.0	38.0	25.7	21.5	26.8	31.3	0.0	9.0	26.6	12.1	21
30.1	24.9	25.2	29.7	49.1	36.9	30.0	36.5	26.5	22.2	27.1	32.2	0.0	9.5	29.2	13.5	29
9.8	20.1	25.5	15.6	52.0	31.1	20.8	35.5	25.5	21.6	25.4	30.5	0.0	6.0	19.2	9.2	28
32.2	26.7	24.8	31.5	48.0	327.0	30.2	41.1	26.8	23.5	26.9	31.9	0.0	6.9	21.2	10.3	34

Table A.9. Temperature, humidity, flow rate, pressure difference (between supply and return side) and concentration data for acetic acid tests in molecular sieve coated energy wheel.

Temperature (°C)				Relative humidity (%)				Mass flow rate (g/s)				Concentration (ppm)				Pressure (Pa)
OA	SA	RA	EA	OA	SA	RA	EA	OA	SA	RA	EA	OA	SA	RA	EA	Ps-Pr
24.6	25.8	25.9	24.9	38	38.9	39.2	38.1	28.6	24.5	27.6	32.5	0.0	9.3	20.5	7.9	34
-21.2	15.6	21.4	-6.1	23.7	50.6	46.3	58.9	30.1	24.4	26.9	32.6	0.0	15.4	34.3	22.2	32
-16.6	17.0	21.7	-2.5	26.3	43.8	45.0	50.3	30.1	24.3	29.5	34.5	0.0	16.2	36.9	17.9	36
-13.6	18.6	22.5	0.3	25.3	39.0	43.2	43.9	29.1	22.9	26.9	32.6	0.0	14.8	31.5	12.5	39
-7.1	20.2	24.3	4.0	45.4	53.5	52.4	66.0	30.3	24.3	26.5	32.9	0.0	16.9	36.7	13.1	35
27.0	25.1	25.1	25.5	12.3	13.1	12.8	12.6	27.7	23.4	26.9	32.9	0.0	16.3	32.5	12.9	32
32.2	26.2	24.7	30.3	50.2	48.9	50.8	42.1	26.5	22.5	26.9	31.3	0.0	15.5	32.9	11.8	34
32.6	26.7	24.5	29.9	53.5	54.2	46.0	56.5	26.9	22.2	27.3	33.4	0.0	18.2	38.5	13.6	28
32.0	26.8	24.5	30.7	60.0	54.8	47.3	62.1	26.3	21.9	26.5	31.4	0.0	15.0	30.5	14.5	35
32.8	26.8	24.9	30.2	71.1	59.0	49.6	67.1	27.5	21.2	27.4	34.6	0.0	17.8	35.5	--	36
33.0	26.8	24.5	30.7	85.5	61.8	47.6	76.3	27.1	22.3	27.6	32.5	0.0	15.2	30.7	--	31
23.8	24.1	24.3	23.6	14.7	14.1	13.6	14.3	25.7	23.5	26.3	28.5	0.0	18.9	34.4	10.2	-75
24.0	24.4	24.4	24.0	14.7	14.1	13.6	14.3	26.2	22.8	25.5	28.7	0.0	19.9	35.5	11.1	-25
24.0	24.3	24.4	24.0	14.7	14.1	13.6	14.3	26.6	22.5	26.1	30.3	0.0	19.2	36.2	11.2	-10
24.1	24.5	24.5	24.0	14.7	14.1	13.6	14.3	26.8	22.1	26.9	32.4	0.0	14.5	31.5	11.8	25
24.1*	24.6	24.6	24.0	14.7	14.1	13.6	14.3	26.4	22.3	27.1	32.1	0.0	15.3	34.8	12.3	52
27.1	25.1	25.1	25.5	12.2	13.1	12.8	12.7	38.8	33.6	39.1	45.5	0.0	10.0	24.3	9.3	21
24.9	24.2	24.2	24.1	13.8	13.9	13.5	13.8	32.4	25.3	32.2	39.4	0.0	11.1	24.1	10.1	23
21.7	23.1	23.0	22.3	16.4	14.9	14.7	15.5	20.4	15.9	20.2	25.1	0.0	17.0	23.9	9.8	25
21.2	22.8	22.9	22.0	17.0	15.3	14.9	16.1	14.5	9.2	15.4	19.7	0.0	19.2	24.0	9.1	46
9.0	19.4	20.7	13.1	51.1	40.3	18.8	37.5	28.9	23.6	27.5	32.6	0.0	16.2	32.3	10.3	29
30.8	25.6	25.4	29.6	49.8	37.2	31.2	37.2	29.1	23.8	27.3	32.8	0.0	16.7	34.2	11.2	34
10.4	20.5	25.1	15.0	52.1	32.6	20.2	36.1	28.8	24.1	27.4	33.0	0.0	19.3	39.2	12.9	28
32.9	36.8	25.1	32.9	47.6	32.1	30.1	40.4	29.3	24.1	27.1	32.7	0.0	15.6	31.8	11.9	32

Table A.10. Temperature, humidity, flow rate, pressure difference (between supply and return side) and concentration data for ammonia tests in molecular sieve coated energy wheel.

Temperature (°C)				Relative humidity (%)				Mass flow rate (g/s)				Concentration (ppm)				Pressure (Pa)
OA	SA	RA	EA	OA	SA	RA	EA	OA	SA	RA	EA	OA	SA	RA	EA	Ps-Pr
24.6	25.8	25.9	24.9	38	38.9	39.2	38.1	28.6	24.5	27.6	32.5	0.0	36.1	50.2	7.9	34
-21.2	15.6	21.4	-6.1	23.7	50.6	46.3	58.9	30.1	24.4	26.9	32.6	0.0	14.8	21.5	8.2	32
-16.6	17.0	21.7	-2.5	26.3	43.8	45.0	50.3	30.1	24.3	29.5	34.5	0.0	15.0	22.0	7.9	36
-13.6	18.6	22.5	0.3	25.3	39.0	43.2	43.9	29.1	22.9	26.9	32.6	0.0	14.4	20.9	9.6	39
-7.1	20.2	24.3	4.0	45.4	53.5	52.4	66.0	30.3	24.3	26.5	32.9	0.0	12.1	18.9	6.7	35
27.0	25.1	25.1	25.5	12.3	13.1	12.8	12.6	27.7	23.4	26.9	32.9	0.0	13.6	20.0	5.4	32
32.2	26.2	24.7	30.3	50.2	48.9	50.8	42.1	26.5	22.5	26.9	31.3	0.0	14.3	22.0	5.5	34
32.6	26.7	24.5	29.9	53.5	54.2	46.0	56.5	26.9	22.2	27.3	33.4	0.0	12.3	19.2	6.3	28
32.0	26.8	24.5	30.7	60.0	54.8	47.3	62.1	26.3	21.9	26.5	31.4	0.0	16.5	24.3	5.2	35
32.8	26.8	24.9	30.2	71.1	59.0	49.6	67.1	27.5	21.2	27.4	34.6	0.0	14.5	22.0	--	36
33.0	26.8	24.5	30.7	85.5	61.8	47.6	76.3	27.1	22.3	27.6	32.5	0.0	15.3	21.5	--	31
23.8	24.1	24.3	23.6	15.3	14.9	14.4	15.0	25.7	23.5	26.3	28.5	0.0	17.4	22.3	8.5	-75
24.0	24.4	24.4	24.0	14.9	14.3	14.0	14.5	26.2	22.8	25.5	28.7	0.0	16.0	21.6	3.9	-25
24.0	24.3	24.4	24.0	14.8	14.2	13.8	14.3	26.6	22.5	26.1	30.3	0.0	16.3	22.9	5.4	0
24.1	24.5	24.5	24.0	14.6	14.0	13.8	14.2	26.8	22.1	26.9	32.4	0.0	14.9	22.3	6.9	25
24.1	24.6	24.6	24.0	14.7	14.0	13.7	14.3	26.4	22.3	27.1	32.1	0.0	12.7	18.4	5.8	52
27.1	25.1	25.1	25.5	12.2	13.1	12.8	12.7	38.8	33.6	39.1	45.5	0.0	9.6	19.2	11.2	21
24.9	24.2	24.2	24.1	13.8	13.9	13.5	13.8	32.4	25.3	32.2	39.4	0.0	12.5	21.6	8.5	23
21.7	23.1	23.0	22.3	16.4	14.9	14.7	15.5	20.4	15.9	20.2	25.1	0.0	18.2	24.2	5.4	25
21.2	22.8	22.9	22.0	17.0	15.3	14.9	16.1	14.5	9.2	15.4	19.7	0.0	27.5	30.6	7.1	46
9.0	19.4	20.7	13.1	51.1	40.3	18.8	37.5	28.9	23.6	27.5	32.6	0.0	14.2	21.2	5.9	29
30.8	25.6	25.4	29.6	49.8	37.2	31.2	37.2	29.1	23.8	27.3	32.8	0.0	16.7	23.4	3.9	34
10.4	20.5	25.1	15.0	52.1	32.6	20.2	36.1	28.8	24.1	27.4	33.0	0.0	16.3	23.6	5.4	28
32.9	36.8	25.1	32.9	47.6	32.1	30.1	40.4	29.3	24.1	27.1	32.7	0.0	16.1	22.4	5.8	32

Table A.11. Temperature, humidity, flow rate, pressure difference (between supply and return side) and concentration data for carbon dioxide tests in silica gel coated energy wheel.

Temperature (°C)				Relative humidity (%)				Mass flow rate (g/s)				Concentration (ppm)				Pressure (Pa)
OA	SA	RA	EA	OA	SA	RA	EA	OA	SA	RA	EA	OA	SA	RA	EA	Ps-Pr
22.4	25.7	26.6	23.4	24.1	19.8	18.5	24.2	27.3	23.8	26.9	29.7	466.6	702.2	3442.5	2840.6	58

Table A.12. Temperature, humidity, flow rate, pressure difference (between supply and return side) and concentration data for sulfur hexafluoride tests in silica gel coated energy wheel.

Temperature (°C)				Relative humidity (%)				Mass flow rate (g/s)				Concentration (ppm)				Pressure (Pa)
OA	SA	RA	EA	OA	SA	RA	EA	OA	SA	RA	EA	OA	SA	RA	EA	Ps-Pr
21.2	25.2	26.5	22.1	28.7	21.8	19.9	27.2	26.9	23.5	27.1	30.0	0.0	4.5	74.1	63.2	38

Table A.13. Temperature, humidity, flow rate, pressure difference (between supply and return side) and concentration data for n-hexane tests in silica gel coated energy wheel.

Temperature (°C)				Relative humidity (%)				Mass flow rate (g/s)				Concentration (ppm)				Pressure (Pa)
OA	SA	RA	EA	OA	SA	RA	EA	OA	SA	RA	EA	OA	SA	RA	EA	Ps-Pr
24.8	25.9	25.9	25.3	38.0	36.9	37.6	37.4	27.6	23.1	26.3	30.2	0.0	4.1	13.21	7.5	42

Table A.14. Temperature, humidity, flow rate, pressure difference (between supply and return side) and concentration data for acetaldehyde tests in silica gel coated energy wheel.

Temperature (°C)				Relative humidity (%)				Mass flow rate (g/s)				Concentration (ppm)				Pressure (Pa)
OA	SA	RA	EA	OA	SA	RA	EA	OA	SA	RA	EA	OA	SA	RA	EA	Ps-Pr
25.0	25.8	26.9	24.7	20.0	18.9	17.3	22.1	27.7	23.9	26.7	29.9	0.0	5.5	7.61	3.0	39

Table A.15. Temperature, humidity, flow rate, pressure difference (between supply and return side) and concentration data for ammonia tests in silica gel coated energy wheel.

Temperature (°C)				Relative humidity (%)				Mass flow rate (g/s)				Concentration (ppm)				Pressure (Pa)
OA	SA	RA	EA	OA	SA	RA	EA	OA	SA	RA	EA	OA	SA	RA	EA	Ps-Pr
25.4*	25.6	25.8	25.1	16.9	17.5	17.4	19.3	27.5	23.9	27.6	30.6	0.0	3.6	14.4	1.2	40
25.4*	25.6	25.8	25.1	47.0	46.0	48.0	47.0	27.5	23.9	27.6	30.6	0.0	9.0	14.4	1.9	
25.4	25.6	25.8	25.1	47.0	46.0	48.0	47.0	27.5	23.9	27.6	30.6	0.0	11.3	14.4	2.2	
25.4	25.6	25.8	25.1	47.0	46.0	48.0	47.0	27.5	23.9	27.6	30.6	0.0	11.7	14.4	2.2	

Table A.16. Temperature, humidity, flow rate, pressure difference (between supply and return side) and concentration data for MIBK tests in silica gel coated energy wheel.

Temperature (°C)				Relative humidity (%)				Mass flow rate (g/s)				Concentration (ppm)				Pressure (Pa)
OA	SA	RA	EA	OA	SA	RA	EA	OA	SA	RA	EA	OA	SA	RA	EA	Ps-Pr
26.4*	24.2	24.1	25.1	12.5	12.5	12.5	14.2	27.2	23.7	27.2	30.4	0.0	3.1	50.4	5.8	61
26.4*	24.2	24.1	25.1	12.5	12.5	12.5	14.2	27.2	23.7	27.2	30.4	0.0	5.3	51.0	6.6	61
26.4*	24.2	24.1	25.1	12.5	12.5	12.5	14.2	27.2	23.7	27.2	30.4	0.0	6.2	51.0	6.6	61
26.4*	24.2	24.1	25.1	12.5	12.5	12.5	14.2	27.2	23.7	27.2	30.4	0.0	7.2	40.6	5.8	61
26.4*	24.2	24.1	25.1	12.5	12.5	12.5	14.2	27.2	23.7	27.2	30.4	0.0	8.2	40.6	6.3	61
26.4*	24.2	24.1	25.1	12.5	12.5	12.5	14.2	27.2	23.7	27.2	30.4	0.0	9.3	40.6	6.5	61

Table A.17. Temperature, humidity, flow rate, pressure difference (between supply and return side) and concentration data for phenol tests in silica gel coated energy wheel.

Temperature (°C)				Relative humidity (%)				Mass flow rate (g/s)				Concentration (ppm)				Pressure (Pa)
OA	SA	RA	EA	OA	SA	RA	EA	OA	SA	RA	EA	OA	SA	RA	EA	Ps-Pr
25.4*	24.8	25.0	24.8	13.0	14.9	14.6	15.9	26.8	23.6	26.9	30.2	0.0	1.4	16.2	1.8	48
25.4*	24.8	25.0	24.8	13.0	14.9	14.6	15.9	26.8	23.6	26.9	30.2	0.0	1.9	17.3	2.1	48

Table A.18. Temperature, humidity, flow rate, pressure difference (between supply and return side) and concentration data for isopropanol tests in silica gel coated energy wheel.

Temperature (°C)				Relative humidity (%)				Mass flow rate (g/s)				Concentration (ppm)				Pressure (Pa)
OA	SA	RA	EA	OA	SA	RA	EA	OA	SA	RA	EA	OA	SA	RA	EA	Ps-Pr
23.7*	26.0	27.0	24.3	18.5	15.6	14.4	19.2	27.2	24.1	27.4	29.8	0.0	5.2	65.3	3.0	40
23.7*	26.0	27.0	24.3	18.5	15.6	14.4	19.2	27.2	24.1	27.4	29.8	0.0	9.2	65.3	3.9	40
23.7*	26.0	27.0	24.3	18.5	15.6	14.4	19.2	27.2	24.1	27.4	29.8	0.0	12.1	65.3	5.1	40
23.7*	26.0	27.0	24.3	18.5	15.6	14.4	19.2	27.2	24.1	27.4	29.8	0.0	14.6	65.3	4.7	40
23.7*	26.0	27.0	24.3	18.5	15.6	14.4	19.2	27.2	24.1	27.4	29.8	0.0	16.3	65.3	5.2	40
23.7*	26.0	27.0	24.3	18.5	15.6	14.4	19.2	27.2	24.1	27.4	29.8	0.0	17.5	65.3	6.2	40
23.7*	26.0	27.0	24.3	18.5	15.6	14.4	19.2	27.2	24.1	27.4	29.8	0.0	18.1	65.3	6.8	40
23.7*	26.0	27.0	24.3	18.5	15.6	14.4	19.2	27.2	24.1	27.4	29.8	0.0	21.5	65.3	7.2	40
23.7*	26.0	27.0	24.3	18.5	15.6	14.4	19.2	27.2	24.1	27.4	29.8	0.0	28.0	65.3	8.4	40
23.7*	26.0	27.0	24.3	18.5	15.6	14.4	19.2	27.2	24.1	27.4	29.8	0.0	28.2	65.3	9.0	40
23.7*	26.0	27.0	24.3	18.5	15.6	14.4	19.2	27.2	24.1	27.4	29.8	0.0	27.4	65.3	9.0	40

Table A.19. Temperature, humidity, flow rate, pressure difference (between supply and return side) and concentration data for methanol tests in silica gel coated energy wheel.

Temperature (°C)				Relative humidity (%)				Mass flow rate (g/s)				Concentration (ppm)				Pressure (Pa)
OA	SA	RA	EA	OA	SA	RA	EA	OA	SA	RA	EA	OA	SA	RA	EA	Ps-Pr
22.4*	25.7	26.6	23.4	24.1	19.8	18.5	24.2	27.3	23.8	26.9	29.7	0.0	17.8	36.8	1.3	50
22.4*	25.7	26.6	23.4	24.1	19.8	18.5	24.2	27.3	23.8	26.9	29.7	0.0	23.6	36.8	3.8	50
22.4*	25.7	26.6	23.4	24.1	19.8	18.5	24.2	27.3	23.8	26.9	29.7	0.0	25.8	36.8	4.5	50
22.4	25.7	26.6	23.4	24.1	19.8	18.5	24.2	27.3	23.8	26.9	29.7	0.0	29.1	36.8	5.5	50
22.4	25.7	26.6	23.4	24.1	19.8	18.5	24.2	27.3	23.8	26.9	29.7	0.0	28.9	36.8	5.5	50
22.4	25.7	26.6	23.4	24.1	19.8	18.5	24.2	27.3	23.8	26.9	29.7	0.0	34.2	46.6	9.3	50
22.4	25.7	26.6	23.4	24.1	19.8	18.5	24.2	27.3	23.8	26.9	29.7	0.0	34.0	46.6	9.3	50
22.4	25.7	26.6	23.4	24.1	19.8	18.5	24.2	27.3	23.8	26.9	29.7	0.0	35.5	46.6	9.8	50
19.9	26.8	28.6	22.6	48.6	26.7	12.6	37.3	19.9	26.8	28.6	22.6	0.0	39.9	50.1	15.1	61
20.1	24.5	25.5	21.8	47.1	46.2	45.5	46.9	28.3	22.5	27.2	31.6	0.0	34.1	43.9	13.2	61

Table A.20. Temperature, humidity, flow rate, pressure difference (between supply and return side) and concentration data for p-xylene tests in silica gel coated energy wheel.

Temperature (°C)				Relative humidity (%)				Mass flow rate (g/s)				Concentration (ppm)				Pressure (Pa)
OA	SA	RA	EA	OA	SA	RA	EA	OA	SA	RA	EA	OA	SA	RA	EA	P_s-P_r
25.9*	25.2	25.2	25.2	11.8	11.5	11.1	14.2	26.8	23.3	26.9	29.8	0.0	2.8	15.7	2.8	51
25.9*	25.2	25.2	25.2	11.8	11.5	11.1	14.2	26.8	23.3	26.9	29.8	0.0	4.3	15.7	3.2	51
25.9*	25.2	25.2	25.2	11.8	11.5	11.1	14.2	26.8	23.3	26.9	29.8	0.0	5.2	15.7	3.5	51
25.9*	25.2	25.2	25.2	11.8	11.5	11.1	14.2	26.8	23.3	26.9	29.8	0.0	5.6	15.7	3.6	51
25.9*	25.2	25.2	25.2	11.8	11.5	11.1	14.2	26.8	23.3	26.9	29.8	0.0	5.7	14.5	3.8	51
25.9*	25.2	25.2	25.2	11.8	11.5	11.1	14.2	26.8	23.3	26.9	29.8	0.0	6.2	14.5	4.1	51
25.9*	25.2	25.2	25.2	11.8	11.5	11.1	14.2	26.8	23.3	26.9	29.8	0.0	6.5	14.5	4.0	51
25.9*	25.2	25.2	25.2	11.8	11.5	11.1	14.2	26.8	23.3	26.9	29.8	0.0	6.7	14.1	4.4	51
25.9*	25.2	25.2	25.2	11.8	11.5	11.1	14.2	26.8	23.3	26.9	29.8	0.0	6.6	14.1	4.4	51
25.9*	25.2	25.2	25.2	11.8	11.5	11.1	14.2	26.8	23.3	26.9	29.8	0.0	6.8	13.9	4.5	51
25.9*	25.2	25.2	25.2	11.8	11.5	11.1	14.2	26.8	23.3	26.9	29.8	0.0	7.2	14.3	4.8	51
25.9*	25.2	25.2	25.2	11.8	11.5	11.1	14.2	26.8	23.3	26.9	29.8	0.0	7.2	14.3	4.8	51

Table A.21. Temperature, humidity, flow rate, pressure difference (between supply and return side) and concentration data for acetic acid tests in silica gel coated energy wheel.

Temperature (°C)				Relative humidity (%)				Mass flow rate (g/s)				Concentration (ppm)				Pressure (Pa)
OA	SA	RA	EA	OA	SA	RA	EA	OA	SA	RA	EA	OA	SA	RA	EA	Ps-Pr
25.5*	25.8	25.1	25.7	17.4	17.2	19.3	17.1	27.3	23.3	27.6	30.3	0.0	3.84	40.79	2.69	52
25.5*	25.8	25.1	25.7	17.4	17.2	19.3	17.1	27.3	23.3	27.6	30.3	0.0	3.8	40.79	2.72	52
25.5*	25.8	25.1	25.7	17.4	17.2	19.3	17.1	27.3	23.3	27.6	30.3	0.0	5.03	40.79	2.87	52
25.5*	25.8	25.1	25.7	17.4	17.2	19.3	17.1	27.3	23.3	27.6	30.3	0.0	5.35	40.79	2.82	52
25.5*	25.8	25.1	25.7	17.4	17.2	19.3	17.1	27.3	23.3	27.6	30.3	0.0	9	41.68	3.82	52
25.5*	25.8	25.1	25.7	17.4	17.2	19.3	17.1	27.3	23.3	27.6	30.3	0.0	9.2	41.68	3.71	52
25.5*	25.8	25.1	25.7	17.4	17.2	19.3	17.1	27.3	23.3	27.6	30.3	0.0	11.44	42.47	4.75	52
25.5*	25.8	25.1	25.7	17.4	17.2	19.3	17.1	27.3	23.3	27.6	30.3	0.0	11.08	42.47	4.5	52
25.5*	25.8	25.1	25.7	17.4	17.2	19.3	41.2	27.3	23.3	27.6	30.3	0.0	12.13	42.47	4.59	52
25.5*	25.8	25.1	25.7	17.4	17.2	19.3	41.2	27.3	23.3	27.6	30.3	0.0	14.7	39.62	5.25	52
25.5*	25.8	25.1	25.7	17.4	17.2	19.3	41.2	27.3	23.3	27.6	30.3	0.0	14	39.62	5.2	52

Table A.22. Temperature, humidity, flow rate, pressure difference (across the wheel) and concentration data for frosting test using methanol in molecular sieve coated energy wheel.

Temperature (°C)				Relative humidity (%)				Mass flow rate (g/s)				Concentration (ppm)				Pressure (Pa)
OA	SA	RA	EA	OA	SA	RA	EA	OA	SA	RA	EA	OA	SA	RA	EA	Ps-Pr
-21.9	17.3	23.5	-4.1	29.1	59.1	49.9	58.5	30.5	21.6	26.8	35.6	0.0	24.9	42.8	21.0	59
-23.2	17.4	23.8	-4.7	28.2	60.6	50.0	60.1	30.2	21.5	26.8	35.1	0.0	25.4	42.8	20.5	59
-22.8	17.3	23.9	-3.6	31.1	61.0	50.3	62.0	29.9	21.5	26.1	34.8	0.0	25.7	42.8	19.1	71
-21.3	17.2	24.5	-2.0	31.0	59.7	47.7	62.0	29.8	21.2	26.1	34.3	0.0	27.1	42.8	18.6	165
-20.3	16.6	24.3	-1.5	32.6	60.8	48.8	62.1	28.9	20.9	26.5	34.3	0.0	28.5	43.1	17.2	348

Table A.23. Temperature, humidity, flow rate, pressure difference (across the wheel) and concentration data for frosting test using carbon dioxide in molecular sieve coated energy wheel.

Temperature (°C)				Relative humidity (%)				Mass flow rate (g/s)				Concentration (ppm)				Pressure (Pa)
OA	SA	RA	EA	OA	SA	RA	EA	OA	SA	RA	EA	OA	SA	RA	EA	Ps-Pr
-22.2	15.5	22.0	-6.0	25.5	46.0	39.8	54.2	30.4	23.1	26.8	34.7	489.5	510	1639	1298.1	59
-23.6	15.2	21.9	-6.8	25.3	47.5	39.8	55.6	30.5	23.1	26.8	34.7	489.5	510	1676	1298.1	61
-23.7	14.9	21.2	-7.0	25.0	51.2	43.4	57.2	30.6	22.8	26.9	34.6	489.5	510	1640	--	60
-23.8	14.8	21.2	-7.3	24.6	51.4	43.5	56.3	30.6	22.8	26.9	34.5	489.5	516	1603	--	93
-23.8	14.9	21.1	-7.1	24.2	52.0	44.5	57.0	30.0	22.5	26.7	34.2	489.5	540	1621	--	163

APPENDIX B

This appendix provides the literature review on test methods for gaseous contaminant transfer in energy exchangers. A summary of test data and properties of gaseous contaminants reported in Chapter 2 of this report are elaborated in this appendix. The mechanisms behind contaminant transfer, available experimental data, and the findings and analysis of literature data are presented in detail. This manuscript was published in the ASHRAE journal, Science and Technology for the Built Environment. (doi: https://doi.org/10.1080/23744731.2022.2113705) and included here with the permission of the ASHRAE.

A REVIEW OF EXPERIMENTAL STUDIES ON CONTAMINANT TRANSFER IN ENERGY EXCHANGERS (RP-1780)

ABSTRACT

This paper presents a literature review on experimental studies for measuring gaseous contaminant transfer in different energy exchangers. The experimental methods, measured contaminant transfer rates and uncertainties (where available) for different gases are summarized, although most studies do not include any uncertainty analysis. The measured transfer rates vary between 0% to 75%, with uncertainties between 1% to 30%. The literature review shows that mechanisms for gaseous contaminant transfer in energy exchangers are air leakage, carryover, and phase change mechanisms such as: adsorption/desorption, condensation/evaporation, and absorption/evaporation. There is an established test methodology to quantify the gaseous contaminant transfer in energy exchangers due to air leakage and carryover; however, there is no method in the literature to quantify gaseous contaminant transfer due to the phase change mechanisms. Thus, a method to determine the contaminant transfer due to the phase change mechanisms is proposed and applied to the available literature data.

Keywords: Energy exchangers, Adsorption/desorption, Contaminant transfer, Exhaust air transfer ratio.

Nomenclature

A_s	total heat transfer area (m^2)	IAQ	indoor air quality
C	concentration of contaminant	IER	ion exchanger resin
Cr*	matrix heat capacity rate ratio	HVAC	heating ventilation and air-conditioning
h	specific enthalpy (kJ/kg)	LAMEE	liquid-to-air membrane energy exchanger
M	mass of the matrix (kg)	RAMEE	run around membrane energy exchanger
$\dot{m}$	mass flow rate of air (kg/s)	SG	silica gel
NTU	number of transfer units	VOCs	volatile organic compounds
P	pressure	**Greek Symbols**	
T	temperature (°C)	ε	effectiveness (%)
U	overall heat transfer coefficient ($W/m^2 K$)	ω	rotational speed (rpm)
V	velocity (m/s)	**Subscripts**	
W	humidity ratio (kg_w/kg_a)	ad	adsorption
Abbreviations		1, 2, 3, 4	measurement station numbers in ASHRAE Std 84 (2020) at the inlets and outlets of the test section.
AAEE	air-to-air energy exchanger		
EATR	exhaust air transfer ratio		
ECTR	exhaust contaminant transfer ratio		

1. INTRODUCTION

People spend 90% of their time indoors, and indoor air quality (IAQ) and thermal comfort significantly affect the occupants' health and productivity (Brown, Sim, Abramson, & Gray, 1994). A high concentration of gaseous and particulate contaminants in indoor air could diminish the air quality in buildings. There are various indoor sources that generate contaminants such as carpets, floor coverings, curtains, and other building materials (Harčárová, Vilčeková, & Balintova, 2020; Roulet, Pibiri, Knutti, Pfeiffer, & Weber, 2002; Yurdakul et al., 2017). More than 300 indoor

contaminants have been identified in different countries, and many of them cause adverse health effects such as headaches, drowsiness, difficulty in breathing, and allergic reactions (Patel et al., 2014; Roulet et al., 2002). To provide fresh air to buildings and maintain thermal comfort conditions, Heating, Ventilating, and Air-Conditioning (HVAC) systems are needed (Kassai, 2019; Wang, Sadeghian, & Sadrizadeh, 2019). Conditioning outdoor air is an energy-intensive process, and it accounts for about 60% of commercial building energy consumption in developed countries (Natural Resources Canada, 2020). One way to reduce energy consumption for conditioning the outdoor air is to use air-to-air energy exchangers (AAEEs) (Besant & Simonson, 2000) that exchange heat and moisture between the building exhaust and supply airstreams.

Figure 2 shows a schematic of an HVAC system that provides conditioned air into a building. The supply fan provides fresh outdoor air into the building, and the exhaust fan removes stale/contaminated air from the building. The outdoor air can be heated or cooled depending on the outdoor climatic conditions. The energy exchanger is used to transfer energy between the return airstream and supply airstream. As the energy exchanger exchanges heat and moisture between the supply and the return airstreams, contaminants generated at indoors may also transfer (through return airstream) to the supply airstream. Energy wheels (Simonson & Besant, 1999), membrane exchangers (Ghadiri Moghaddam, Besant, & Simonson, 2015) and fixed-bed regenerators (Krishnan, Ramin, Gurubalan, & Simonson, 2021) are the commonly used energy exchangers. Energy wheels and fixed-bed systems are regenerative, in which energy storage and release take place intermittently whereas membrane exchangers are recuperative in nature. It should also be noted that some exchangers such as heat wheels (Rabah, Fekete, & Kabelac, 2009), flat plate exchangers (Shokouhmand & Hasanpour, 2020), and heat pipes (ASHRAE, 2012) are capable of transferring only heat between the air streams.

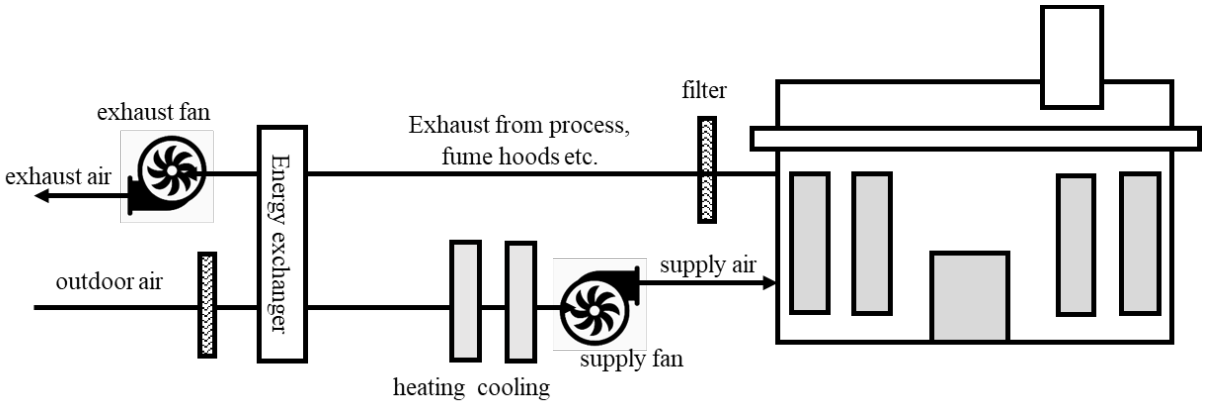

Figure 2. Schematic of an HVAC system providing conditioned (heated/cooled) outdoor air to a building.

Over the past decades, researchers and engineers have investigated gaseous contaminant transfer in different AAEEs (Bayer, 2011; Fisk, Pedersen, Hekmat, Chant, & Kaboli, 1985; Kodama, 2010; Patel et al., 2014; Shang, Wawryk, & Besant, 2001). A comprehensive literature review on this topic shows that there are fifteen studies on gaseous contaminant transfer in energy exchangers. Many of these studies were performed using different contaminants at various operating conditions. The transfer rate of contaminants, the effect of operating conditions, and exchanger design parameters on contaminant transfer are not clearly summarized in the open literature. In this paper, the available literature in experimental studies of gaseous contaminant transfer in energy exchangers are summarized based on the transfer mechanisms. The various contaminant transfer mechanisms in energy exchangers are: (i) air leakage, (ii) carryover (iii) adsorption/desorption, (iv) condensation/evaporation, and (v) absorption/evaporation. Each of these mechanisms will be discussed in detail in the next section. It should also be noted that the gaseous contaminant transfer due to carryover and leakage are reported together as their contributions have been typically investigated simultaneously. The major findings and the contribution of published articles, comparison of gaseous contaminant transfer results, and effects of operating conditions on gaseous contaminant transfer results will be presented.

2. CONTAMINANT TRANSFER MECHANISMS IN ENERGY EXCHANGERS

Carryover, air leakage, and adsorption/desorption are the three major mechanisms responsible for contaminant transfer in energy exchangers. The contaminant transfer is also possible because of absorption/evaporation and condensation/evaporation. All the three mechanisms are present in energy wheels. These mechanisms are discussed in detail in the following sections.

2.1. Carryover

The contaminant transfer due to carryover occurs when return air flows through energy wheel, and part of the air transfers to supply airstream through the wheel rotation. Figure 1.2 presents a schematic of carryover in the energy wheel. As shown in the figure, some of the air from the exhaust side remains in the matrix of the wheel as it rotates to the supply side. This exhaust air mixes with fresh incoming outdoor air and is supplied to indoor space. The contaminants present in the return airstream will also get transferred through this mechanism.

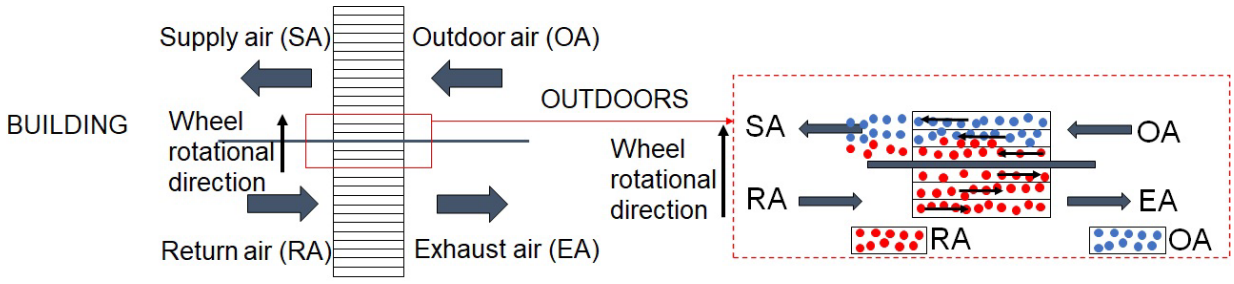

Figure 3. Schematic of carryover mechanism in energy wheels.

The carryover can be limited by using a purge section in energy wheel, and a good installation and proper maintenance of energy wheel (Roulet et al., 2002; Shang & Besant, 2008). Figure 3 shows a schematic of a purge section in an energy wheel that prevents carryover from return airstream to supply airstream. The purge isolates a section of the wheel on the boundary

between the supply and return airstreams and displaces the entrapped return air (from the exhaust side) along with some outdoor air to the exhaust side. Contaminant transfer due to the carryover is independent of the gas since contaminants are simply carried in the air from one side to other.

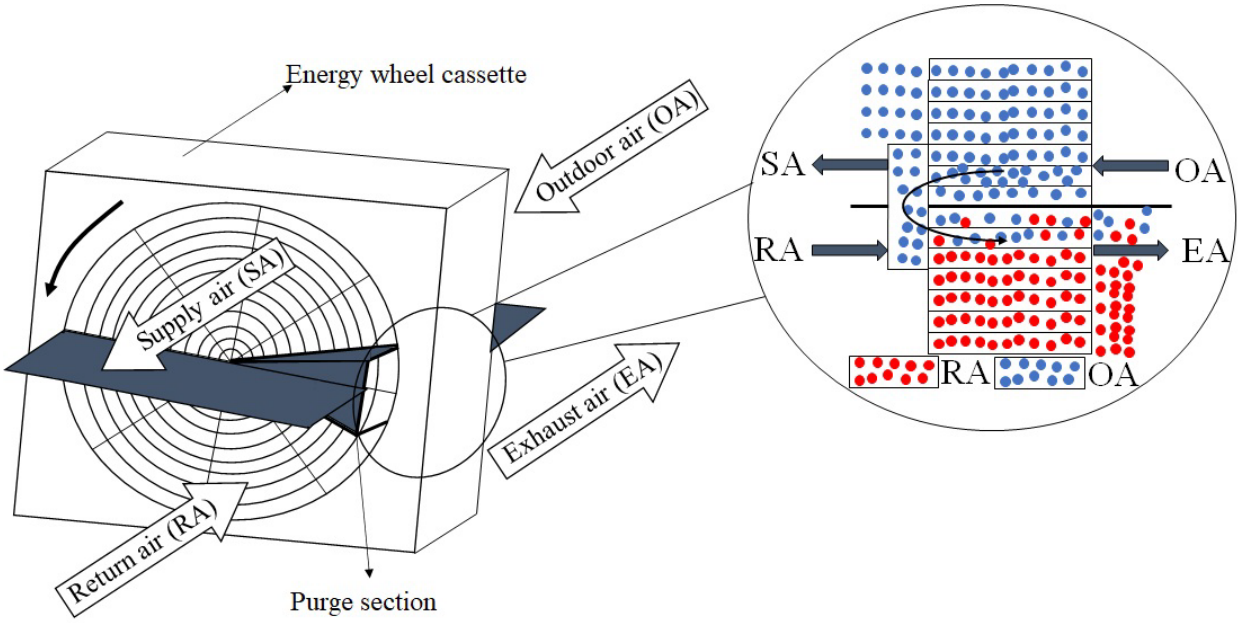

Figure 4. Schematic showing a purge section in an energy wheel that transfers outdoor air to exhaust air and prevents carryover from return air to supply air.

2.2. Air leakage

The contaminant transfer by air leakage occurs due to pressure difference between supply and return airstreams. In this case, air leaks through the interface (seals) of return and supply airstreams as shown in

Figure **1.4**. The leakage can occur either from supply to return airstream or vice versa, depending on the airstream pressure. The leakage to the supply side from the exhaust side can be minimized by maintaining high pressure on the supply side ($P_{supply} > P_{return}$). The locations of the fans in outdoor, supply, return, and exhaust airstreams play an important role in air leakage direction (Khoury, Chang, Lessley, Abdelghani, & Anderson, 1988).

Figure **1.4** shows a schematic of the air leakage mechanism in an energy wheel, where the supply air has a higher pressure than return air.

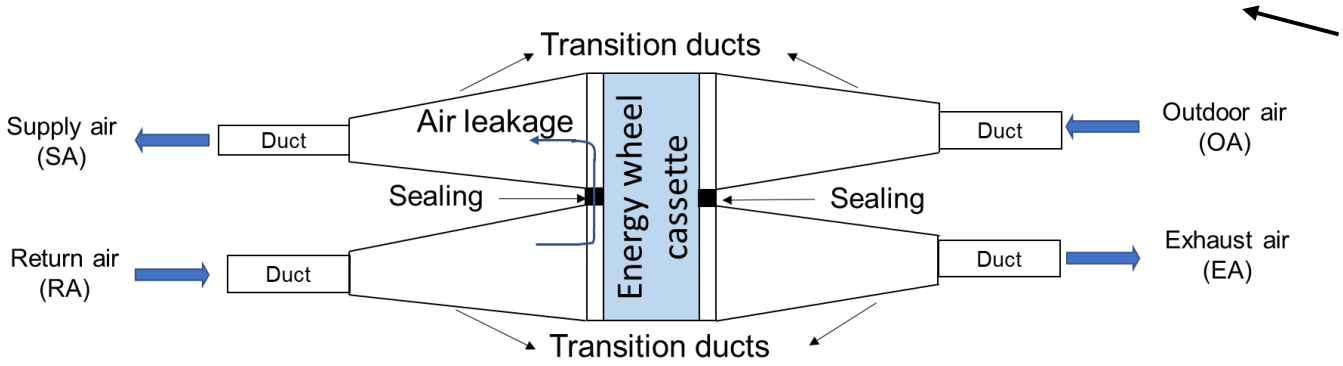

Figure 5. Schematic of air leakage mechanism in energy wheels.

2.3. Adsorption/desorption

Contaminant transfer due to adsorption/desorption occurs when the desiccant-coated energy wheel has the capacity to adsorb the contaminant in one airstream, store the contaminant until it is desorbed in the other airstream (similar to transfer of water vapor). Figure 1.5 presents a schematic of adsorption/desorption mechanism in an aluminum sheet coated with desiccants.

The sorption capacity will vary for different contaminants and desiccants. Contaminant transfer between the airstream and the desiccant occurs because of the difference in the vapor pressure of the contaminant between the airstream and the desiccant (Okano et al., 2001). Adsorption occurs when the vapor pressure is higher in the air than on the desiccant surface and desorption occurs when the vapor pressure is higher on the desiccant surface than in the air. Contaminant transfer in energy wheels through adsorption/desorption mechanism is expected to depend on many parameters such as the air conditions (temperature and humidity), the properties

of the contaminants, desiccants (Kodama, 2010), and design of the wheels (i.e., face velocity, NTU, Cr*, and effectiveness).

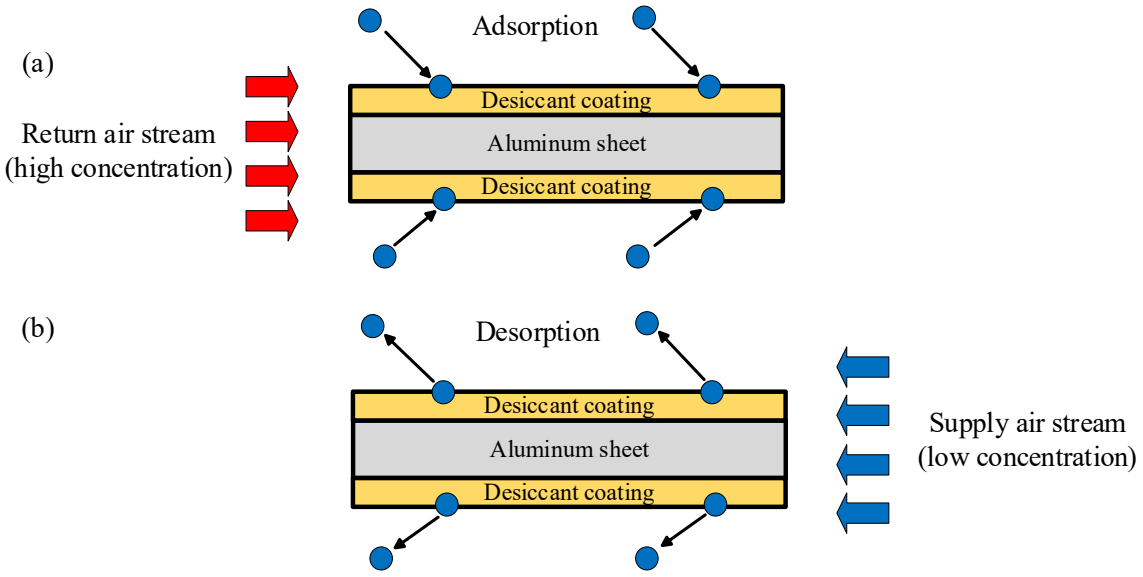

Figure 6. Schematic of adsorption/desorption mechanism, showing (a) adsorption in the return airstream and (b) desorption in the supply airstream.

2.4. Absorption/evaporation

In addition to the main mechanisms mentioned above, some gaseous contaminants in the return airstream get absorbed in the wheel and evaporate on the supply side. For example, when water vapor in return airstream condenses to liquid water (or frost) within energy wheel channels, water soluble gaseous contaminants such as formaldehyde and methanol get absorbed in the liquid (or frozen) water. Gaseous contaminant absorption occurs because of attractive forces between gaseous contaminants and liquid (frozen) water. When the liquid water evaporates into the supply airstream, the absorbed contaminants may evaporate and transfer to the supply air.

2.5. Condensation/evaporation

The condensation of gaseous contaminants would occur if the concentration of the contaminant reached the saturation level. Although such high concentrations are expected to be very rare for AAEE applications, it may be possible for a contaminant to condense on the exhaust side of the wheel and evaporate on the supply side of the wheel. Contaminant transfer by condensation/evaporation in AAEEs is expected to be small.

The literature presented in this paper discusses contaminant transfer mainly focused on three types of desiccant coated wheels: (a) silica gel, (b) molecular sieves, and (c) ion-exchange resins. It is known that both the silica gel and molecular sieves are porous adsorbents. They adsorb moisture onto their pores due to the humidity gradient between the airstream and the desiccant. Hence, considering the same principle, contaminants could also be adsorbed/desorbed because of the concentration gradient in the airstream and the desiccant. The ion-exchange resins are non-porous, selective materials and the driving potential for moisture exchange is their swelling behavior and volume change (Kodama 2010), and its selectivity could be one of the reasons for the low transfer rate of contaminants.

3. TEST STANDARDS AND PERFORMANCE PARAMETERS

ASHRAE Standard 84 (ANSI/ASHRAE, 2020) and CSA C 439-18 (Canadian Standards Association, 2018) standards provide guidelines to conduct the performance tests. The performance of an energy exchanger depends on design parameters and operating conditions. The direction of airflow and the nomenclature of inlet and outlet airstreams as given in ASHRAE standard 84 (ANSI/ASHRAE, 2020) are shown in Figure 7. Major parameters used to quantify the energy and contaminant transfer performance are discussed below.

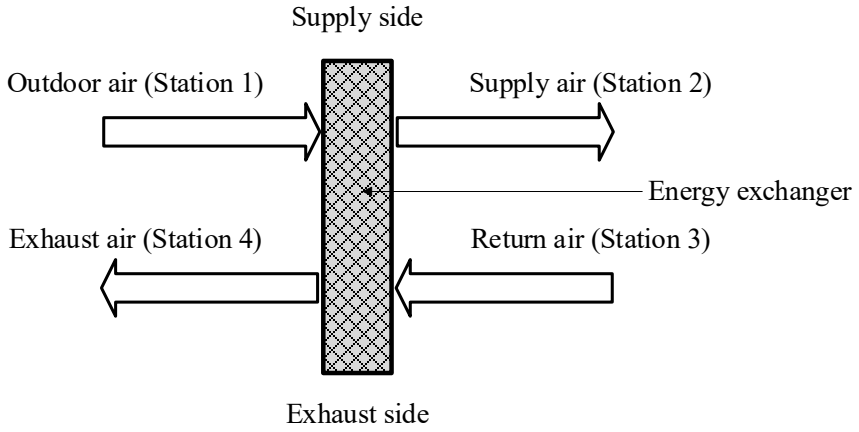

Figure 7. Schematic of an air-to-air energy exchanger showing the airflow and measurement stations.

3.1. Effectiveness (ε):

Effectiveness is defined as the ratio of actual energy transfer rate at a specific test condition to the maximum energy transfer at the same test condition (Shah & Sekulic, 2003). The sensible, latent, and total effectiveness can be determined using Eqs. (1), (2) and (3) according to ASHRAE Standard 84 (ANSI/ASHRAE, 2020).

$$\varepsilon_{sensible} = \frac{\dot{m}_2(C_{p,1}T_1 - C_{p,2}T_2)}{\dot{m}_{minimum\ (2,3)}\ (C_{p,1}T_1 - C_{p,3}T_3)} \tag{1}$$

$$\varepsilon_{latent} = \frac{\dot{m}_2(W_1 - W_2)}{\dot{m}_{minimum\ (2,3)}\ (W_1 - W_3)} \tag{2}$$

$$\varepsilon_{latent} = \frac{\dot{m}_2(h_1 - h_2)}{\dot{m}_{minimum\ (2,3)}\ (h_1 - h_3)} \tag{3}$$

Where $\dot{m}, T, W, C_p\ and\ h$ represent the mass flow rate, temperature, humidity ratio, specific heat, and specific enthalpy at stations 1, 2, and 3 according to the subscripts.

3.2. Outdoor air correction factor (OACF):

ASHRAE Standard 84 (ANSI/ASHRAE, 2020) defines the outdoor air correction factor as the ratio of entering supply airflow to the leaving supply airflow as shown in Eq. (4).

$$OACF = \frac{\dot{m}_1}{\dot{m}_2} \tag{4}$$

3.3. Exhaust air transfer ratio (EATR):

Exhaust air transfer ratio (EATR) is used to express the percentage of an inert tracer gas transferred from exhaust side (station 3) to supply side (Station 2). It is defined as the ratio of tracer gas concentration difference between the supply and the outdoor air streams, to the tracer gas concentration difference between the return and the outdoor air streams (ANSI/ASHRAE, 2020), and can be calculated using Eq. (5).

$$EATR = \frac{C_2 - C_1}{C_3 - C_1} \tag{5}$$

where C_1, C_2, and C_3 are the tracer gas concentration measured at the stations 1, 2 and 3, respectively. It should be noted that EATR is a measure of bulk leakage of air within the energy exchanger and is not directly applicable to the measurement of other gaseous contaminants in the device as described in ASHRAE standard 84 (ANSI/ASHRAE, 2020).

The uncertainty in EATR (Eq. (6)) can be calculated using uncertainty propagation methods as (ASME/ANSI, 1998):

$$U_{EATR} = \sqrt{(U_{C_2}\frac{1}{(C_3 - C_1)})^2 + (U_{C_1}\frac{C_2 - C_3}{(C_3 - C_1)^2})^2 + (U_{C_3}\frac{C_1 - C_2}{(C_3 - C_1)^2})^2} \tag{6}$$

where U_{C_1}, U_{C_2} and U_{C_3} are uncertainty in tracer gas concentration measurement in stations 1, 2 and 3, respectively.

Tracer gas measurement procedure: To measure the EATR, an inert tracer gas is injected into the turbulent region of the return air stream. Then the air samples draw from each station, and the concentration of tracer gas will be measured using calibrated gas analyzers. The air sampling lines

must be maintained short enough to avoid dilution and sample line transients. The maximum allowed uncertainty in ASHRAE standard 84 (ANSI/ASHRAE, 2020) for EATR is less than 3%. The requirements of sampling equipment and recommendations on the sampling grid are also provided in the test standards (ANSI/ASHRAE, 2020; Canadian Standards Association, 2018).

3.4. Energy and mass inequalities

During every performance test, in addition to the performance parameters, the test data should satisfy the energy and mass inequalities (ANSI/ASHRAE, 2020; Canadian Standards Association, 2018). The inequality equations for (i) energy transfer, (ii) dry air mass flow rate, (iii) water vapor mass and (iii) contaminants mass are provided in Eqs. (7), (8), (9) and (10) (ANSI/ASHRAE, 2020).

For sensible energy transfer:

$$\frac{\left|\dot{m}_1 C_p T_1 - \dot{m}_2 C_p T_2 + \dot{m}_3 C_p T_3 - \dot{m}_4 C_p T_4\right|}{\dot{m}_{minimum\ (1,3)}\ C_p\ |T_1 - T_3|} < 0.20 \tag{7}$$

For water vapor transfer:

$$\frac{|\dot{m}_1 W_1 - \dot{m}_2 W_2 + \dot{m}_3 W_3 - \dot{m}_4 W_4|}{\dot{m}_{minimum\ (1,3)}\ C_p\ |W_1\ - W_3|} < 0.20 \tag{8}$$

For enthalpy transfer:

$$\frac{|\dot{m}_1 h_1 - \dot{m}_2 h_2 + \dot{m}_3 h_3 - \dot{m}_4 h_4|}{\dot{m}_{minimum\ (1,3)}\ C_p\ |h_1 - h_3|} < 0.20 \tag{9}$$

For tracer gas mass inequality:

$$\frac{|\dot{m}_1 C_1 - \dot{m}_2 C_2 + \dot{m}_3 C_3 - \dot{m}_4 C_4|}{\dot{m}_{minimum\ (1,3)}\ |C_1 - C_3|} < 0.15 \tag{10}$$

3.5. Energy wheel design parameters

In addition to these performance parameters, some important non-dimensional parameters that are used to define exchangers are number of transfer unit (NTU) and matrix heat capacity rate ratio (Cr*) which can be evaluated using Eqs. (11) and (12) (Shah & Sekulic, 2003).

$$NTU = \frac{UA}{C_{min.}} \quad (11)$$

$$Cr^* = \frac{(M)_{matrix}\omega}{(C_{min.})_{air}} \quad (12)$$

Here, U, A, M, C, ω, $\dot{m}$ are overall heat transfer coefficient, heat transfer area, mass of the matrix, heat capacity rate, rotational speed, and air mass flow rate, respectively.

4. SUMMARY OF RESEARCH ON CONTAMINANT TRANSFER IN ENERGY EXCHANGERS

The following section summarizes the research on contaminant transfer in energy exchangers and the effect of operating conditions on the transfer rate for various contaminants. Most of the studies have applied the concept of EATR for gaseous contaminants, even for gases that are not inert gases as specified in the test standards (ANSI/ASHRAE, 2020; Canadian Standards Association, 2018). The measurements of non-inert gases, therefore, include all the contaminant transfer mechanisms (carryover, leakage, and adsorption/desorption). The studies will be sorted into groups based on the main transfer mechanisms and the type of gaseous contaminant (inert or non-inert) and will be presented in chronological order within each section.

4.1. Carryover and air leakage of inert gases

4.1.1. ***Fisk et al.*** (Fisk et al., 1985)

Fisk et al. (Fisk et al., 1985) studied the gaseous contaminant transfer from the return airstream to the supply airstream in an energy wheel. Propane (C_3H_8) and sulfur hexafluoride (SF_6) were used to determine air leakage in the energy wheel. C_3H_8 and SF_6 were injected upstream of the energy wheel in exhaust side. To improve the mixing of the tracer gases in the airstream, tracer gases were injected through a manifold upstream of an orifice plate and mixing vanes. The concentrations of contaminants were monitored using infrared analyzers. The results showed that

SF_6 and C_3H_8 transfer rates were between 6-7% and 5-7%, respectively, indicating that the transfer of propane could be mainly due to the carryover and leakage. These experiments were performed at summer (≈ 32°C, 20-55% RH) and winter operating conditions (≈ 4°C, 70% RH).

*4.1.2. **Khoury et al.*** (Khoury et al., 1988)

Khoury et al. (Khoury et al., 1988) studied SF_6 transfer in a heat wheel. SF_6 was stored in a gas chamber and injected into return airstream with a rotameter. In the experiments, three-meter-long sampling tubes were used to collect air samples from the center of the air ducts. Air samples were collected into 15 L Tedlar sampling bags. The concentration of SF_6 in the collected air samples was measured using infrared spectroscopy with a calibrated MIRAN 1A gas analyzer. The results showed that an average of 1% of SF_6 was transferred by the heat wheel from the return air to the fresh supply air. A mass balance showed that 30% of the injected SF_6 was lost during an experiment. They suggested that the SF_6 could have been adsorbed onto wheel cassette. Their experimental data did not include uncertainty analysis and the operating conditions.

*4.1.3. **Andersson et al.*** (Andersson, Andersson, Sundell, & Zingmark, 1993)

Andersson et al. (Andersson et al., 1993) studied formaldehyde transfer in six energy wheels with and without a purge section. They measured carryover and air leakage with nitrous oxide (N_2O). A vacuum pump and metal tubes were used to draw air samples from the outdoor, supply, return, and exhaust airstreams. An infrared spectrophotometer was used to determine the N_2O concentration in the air samples. Test results showed that 3% of injected N_2O was transferred from the return airstream to the supply airstream for the energy wheels without a purge section (i.e., carryover and air leakage) and 1% of injected N_2O was transferred with a purge section (i.e., air leakage assuming a well-designed purge section). Results showed that standard deviations were

1-12% for N_2O concentration. Andersson et al. also conducted experiments with formaldehyde and these tests are described in Section 4.2.2.

*4.1.4. **Shang et al.*** (Shang et al., 2001)

Shang et al. (Shang et al., 2001) studied N_2O crossover in an energy wheel with and without a purge section. Five pressure differences were applied between exhaust airstream and outdoor airstream ranging from -254 Pa to 254 Pa. The schematic of their test facility is provided in Figure 8.

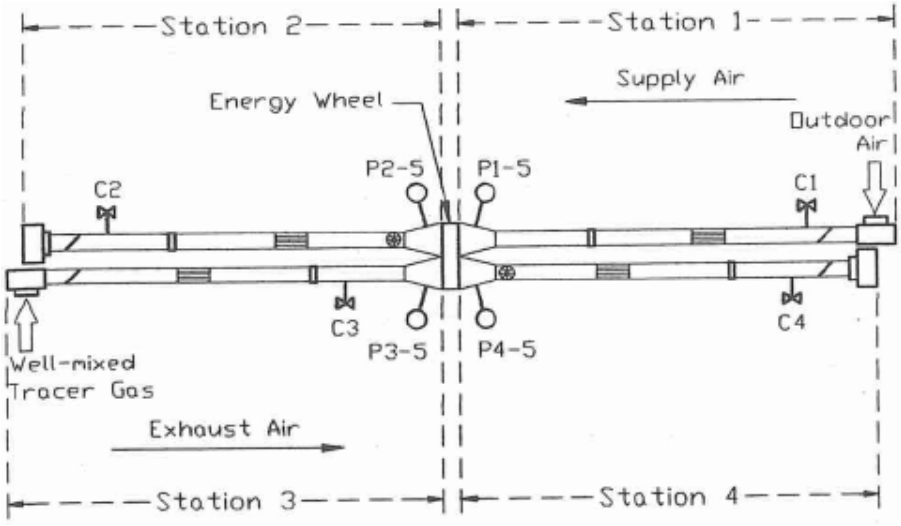

Figure 8. Schematic of test facility used by Shang et al. (2001) for N_2O crossover experiments (Shang et al., 2001).

Experiments started with injecting N_2O into return airstream with a concentration of 150 ppm. Air samples were collected in sampling bags with 100 L volume and analyzed with a gas analyzer. Details of gas measurement techniques such as the gas analyzer model were not provided.

Result for experiments on the energy wheel without a purge section showed that EATR was 33% when pressure difference (P_{supply}-$P_{exhaust}$) was -254 Pa and reduced to 1% when pressure difference was 254 Pa. Results for experiments on the energy wheel with a purge section showed

that EATR was 54% for pressure difference of -246 Pa and reduced to 1.1% for a pressure difference of 250 Pa. The highest EATR uncertainty was ±3% at a pressure difference of 250 Pa. They suggested that a purge section increased EATR and uncertainty in measurement when the exhaust side pressure is higher than supply side pressure and therefore, the purge section may not always be beneficial.

*4.1.5. **Sparrow et al.*** (Sparrow, Abraham, Martin, & Tong, 2001)

Sparrow et al. (Sparrow et al., 2001) studied CO_2 transfer in a flat plate enthalpy exchanger using a novel semi-permeable membrane. The membrane was coated with polymer material which allowed penetration of water vapor and prevented other gases from passing through it. This was due to polymer coatings that were synthesized in order to fit water vapor molecular size. A pressurized cylinder of CO_2 was connected to four distribution tubes for ensuring a uniform concentration of CO_2 in the return airstream. An orifice plate was used for achieving desired concentration of CO_2 in return airstream. The authors assumed mass balance for CO_2 in order to reduce the costs of measuring CO_2 at different airstreams. An infrared spectroscopy technique was used with a resolution of 1 ppm for measuring CO_2 concentration in return, outdoor and supply airstreams. The CO_2 concentration for their experiments was reported as 300-900 ppm.

Mass transfer effectiveness for water vapor was reported as 50% at face velocities between 0.25-0.5 m/s (50-100 fpm) and transfer of CO_2 was reported as 1% at a face velocity of 1.5 m/s (300 fpm). A selectivity parameter was introduced for quantifying gas transfer through applied polymer membrane. This parameter was the ratio of water vapor transfer rate to CO_2 transfer rate and ranged between 21 and 61. Results showed that the membrane transferred water vapor while prevented CO_2 transfer through the membrane. This study did not provide uncertainty analysis of results.

*4.1.6. **Roulet et al.*** (Roulet et al., 2002)

Roulet et al. (Roulet et al., 2002) studied SF_6 transfer in energy wheels in an auditorium, a laboratory, and a building. Tracer gas experiments with SF_6 showed that transfer rate through air leakage and carryover mechanisms were 7±4% in auditorium, 5±11% in laboratory and 26±16% in building. The higher transfer rate in the building might have been due to higher air flow rate in return airstream than that of supply airstream. Roulet et al. (2002) reported experimental data for other contaminants, which will be provided in Section 4.2.4 as the adsorption mechanism is predominant for those contaminants.

*4.1.7. **Wolfrum et al.*** (Wolfrum, Peterson, & Kozubal, 2008)

Wolfrum et al. (Wolfrum et al., 2008) studied toluene and n-hexane transfer in a desiccant wheel coated with silicate-based desiccant. Preliminary tracer gas experiments with SF_6 showed 1% air leakage and carryover from return airstream to supply airstream. Pressure difference between return and supply airstream was set to zero in his experiments. Experimental data for other contaminants will be described in Section 4.2.5.

*4.1.8. **Patel et al.*** (Patel et al., 2014)

Patel et al. (Patel et al., 2014) performed experiments to measure formaldehyde and toluene transfer in a run-around membrane energy exchanger (RAMEE). A RAMEE consists of two energy exchangers, a liquid desiccant running loop and a pump to run liquid desiccant between energy exchangers. These energy exchangers are called liquid-to-air membrane energy exchangers (LAMEEs). Figure 9 shows a schematic of a RAMEE.

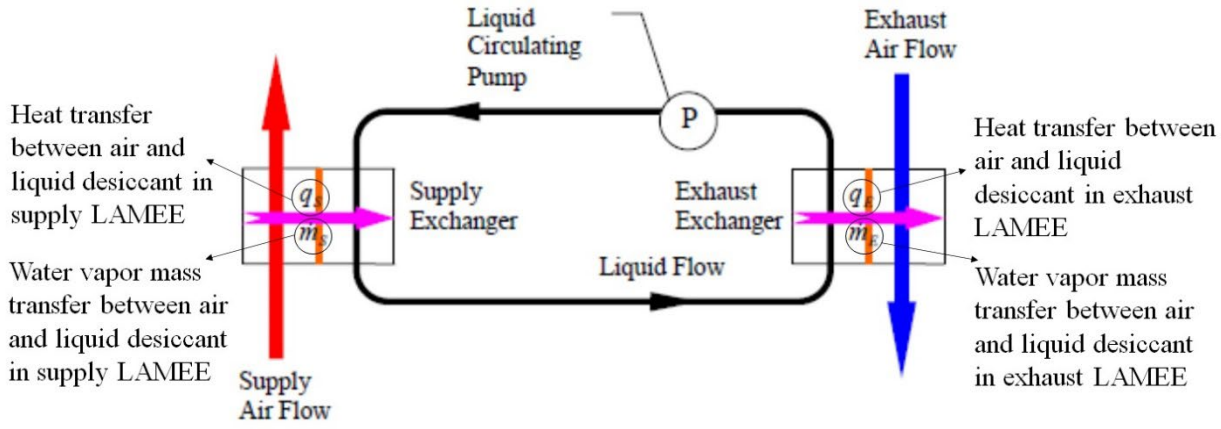

Figure 9. Schematic of a RAMEE (Fan, Simonson, Besant, & Shang, 2006).

Experiments with SF_6 showed that EATR was almost zero which was due to its very low solubility in water. EATR results for the formaldehyde and toluene will be provided in Section 4.2.8.

*4.1.9. **Hult et al.*** (Hult, Willem, & Sherman, 2014)

Hult et al. (Hult et al., 2014) studied gaseous contaminants (CO_2, SF_6 and formaldehyde) transfer in energy wheels using field and chamber experiments. CO_2 concentration in outdoor, supply and return airstreams were measured for determining contributions of air leakage and carryover mechanisms in cross-contamination in energy wheel. Air samples were collected in silica gel cartridges coated with 2,4-dinitrophenylhydrazine. Sampling cartridges were extracted into 2 mL of high purity acetonitrile. Sample extracts were analyzed using HPLC technique.

Chamber experiments were done in order to validate field experiments at air flow rates between 120-340 m^3/hr. Chamber experiments started with injecting SF_6 into return airstream. Air samples were collected using sampling bags and analyzed using a gas chromatography technique. Measured SF_6 concentration was between 20-1200 $\mu g/m^3$.

4.1.10. Kassai (Kassai, 2018)

Kassai (Kassai, 2018) studied CO_2 transfer in an energy wheel coated with a 3Å molecular sieve desiccant. CO_2 was injected into return airstream from a 50 L volume cylinder. A TESTO multifunctioning metering instrument was used for measuring CO_2 concentration at different airstreams. Results showed that CO_2 transfer from return airstream to supply airstream increased with wheel rotational speed. CO_2 transfer also increased with air volume flow rate in return and outdoor airstreams. For example, at volume flow rate of 400 $\frac{m^3}{h}$ and wheel rotational speed of 2 rpm the CO_2 transfer was 2%, and at volume flow rate of 800 $\frac{m^3}{h}$ and wheel rotational speed of 10 rpm the CO_2 transfer was 4%.

Their results showed that carbon dioxide transfer was between 2-5% depending on wheel speed and flow rate. Relative standard deviation for CO_2 transfer measurements was reported as 0-1%. It was assumed that two major mechanisms for CO_2 transfer were air leakage and carryover. This study did not present contaminant mass conservation in experiments.

4.2. Adsorption/desorption of non-inert gases

In this section, the experimental studies on contaminant transfer due to adsorption/desorption are summarized. It should be noted that the results of contaminant transfer experiments reported in this section also include all the possible mechanisms (carryover, leakage, and adsorption/desorption).

4.2.1. Fisk et al. (Fisk et al., 1985)

Fisk et al. (Fisk et al., 1985) studied formaldehyde transfer in energy wheel. Gaseous formaldehyde was produced by evaporating a methanol-free aqueous formaldehyde solution into a secondary airflow. This secondary airflow containing the gaseous formaldehyde was injected

into the return airstream the same way as injection of SF_6 and C_3H_8. The details of the formaldehyde concentration measurement technique were not provided. Results showed that formaldehyde transfer was between 9-15% in the energy wheel depending on outside air temperature and humidity ratio. Higher outside temperatures and humidity ratios showed higher formaldehyde transfer rates. The difference between the formaldehyde transfer rate and tracer gas transfer rate showed that there were mechanisms other than carryover and leakage that contributed to the contaminant transfer in energy wheel.

Fisk et al. (Fisk et al., 1985) concluded that the higher transfer rates of formaldehyde may be due to adsorption of formaldehyde on surface of flow channels in return airstream and transfer through wheel rotation to supply airstream. Their results showed a 12% uncertainty in the formaldehyde transfer rate.

4.2.2. Andersson et al. (Andersson et al., 1993)

Andersson et al. (Andersson et al., 1993) conducted experiments with formaldehyde in energy wheels. The concentration of formaldehyde in different airstreams was measured using a chemisorption technique employing 2,4-dinitrophenylhydrazine-impregnated glass fiber filters. Six fiber filters were used for air sampling. In addition, where air flow was not homogenous, air sampling was done using grids of metal tubes (1 mm diameter) located perpendicular to the airstream. These metal tubes were used for collecting air samples in a bottle. The bottle contained filters for adsorbing formaldehyde, and the filters were analyzed with high performance liquid chromatography (HPLC) technique. It was found that in the worst-case scenario 9% of the formaldehyde transferred from return airstream to supply airstream with a standard deviation between 15-29%. Results agreed with results reported by Fisk et al. (who measured a formaldehyde transfer rate of 9-15%).

Andersson et al. (Andersson et al., 1993) determined effects of formaldehyde transfer in energy wheels on concentration of formaldehyde in building. An example was put forward in their published article. It was assumed that formaldehyde concentration was 20 μg/m^3 in building, ventilation rate was 1 air change per hour, and formaldehyde transfer from return airstream to supply airstream was 10%. Figure 10 shows that after 2 hours operation of ventilation system, the formaldehyde concentration remained constant in building. After two hours of initial transient operation, the formaldehyde generation from the source and its dilution due to the ventilation resulted in an equilibrium concentration of 22 μg/m^3 (around 10% increase in the concentration due to the cross contamination).

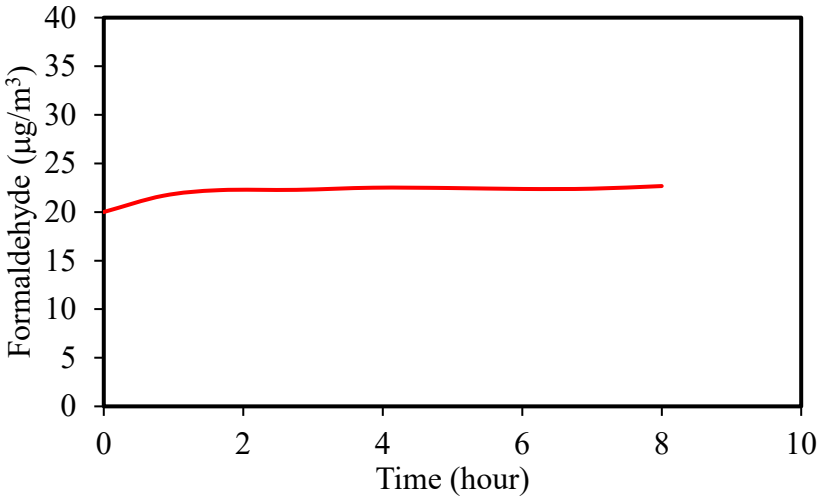

Figure 10. Calculated formaldehyde concentration in a building during 8 hours with 10% EATR in an energy wheel (Andersson et al., 1993).

4.2.3. Okano et al. (Okano et al., 2001)

Okano et al. (Okano et al., 2001) studied contaminant transfer in energy wheels coated with different desiccants, namely ion exchange resin (IER) and silica gel (SG). The ion exchange resin was selected because it is nonporous and little contaminant transfer by adsorption/desorption is expected, while the silica gel was selected since it is a commonly used desiccant material.

Experiments started with generating gaseous contaminants in a box and injecting them into the return airstream. Contaminants tested were ammonia, isopropyl alcohol (IPA), toluene, acetic acid, formaldehyde, styrene, acetone, xylene, ethyl methyl ketone, ethyl acetate, butyl acetate, ethyl alcohol, and methanol.

A sorption test was conducted to determine sorption capacity of desiccants. The sorption test showed that ion exchange resin adsorbed 3% mass fraction of IPA and silica gels adsorbed 17-19% mass fraction of IPA. Concentration of IPA were not reported in these tests. The concentration of ammonia, formaldehyde and acetic acid was measured using gas detector tubes, whereas gas chromatography technique was used for remaining contaminants. Details of instrumentation in contaminant injection and contaminant concentration measurement were not described in the paper.

Experiments with the energy wheel coated with the ion exchange resin showed that ammonia, acetic acid, and formaldehyde transfers were 10%, 7% and 5%, respectively. Other contaminants showed no transfer rate in the energy wheel. Measured results for ammonia from [18] are presented in Figure 11, and these results show that as the face velocity increases, EATR decreases. In order to determine if this trend is mainly due to a decrease in actual contaminant transfer rate or due to an increase in dilution at higher face velocities (i.e., higher flow rates), a dashed line is added to Figure 11 which represents change in EATR that would result due to dilution only (i.e., a constant contaminant transfer rate that is diluted more by a higher air flow rate), and is calculated as Eq. (13):

$$EATR_2 = \frac{EATR_1 \cdot V_1}{V_2} \tag{13}$$

where V is the face velocity. Since the measured results follow a similar trend as the dashed line in Figure 11, it can be concluded that the measured decreases in EATR with increasing face velocity are mainly due to dilution and not due to a decrease in actual contaminant transfer rate.

Figure 11 also shows that EATR increases with increasing outdoor air relative humidity in an energy wheel coated with SG and remains constant with increasing outdoor air relative humidity in energy wheel coated with IER.

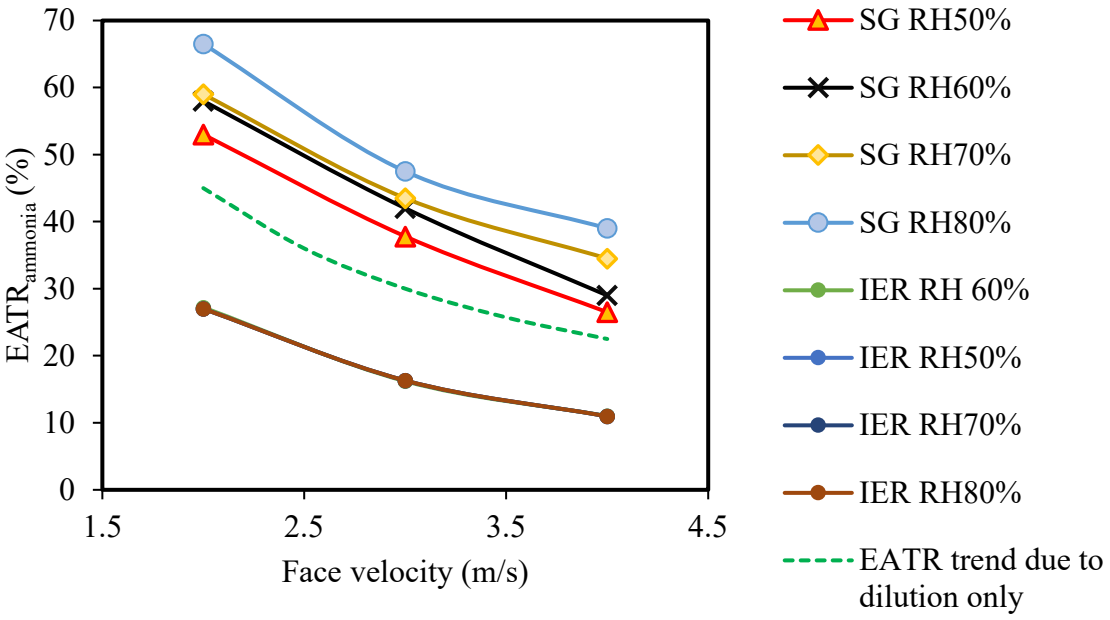

Figure 11. EATR as a function of face velocity at different outdoor air relative humidities and with wheels coated with silica gel (SG) and ion exchange resin (IER) desiccants (OA conditions: T: 30°C, RH: 50-80%, rotational speed: 16 rpm) (Okano et al., 2001). An addition is included (dashed line) which represents the change in EATR that would occur due to dilution of a constant contaminant transfer rate.

Further experiments on different desiccants showed that ion exchange resin, synthesized zeolite, silica gel, and lithium chloride showed 17%, 36%, 43%, and 60% ammonia transfer rate, respectively. Authors discussed that the desiccants with smaller pore sizes showed stronger desiccating capacity and transferred lower amounts of contaminants.

4.2.4. Roulet et al. (Roulet et al., 2002)

Roulet et al. (Roulet et al., 2002) performed contaminant transfer experiments as VOCs with different physical and chemical properties (e.g., saturation degree, boiling point, and polarity) were selected. Studied contaminants included *n*-decane, *n*-butanol, 1-hexanol, phenol, 1,6-dicholorhexane, hexanal, benzaldehyde, limonene, *m*-xylene, mesitylene, and dipropyl ether. A liquid mixture of VOCs was used such that one milliliter of mixture with equal masses of all VOCs was injected into a 200 ℃ air flow at a duration of 30 s. Pulse injection technique was used for injecting mixture. Hot air flow over the injected mixture evaporated contaminants into air and contaminated air delivered to return airstream. Pumps were used for collecting air samples in outdoor, supply, return, and exhaust airstreams. Air samples passed through tubes coated with adsorbing agents. For identifying VOCs concentration, tubes were heated, and adsorbed VOCs were released and stored in a cold trap. VOCs in the cold trap were analyzed using a gas chromatograph. A mass spectrometer was used for identifying each contaminant and a flame ionization detector was used for measuring contaminant concentration.

Experimental results showed that contaminant transfer is related to VOCs boiling point. Chemical compounds with higher boiling points showed higher transfer rates. For example, phenol with a boiling point of 182 ℃ showed a transfer rate of 48% and limonene with a boiling point of 177 ℃ showed a transfer rate of 4%. A physical reason for this result was not provided. This research did not examine effects of operating conditions on VOCs transfer through adsorption/desorption mechanism in energy wheels.

4.2.5. Wolfrum et al. (Wolfrum et al., 2008)

Wolfrum et al. (Wolfrum et al., 2008) studied toluene and n-hexane transfer in a desiccant wheel. A syringe pump with 10 mL volume was used for injecting a liquid mixture of toluene and

n-hexane into the return airstream. The syringe pump injected the VOCs with a flow rate of 1-10 μL/min to a transfer airstream with a flow rate of 1 SCFM. Transfer airstream was used for the purpose of evaporation and proper mixing of VOCs prior to entering return airstream. The transfer airstream entered the return airstream 20 ft upstream the desiccant wheel. Injecting a mixture of toluene and n-hexane with 50:50 mass basis at 18 μL/min flow rate to a transfer airstream with a flow rate of 600 SCFM resulted in concentration of 100 ppb for gaseous toluene and concentration of 125 ppb for gaseous n-hexane.

Air samples were collected using a vacuum pump and passed through a manifold with 10 sorbent tubes. Adsorbed contaminants by the tubes were desorbed and concentrated using a thermo-desorption technique. Gas chromatography technique was used for identifying VOCs concentration. After identification of VOCs concentration in sorbent tubes, each tube was heated to 325 ℃ for 10 minutes to ensure no contaminant remained in the tube for the next experiment. The desiccant wheel transferred 50-80% of the toluene and 10-30% of the n-hexane from return airstream to supply airstream. A total uncertainty of 5% was included in the results. Results showed that contaminant mass conservation was satisfied.

4.2.6. Kodama (Kodama, 2010)

Kodama (Kodama, 2010) studied gaseous contaminant transfer in energy wheels coated with two types of desiccants, i.e., ion-exchange resin and 3Å zeolite. These desiccants were selected due to the selectivity feature on water vapor adsorption/desorption and preventing gaseous contaminants from adsorption/desorption. Tests were conducted for 0 Pa and 250 Pa pressure difference between supply and return airstreams. Supply airstream had a higher flow rate than that of return airstream. Carbon dioxide, propane, ammonia, and formaldehyde were used. Carbon dioxide and propane were injected at constant flow rates using a mass flow controller. Ammonia

and formaldehyde were injected by aeration mechanism such that airflow was supplied to water solutions of contaminants at a controlled flow rate. Then ammonia and formaldehyde rich air was drawn to return airstream.

Air samples were collected in sampling bags and were analyzed by gas detector tubes and gas chromatography. Carbon dioxide and propane concentrations were measured using gas chromatography technique. Formaldehyde and ammonia concentrations were determined by gas detector tubes. Gas detector tubes with a measuring range of 0.2-20 ppm for ammonia and 0.05-4 ppm for formaldehyde were applied.

Results showed that ammonia transfer was between 20-46%, carbon dioxide transfer was between 1-3%, formaldehyde transfer was between 6-35%, and propane transfer was between 1-4%. Ammonia showed higher transfer rate compared to other VOCs, which was attributed to higher water-solubility and smaller molecular size of ammonia. The ion-exchange resin desiccant showed 2-6 times lower contaminant transfer than the 3Å zeolite desiccant. It was concluded that desiccants which adsorb water and water-soluble substances are more likely to transfer VOCs in energy wheels. This research did not present contaminant mass conservation and uncertainty analysis of results.

*4.2.7. **Bayer*** (Bayer, 2011)

Bayer (Bayer, 2011) studied contaminant transfer in energy wheels coated with 3Å molecular sieve desiccants. The studied contaminants included propane, CO_2, methyl isobutyl ketone (MIBK), isopropyl alcohol (IPA), xylene, acetaldehyde, methanol, and acetic acid. The wheel rotated at 20 rpm and the pressure at the supply air stream was 109 Pa (0.44 inches of water column) higher than that of return air stream.

Air samples were collected in Tedlar sampling bags and analyzed with a photoacoustic spectroscopy technique. The air samples were taken 10 times and the average value of concentration was reported. The published report did not describe contaminant injection method and details of contaminant concentration measurement technique. Experiments on an energy wheel coated with a 3Å molecular sieve desiccant showed that contaminant transfer was zero for all contaminants. This work did not contain an uncertainty analysis of results. It should also be noted that these results are published as a report but not in any peer-reviewed journals.

4.2.8. Patel et al. (Patel et al., 2014)

Patel et al. (Patel et al., 2014) performed experiments with toluene and formaldehyde in a RAMEE. Contaminants were injected using calibrated gas mixture injection technique and contaminant evaporation technique. In calibrated gas mixture injection technique, gaseous toluene with a concentration of 150 ppm and gaseous formaldehyde with a concentration of 30 ppm were injected to exhaust airstream. In the contaminant evaporation technique, liquid contaminants were injected into an evaporation chamber using a syringe pump with flow rates from 0.73 μL/hr to 1500 mL/hr. Evaporated contaminants in the evaporation chamber were driven to the exhaust airstream. Air samples were drawn at supply and exhaust ducts to Teflon sampling bags with 100 L volume. Air samples were analyzed using Fourier Transform Infrared (FTIR) spectroscopy technique.

The contaminant transfer in the RAMEE occurred due to pressure differential between contaminants in airstream and contaminants on the surface of the membrane in LAMEEs. This pressure differential occurred because of contaminant concentration gradient between the two media. For transferring contaminants from exhaust LAMEE to supply LAMEE, contaminants needed to transfer from exhaust airstream to membrane surface through convection and diffusion

mechanisms. Then, contaminants diffused through the membrane toward the liquid desiccant flow where contaminant pressure was low. Contaminants dissolved in liquid desiccant and flowed through the running loop to supply LAMEE. In the supply LAMEE, contaminants diffused through the membrane and reached the supply airstream.

Formaldehyde showed 4-6% EATR and toluene showed 2-3% EATR. Uncertainty for formaldehyde and toluene transfer were 4% and 3%, respectively. Higher EATR for formaldehyde was attributed to higher diffusivity and water solubility than those of toluene. These values are smaller than 71% toluene transfer in a desiccant wheel (Wolfrum et al., 2008) and 8-15% formaldehyde transfer in energy wheels (Andersson et al., 1993; Fisk et al., 1985). Moreover, changes in air flow rate, environmental conditions and liquid desiccant flow rate showed no significant effect on the transfer rate of contaminants in RAMEE.

4.2.9. Hult et al. (Hult et al., 2014)

Hult et al. (Hult et al., 2014) investigated formaldehyde transfer rate in energy wheels. Experiments for formaldehyde cross-contamination started with injecting liquid formalin into an evaporation chamber using a glass syringe pump. Gaseous formaldehyde with a concentration range of 60-75 $\mu g/m^3$ was delivered to the return airstream. Air samples were collected with 2,4-dinitrophenylhydrazine silica samplers at outdoor, supply, return, and exhaust airstreams.

Results from field experiments showed that formaldehyde transfer rate was between 28-29%. CO_2 concentration measurement showed that around 92-100% of formaldehyde transfer occurred due to air leakage and carryover mechanisms, and only 0-8% of formaldehyde transfer occurred due to adsorption/desorption mechanism. Chamber experiments in different air flow rates showed that formaldehyde transfer rate decreased as air flow rate increased.

Similarly, formaldehyde adsorption/desorption decreased as the air flow rate increased. For example, adsorption/desorption contribution in formaldehyde transfer was 30% at air flow rate of 85 m^3/hr. and 10% at air flow rate of 340 m^3/hr. This might have occurred due to reverse relation between air flow rate and residence time of formaldehyde on desiccants. In other words, as air flow rate decreased, there was more time for formaldehyde molecules to adsorb on desiccants. Formaldehyde transfer results were shown with a total uncertainty of 3% for field and chamber experiments.

4.2.10. Nie et al. (Nie, Yang, Fang, & Kong, 2015)

Nie et al. (Nie et al., 2015) studied gaseous contaminant transfer in a flat plate enthalpy exchanger. Toluene, acetone, and ammonia were used. These contaminants were continuously injected in return airstream with a washing bottle connected to the injection port. Details of contaminants injection technique such as operating conditions of washing bottle and mass of injected contaminants were not provided. Air samples were taken at outdoor, supply, return, and exhaust airstreams. Plastic tubes were used for delivering air samples to a photoacoustic multi-gas analyzer.

Results showed that from return airstream to supply airstream toluene transfer was between 7-8%, acetone transfer was between 5-6% and ammonia transfer was between 8-9%. Experiments in different outdoor conditions showed that toluene transfer in flat plate enthalpy exchanger was little affected by different outdoor temperatures and humidity ratios. For example, when outdoor air temperature was 35 ℃ and humidity ratio was 22 g/kg, toluene transfer was 7%. When outdoor air temperature decreased to 11 ℃ and humidity ratio decreased to 6 g/kg, toluene transfer increased to 8%. Similar results were found for acetone and ammonia. This study did not present uncertainty analysis and contaminant mass conservation in experiments.

4.3. Summary of literature review

Table 2.2 provides a summary of EATR and uncertainties measured on various energy exchangers in the literature. An established test methodology for measuring air leakage and carryover in energy wheels is available in ASHRAE Standard 84 (2020) (ANSI/ASHRAE, 2020). However, based on the literature review, a similar test methodology for determining the contribution of adsorption/desorption mechanism in gaseous contaminant transfer in energy wheels is missing.

Table 11. Summary of the gaseous contaminant transfer rates and uncertainties measured on various energy exchangers.

Gaseous contaminants	Energy exchanger	Transfer rate	Uncertainty	Reference
17. Acetaldehyde	Energy wheel	17%	NR	(Bayer, 2011)
18. Ammonia	Energy wheel	10-46%	NR	(Okano et al., 2001), (Kodama, 2010).
	Flat plate enthalpy exchanger	8-9%		(Nie et al., 2015)
19. Acetic acid	Energy wheel	7-36%	NR	(Okano et al., 2001), (Bayer, 2011).
20. Methanol	Energy wheel	0-11%	NR	(Okano et al., 2001), (Bayer, 2011).
21. Isopropyl alcohol	Energy wheel	0-4%	NR	(Okano et al., 2001), (Bayer, 2011).
22. Methyl isobutyl ketone	Energy wheel	0-3%	NR	(Okano et al., 2001), (Bayer, 2011).
23. Xylene	Energy wheel	0-30%	NR	(Okano et al., 2001), (Bayer, 2011), (Roulet et al., 2002).
24. Carbon dioxide	Energy wheel	0.6-5%	NR	(Kodama, 2010), (Bayer, 2011), (Kassai, 2018).
	Flat plate type mass exchanger	1%		(Sparrow et al., 2001).
25. Propane or hexane	Energy wheel	0.2-7%	5%	(Kodama, 2010), (Bayer, 2011), (Fisk et al., 1985).
	Flat plate enthalpy exchanger	6-8%		(Fisk et al., 1985).
	Desiccant wheel	20%		(Wolfrum et al., 2008).
26. Phenol	Energy wheel	30-75%	NR	(Roulet et al., 2002).
27. Sulfur hexafluoride	Energy wheel	5-26%	1%	(Bayer, 2011),

				(Khoury et al., 1988), (Fisk et al., 1985), (Roulet et al., 2002).
	Flat plate enthalpy exchanger	5-8%		(Fisk et al., 1985)
28. Formaldehyde	Energy wheel	6-35%	3-29%	(Okano et al., 2001), (Kodama, 2010), (Andersson et al., 1993), (Bayer, 2011), (Hult et al., 2014), (Fisk et al., 1985).
	Flat plate enthalpy exchanger	7-12%		(Fisk et al., 1985).
	RAMEE	5-6%		(Patel et al., 2014).
29. Nitrous oxide	Energy wheel	1-54%	3%	(Shang et al., 2001).
30. Acetone	Energy wheel	0	NR	(Okano et al., 2001).
	Flat plate enthalpy exchanger	5-6		(Nie et al., 2015).
31. Toluene	RAMEE	2-3%	3-5%	(Patel et al., 2014).
	Desiccant wheel	70%		(Wolfrum et al., 2008).
	Flat plate enthalpy exchanger	7-8%		(Nie et al., 2015).
	Energy wheel	0-30%		(Okano et al., 2001).
32. Inert tracer gas (For measuring air leakage and carryover)	Air-to-air heat/energy exchanger	----	3%	(ANSI/ASHRAE, 2020), CSA Standard C 439-18 (2018) (Canadian Standards Association, 2018).

RAMEE = Run-around membrane energy exchanger, NR = uncertainty not reported

4.4. Literature data analysis

In the following sections, the literature data will be presented to show the effect of different operating and design parameters on EATR.

4.4.1. Effect of temperature on EATR

Figure 12 shows EATR versus outdoor air temperature for different VOCs. There is no clear relationship between EATR and outdoor air temperature because the design and operating parameters are different in each test (e.g., different exchangers, desiccants, face velocities, pressure conditions, and purge sections). Figure 12 tends to indicate that these other parameters play a more important role in contaminant transfer than temperature.

Okano et al. (Okano et al., 2001) studied the effect of outdoor air temperature on EATR for ammonia while keeping other parameters constant. They found that changing outdoor air temperature does not change EATR significantly, as can be seen in Figure 13. Okano et al. (Okano et al., 2001) found that energy wheels with different desiccants (silica gel (SG)) and ion exchange resin (IER)) show very similar trends for EATR versus outdoor air temperature.

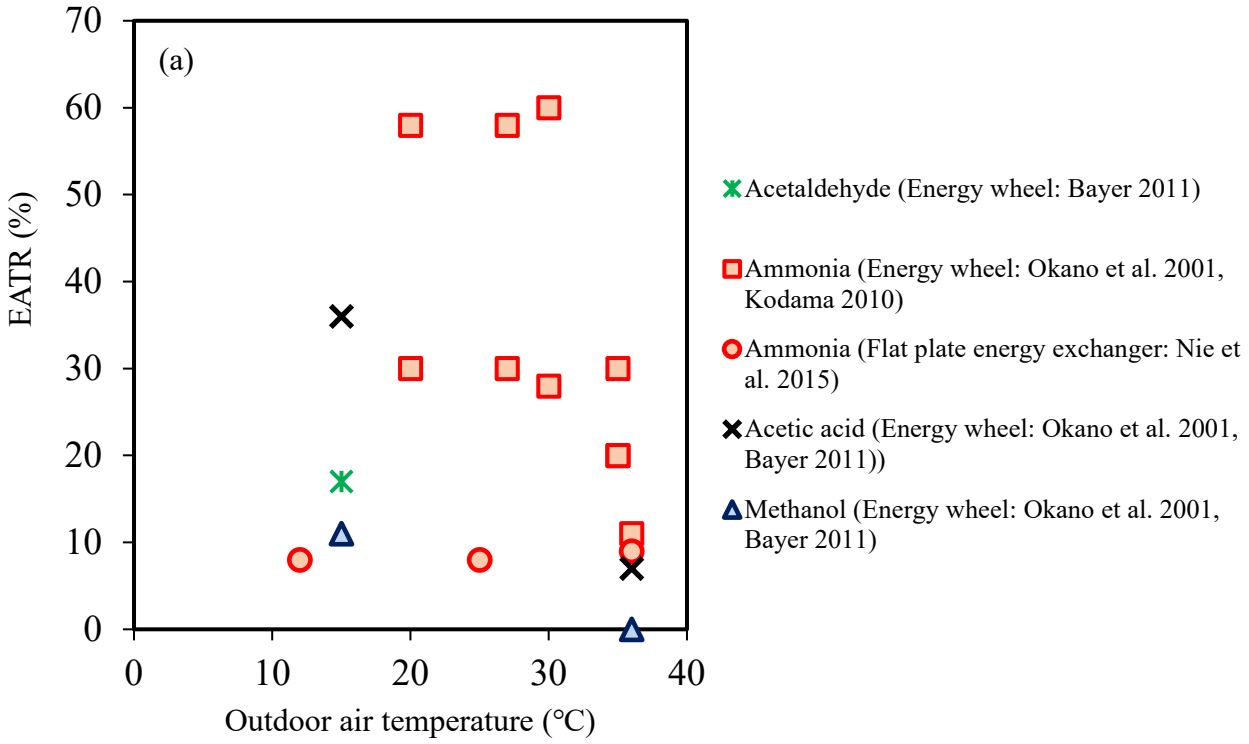

Figure 12. (a) EATR for different VOCs versus outdoor air temperatures at various test conditions.

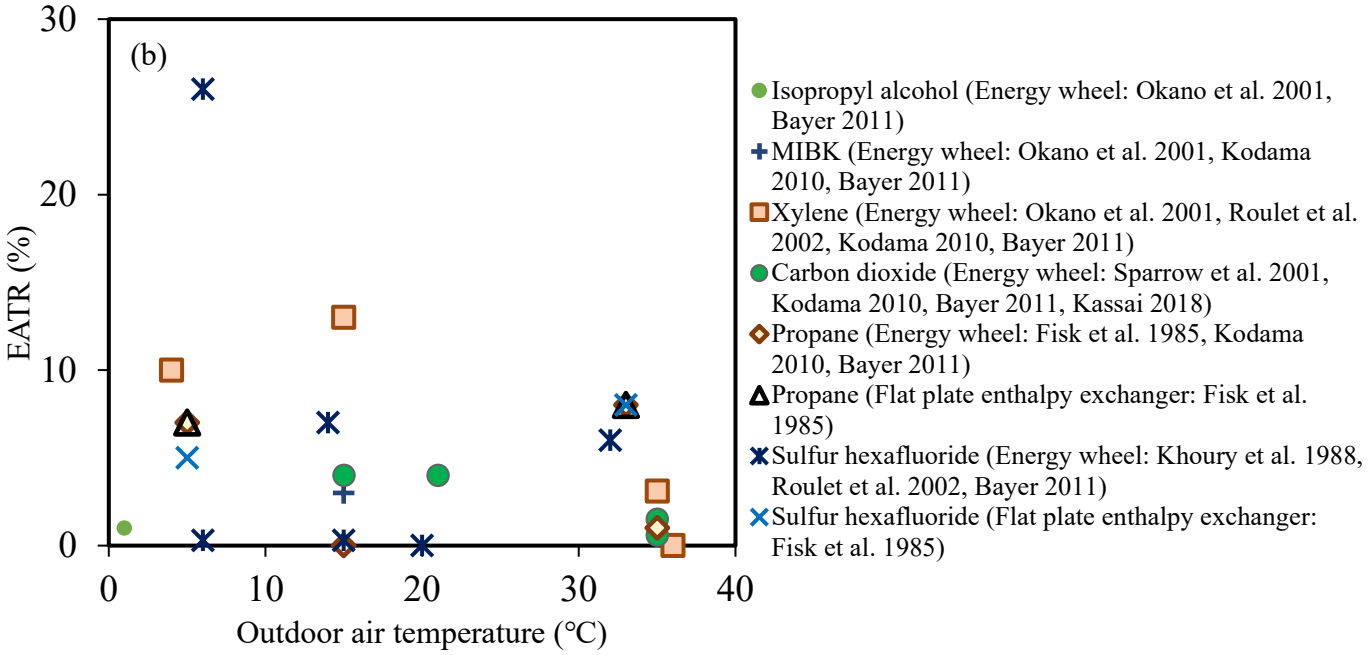

Figure 11. (b) EATR for different VOCs versus outdoor air temperatures at various test conditions.

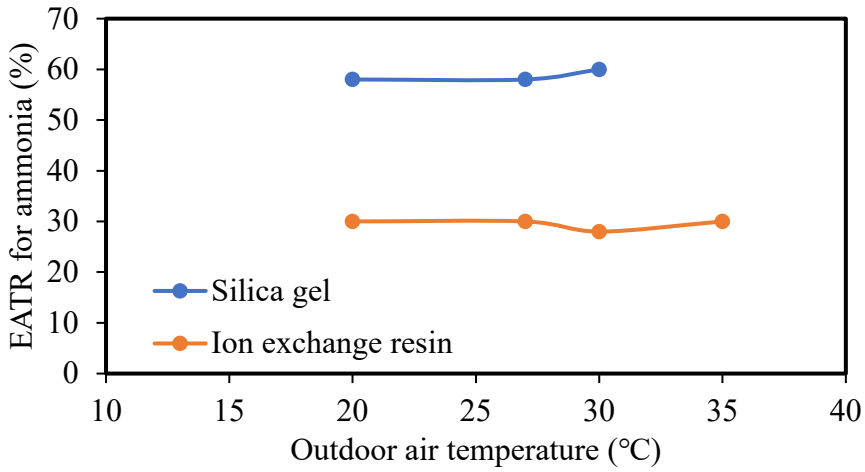

Figure 13. EATR for ammonia versus outdoor air temperature in constant test conditions (Okano et al., 2001).

4.4.2. Effect of humidity on EATR

Figure 14 shows that EATR tends to decrease as the outdoor air relative humidity increases for different VOCs. However, there is a large scatter in the data because the design and operating parameters are not the same in all tests.

Figure 15 presents the effect of outdoor air relative humidity on EATR for ammonia as measured by Okano et al. (Okano et al., 2001). It is seen that EATR increases or remains constant with increasing outdoor air relative humidity depending on the desiccant material coated on energy wheel, which is slightly different than the apparent trend in Figure 14. Okano et al. (Okano et al., 2001) found that increasing the outdoor air relative humidity, increases EATR for ammonia in energy wheels with a silica gel desiccant but does not change EATR in energy wheels with an ion exchange resin desiccant.

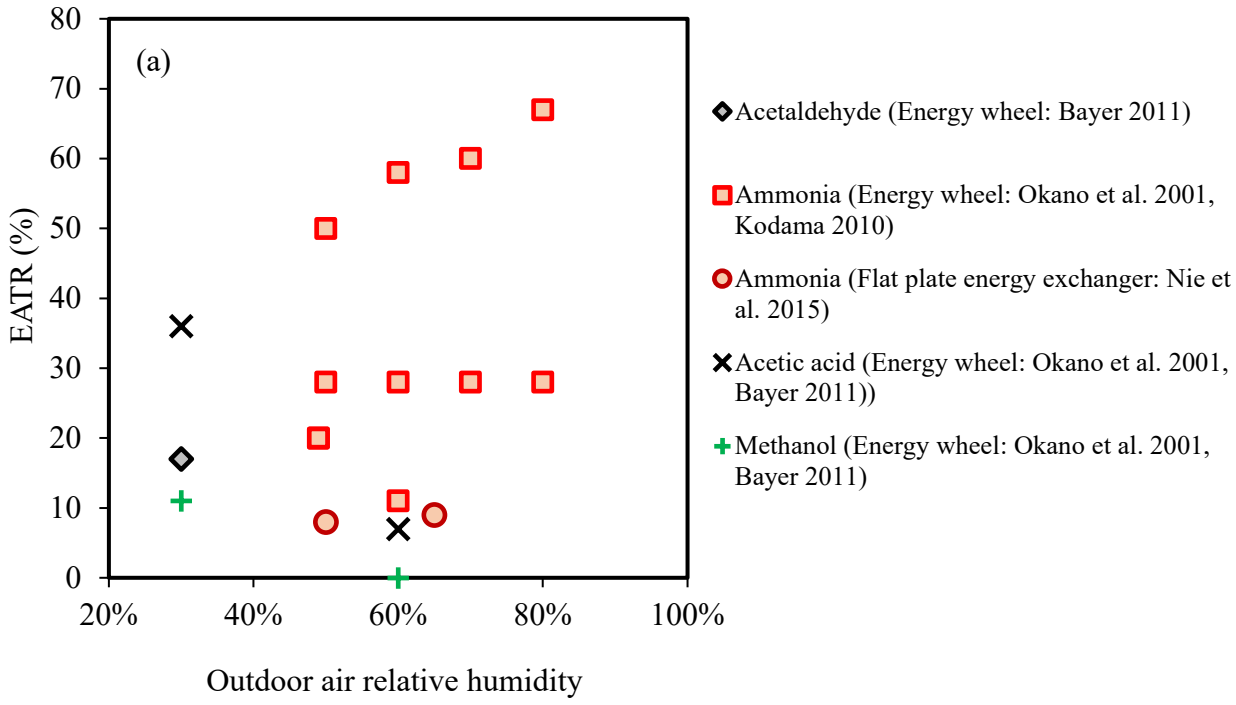

Figure 14. (a) EATR for different VOCs versus outdoor air relative humidity at various test conditions.

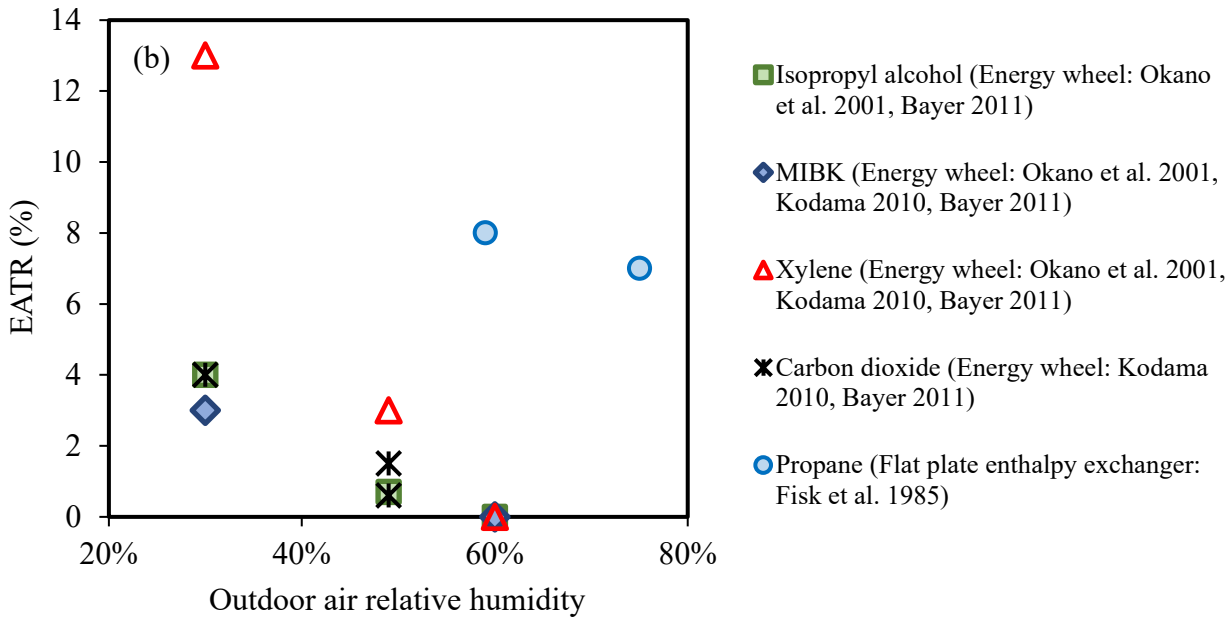

Figure 13. (b) EATR for different VOCs versus outdoor air relative humidity at various test conditions.

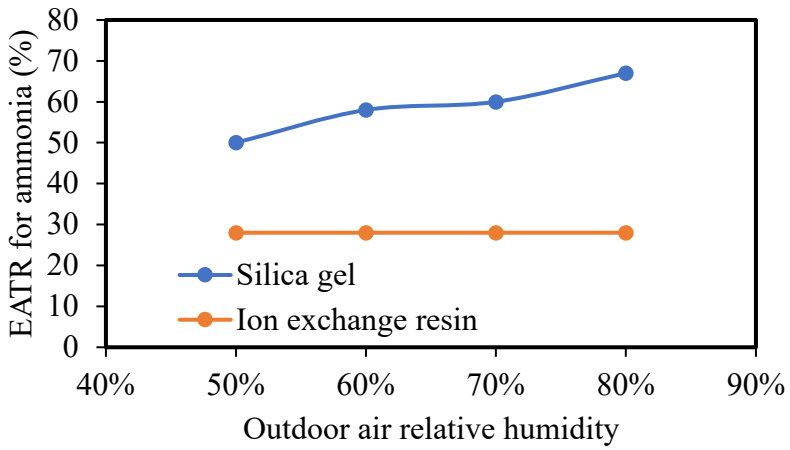

Figure 15. EATR for ammonia versus outdoor air relative humidity in constant test conditions (Okano et al., 2001).

4.4.3. Effect of face velocity on EATR

One may expect the contaminant transfer to depend on the exchanger design (NTU and Cr*). However, since most researchers do not report NTU and Cr* or provide enough information to calculate NTU and Cr*, the effect of face velocity will be presented here. According to Eqs. (11) and (12), NTU and Cr* are inversely proportional to face velocity (Kays & A. L. London, 1984; Shah & Sekulic, 2003).

The effect of face velocity on EATR was studied by Okano et al. (Okano et al., 2001) and is presented in Figure 16. Figure 16 shows a consistent trend of decreasing EATR with increasing face velocity (decreasing NTU and Cr*) regardless of the desiccant. This trend may be due to the fact that if the contaminant transfer rate is constant, the percent carryover will decrease as the face velocity (flow rate of air) increases. Figure 16 also contains dashed lines to indicate how EATR would change if the contaminant transfer rate was constant for the measured contaminant transfer rate at a face velocity of 2 m/s using Eq. (13) in Section 4.2.3. Comparing the solid lines (measured data) and the dashed lines (data based on a constant contaminant transfer rate and dilution) shows that the actual EATR is quite similar (within ±5%) to the EATR that would exist due to a constant contaminant transfer rate and dilution. This indicates that the actual contaminant transfer rate seems to change little with face velocity but the dilution of the contaminant changes with flow rate as expected. It should also be noted that this study (Okano et al., 2001) did not report uncertainty analysis of the EATR results.

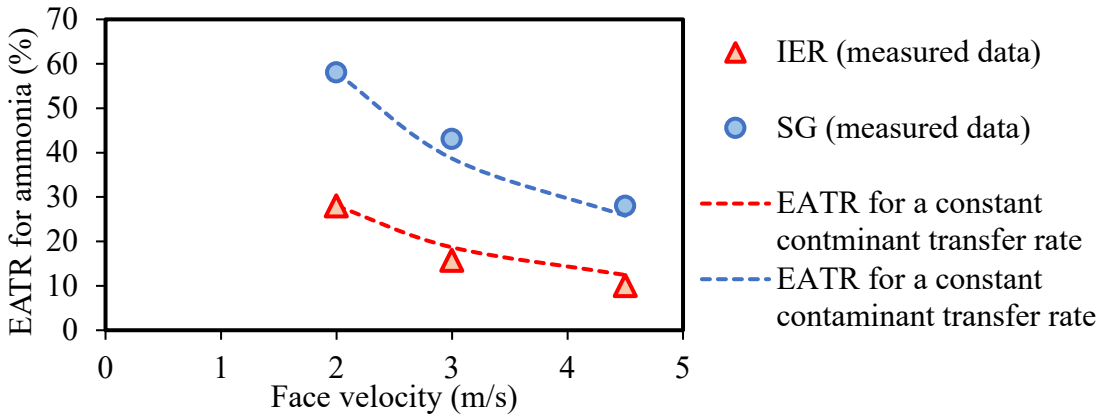

Figure 16. EATR for ammonia versus air face velocity in constant test conditions (solid lines) (Okano et al., 2001) compared to EATR that would exist if the total transfer rate were constant at 2 m/s (dashed lines).

4.4.4. Effect of effectiveness on EATR

Figure 17 presents EATR versus total effectiveness for different energy exchangers with different contaminants. In general, EATR increases with the total effectiveness. For example, for acetic acid, when the total effectiveness increases from 75% to 90%, EATR increases almost 5 times (from 7% to 36%). This might be due to decrease in face velocity, which would increase contaminant transfer through carryover as noted in the previous section, or due to the increased adsorption/desorption in the energy wheels (adsorption of water vapor also increases as the effectiveness increases). For some VOCs and exchangers (e.g., ammonia in the flat plate energy exchanger (Nie et al., 2015) and propane in energy wheel (Bayer, 2011; Fisk et al., 1985; Kodama, 2010)), EATR decreases as the total effectiveness increases.

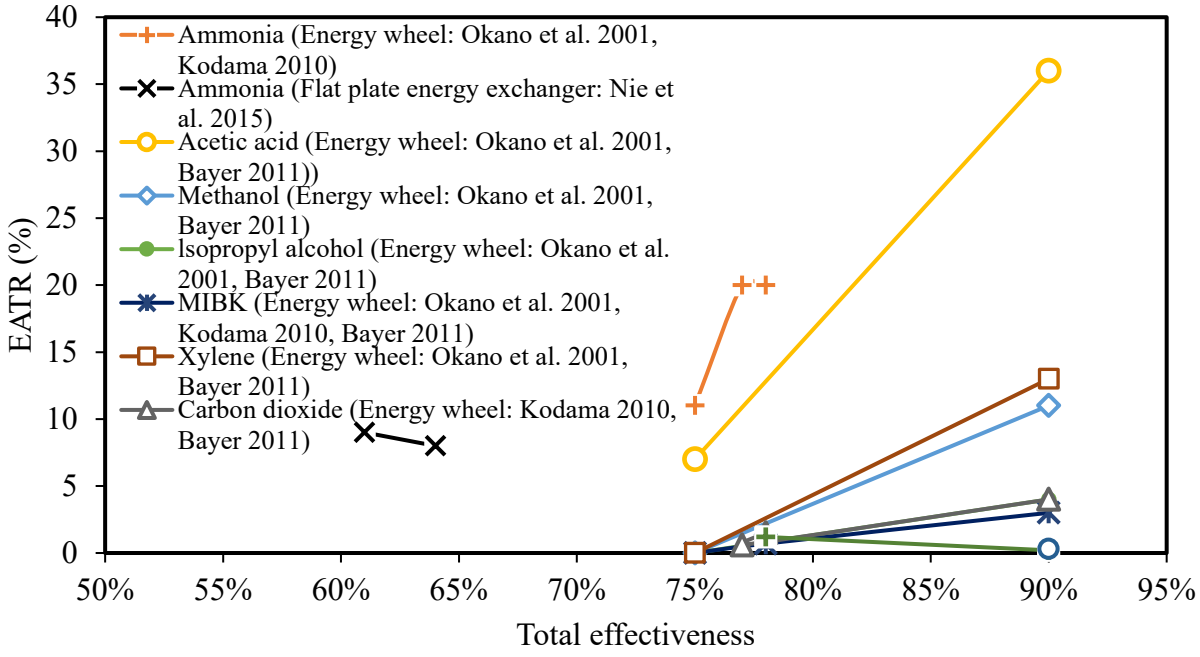

Figure 17. EATR versus total effectiveness of different energy exchangers.

5. NEW METHOD TO DETERMINE THE CONTAMINANT TRANSFER DUE TO ADSORPTION/DESORPTION

The ASHRAE Standard 84 (ANSI/ASHRAE, 2020) and CSA C 439-18 (Canadian Standards Association, 2018) test standards require an inert tracer gas such as sulfur hexafluoride and same inlet conditions (temperature and relative humidity) for contaminant transfer experiments. These experiments measure contaminant transfer in terms of EATR by bulk airflow only. They do not include the contaminant transfer due to phase change mechanisms such as adsorption/desorption and transfer during extreme conditions such as condensation and frosting. Therefore, a methodology needs to be developed to consider these effects. The literature review revealed that the phase change mechanisms significantly contribute to gaseous contaminant transfer in energy exchangers. It depends on many factors, such as the nature of the contaminant, type of desiccant material, exchanger design considerations, and operating conditions. Hence, a

new parameter, Exhaust Contaminant Transfer Ratio *(ECTR)* is proposed to quantify the transfer of gaseous contaminants in rotary wheels. The $ECTR_{phase\ change}$ is contribution of the phase change mechanisms in gaseous contaminant transfer in energy exchangers and the *ECTR* is the total contaminant transfer. The $ECTR_{phase\ change}$ is determined by subtracting the EATR measured with an inert tracer gas (SF_6 – according to ASHRAE standard 84 (ANSI/ASHRAE, 2020)) from the *ECTR* measured with a different non-inert gas (e.g. VOCs) as given in Eq. (14).

$$ECTR_{phase\ change} = ECTR - EATR_{inert} \tag{14}$$

The $ECTR_{phase\ change}$ for different gaseous contaminants which were calculated from data in the literature using Eq. (14) are presented in Figure 18. It is observed that $ECTR_{phase\ change}$ is highest for acetic acid, phenol, and acetaldehyde. This may be due to high water solubility and the smaller molecular size of these VOCs. Xylene was studied in two research papers (Bayer, 2011; Roulet et al., 2002) and the $ECTR_{phase\ change}$ for xylene is reported as 3% and 13%. This difference between the $ECTR_{phase\ change}$ values could be due to the different design considerations and test conditions. Additional research is required to verify the proposed method of quantifying contaminant transfer due to the phase change mechanisms $ECTR_{phase\ change}$ and to determine the uncertainty in $ECTR_{phase\ change}$ for various gases and operating conditions.

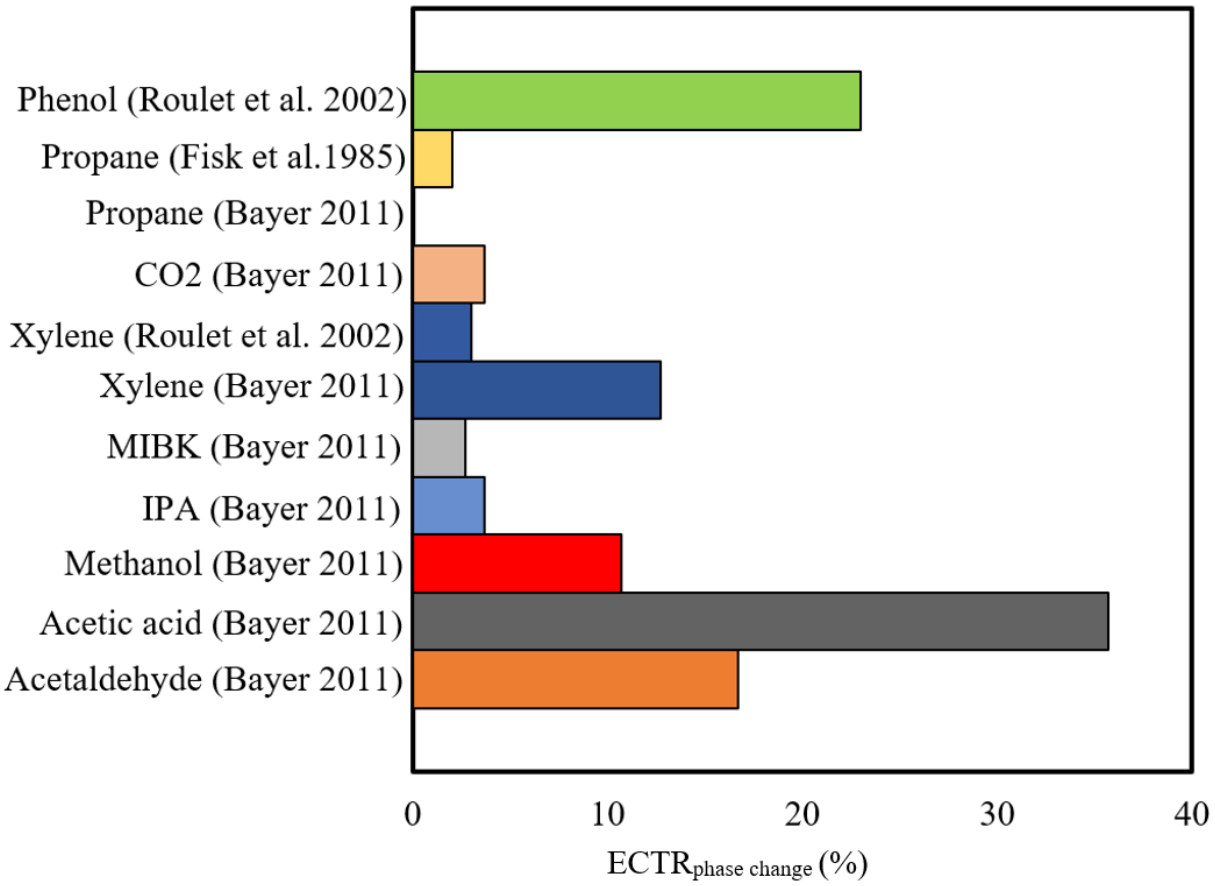

Figure 18. ECTR $_{\text{phase change}}$ for different gaseous contaminants and VOCs reported in the literature.

6. CONCLUSIONS

This paper reviewed the available experimental studies in the area of contaminant transfer in energy exchangers. Several papers have reported the contaminant transfer rate of various contaminants, and most of them were focused on rotary-type energy exchanges. Based on the available literature on contaminant transfer in energy exchangers, the following conclusions can be made:

- There are three main mechanisms that contribute to gaseous contaminant transfer in energy exchangers: air leakage, carryover, and adsorption/desorption.

- Gaseous contaminant transfer due to air leakage and carryover mechanisms has been studied and measured extensively in the literature using inert gases. An established test methodology for measuring contaminant transfer due to air leakage and carryover exists and is included in test standards ASHRAE 84-2020 (ANSI/ASHRAE, 2020) and CSA C439 (Canadian Standards Association, 2018). Contaminant transfer due to air leakage and carryover (i.e., bulk air flow from the exhaust side to the supply side of the exchanger) is quantified using exhaust air transfer ratio (EATR).

- Several researchers have measured contaminant transfer of non-inert gases in energy exchangers. While such measurements inherently include all transfer mechanisms (air leakage, carryover, and adsorption/desorption), no test methods exist in the literature to quantify the adsorption/desorption mechanism. Thus, a method to quantify contaminant transfer due to adsorption/desorption is proposed and applied in this paper. More research is required to verify the proposed method and its uncertainty.

- The literature review showed that gaseous contaminant transfer rates vary between 0% and 75%. The highest transfer rates were measured for phenol, toluene, nitrous oxide, ammonia, acetic acid, and formaldehyde. A common chemical characteristic among these contaminants, except for nitrous oxide (a tracer, and a non-reacting gas) is their high water solubility, which may be a possible reason for high contaminant transfer rates. The high value of EATR for nitrous oxide could be due to higher pressure on the exhaust side than the supply side of the energy wheel.

- The literature review showed that uncertainties in measured EATR varied between 1% and 30%, but most studies did not include a detailed uncertainty analysis. Furthermore, most studies did not determine if the experiments conserved mass of gaseous contaminants.
- The literature review showed that the exchanger design parameters (effectiveness and face velocity) have more significant effect on EATR than the operating conditions (relative humidity and temperature) for the case of energy wheels.

REFERENCES

Andersson, B., Andersson, K., Sundell, J., & Zingmark, P. -A. (1993). Mass transfer of contaminants in rotary enthalpy exchangers. *Indoor Air*, *3*(2), 143–148. https://doi.org/10.1111/j.1600-0668.1993.t01-1-00009.x

ANSI/ASHRAE. (2020). *Standard 84, Method of testing air-to-air heat/energy exchangers*. Atlanta.

ASHRAE. (2012). *HVAC Systems and Equipment*. Atlanta.

ASME/ANSI. (1998). *Performance Test Code 19.1 Test Uncertainty: Instruments and Apparatus*. New York.

Bayer, C. W. (2011). *Total energy recovery wheel contaminant transfer study report*. Prepared for SEMCO LLC, Columbia.

Besant, R. W., & Simonson, C. J. (2000). Air-to-air energy recovery. *ASHRAE Journal*, *42*(May).

Brown, S. K., Sim, M. R., Abramson, M. J., & Gray, C. N. (1994). Concentrations of Volatile

Organic Compounds in Indoor Air - A Review. *Indoor Air*, *4*(2), 123–134. https://doi.org/10.1111/j.1600-0668.1994.t01-2-00007.x

Canadian Standards Association. (2018). *Standard laboratory methods of test for rating the performance of heat/energy-recovery ventilators*. *Canadian Standards Association*. Canada: CSA Group.

Fan, H., Simonson, C. J., Besant, R. W., & Shang, W. (2006). Performance of a run-around system for HVAC heat and moisture transfer applications using cross-flow plate exchangers coupled with aqueous lithium bromide. *HVAC & R Research*, *12*(2), 313–336. https://doi.org/10.1080/10789669.2006.10391181

Fisk, W., Pedersen, B., Hekmat, D., Chant, R., & Kaboli, H. (1985). Formaldehyde and tracer gas transfer between airstreams in enthalpy-type Air-to-air heat exchangers. *ASHRAE Transactions*, *91*(Part 1B), 173–186.

Ghadiri Moghaddam, D., Besant, R. W., & Simonson, C. J. (2015). A methodology for scaling a small-scale energy exchanger performance results to a full-scale energy exchanger. *International Journal of Heat and Mass Transfer*, *82*, 555–567. https://doi.org/10.1016/j.ijheatmasstransfer.2014.11.040

Harčárová, K., Vilčeková, S., & Balintova, M. (2020). Building materials as potential emission sources of VOC in the indoor environment of buildings. *Key Engineering Materials*, *838*, 74–80. https://doi.org/10.4028/www.scientific.net/KEM.838.74

Hult, E. L., Willem, H., & Sherman, M. H. (2014). Formaldehyde transfer in residential energy recovery ventilators. *Building and Environment*.

https://doi.org/10.1016/j.buildenv.2014.01.004

Kassai, M. (2018). Experimental investigation of carbon dioxide cross-contamination in sorption energy recovery wheel in ventilation system. *Building Services Engineering Research and Technology*, *39*(4), 463–474. https://doi.org/10.1177/0143624417744733

Kassai, M. (2019). Newly Developed Direct Current Refrigeration Technique to Improve the Sustainability of Sausage Drying Process. *Journal of Sustainable Development of Energy, Water and Environment Systems*, *7*(4), 631–640. https://doi.org/10.13044/j.sdewes.d7.0278

Kays, W. M., & A. L. London. (1984). *Compact heat exchangers* (Third edit). New York: McGraw-Hill, Inc.

Khoury, G. A., Chang, S. N., Lessley, D. A., Abdelghani, A. A., & Anderson, A. C. (1988). An investigation of reentrainment of chemical fume hood exhaust air in a heat recovery unit. *American Industrial Hygiene Association Journal*, *49*(2), 61–65. https://doi.org/10.1080/15298668891379396

Kodama, A. (2010). Cross-contamination test of an enthalpy wheel loading a strong acidic cation ion-exchange resin or 3A zeolite as a desiccant material. *Journal of Chemical Engineering of Japan*, *43*(10), 901–905. https://doi.org/10.1252/jcej.10we148

Krishnan, E. N., Ramin, H., Gurubalan, A., & Simonson, C. J. (2021). Experimental methods to determine the performance of desiccant coated fixed-bed regenerators (FBRs). *International Journal of Heat and Mass Transfer*.

Natural Resources Canada. (2020). HVAC & Energy Systems. Retrieved July 4, 2020, from https://www.nrcan.gc.ca/energy/efficiency/data-research-and-insights-energy-efficiency

Nie, J., Yang, J., Fang, L., & Kong, X. (2015). Experimental evaluation of enthalpy efficiency and gas-phase contaminant transfer in an enthalpy recovery unit with polymer membrane foils. *Science and Technology for the Built Environment*, *21*(2), 150–159. https://doi.org/10.1080/10789669.2014.967165

Okano, H., Tanaka, H., Hirose, T., Funato, H., Ishihara, S., & Chirarattananon, S. (2001). A novel total heat exchanger with little odor transfer using ion exchange resin as a desiccant. *ASHRAE Transactions*.

Patel, H., Ge, G., Abdel-Salam, M. R. H., Abdel-Salam, A. H., Besant, R. W., & Simonson, C. J. (2014). Contaminant transfer in run-around membrane energy exchangers. *Energy and Buildings*, *70*, 94–105. https://doi.org/10.1016/j.enbuild.2013.11.013

Rabah, A. A., Fekete, A., & Kabelac, S. (2009). Experimental investigation on a rotary regenerator operating at low temperatures. *Journal of Thermal Science and Engineering Applications*, *1*(4), 1–9. https://doi.org/10.1115/1.4001543

Roulet, C. A., Pibiri, M. C., Knutti, R., Pfeiffer, A., & Weber, A. (2002). Effect of chemical composition on VOC transfer through rotating heat exchangers. *Energy and Buildings*, *34*(8), 799–807. https://doi.org/10.1016/S0378-7788(02)00098-1

Shah, R. K., & Sekulic, D. P. (2003). *Fundamentals of Heat Exchanger Design*. Hoboken: John Wiley & Sons, Inc. https://doi.org/10.1002/9780470172605

Shang, W., & Besant, R. W. (2008). Theoretical and experimental methods for the sensible effectiveness of Air-to-Air energy recovery wheels. *HVAC and R Research*, *14*(3), 373–396. https://doi.org/10.1080/10789669.2008.10391015

Shang, W., Wawryk, M., & Besant, R. W. (2001). Air crossover in rotary wheels used for air-to-air heat and moisture recovery. *ASHRAE Transactions*, 72–84.

Shokouhmand, H., & Hasanpour, M. (2020). Effect of number of plates on the thermal performance of a plate heat exchanger with considering flow maldistribution. *Journal of Energy Storage*, *32*(June), 101907. https://doi.org/10.1016/j.est.2020.101907

Simonson, C. J., & Besant, R. W. (1999). Energy wheel effectiveness: Part I-development of dimensionless groups. *International Journal of Heat and Mass Transfer*, *42*(12), 2161–2170. https://doi.org/10.1016/S0017-9310(98)00325-1

Sparrow, E. M., Abraham, J. P., Martin, G. P., & Tong, J. C. Y. (2001). An experimental investigation of a mass exchanger for transferring water vapor and inhibiting the transfer of other gases. *International Journal of Heat and Mass Transfer*, *44*(22), 4313–4321. https://doi.org/10.1016/S0017-9310(01)00044-8

Wang, C., Sadeghian, P., & Sadrizadeh, S. (2019). Effect of staff number on the bacteria contamination in operating rooms with temperature controlled airflow ventilation and turbulent mixing ventilation. *Building Simulation Conference Proceedings*, *2*, 747–753. https://doi.org/10.26868/25222708.2019.210960

Wolfrum, E. J., Peterson, D., & Kozubal, E. (2008). The volatile organic compound (VOC) removal performance of Desiccant-Based dehumidification systems: Testing at Sub-ppm VOC concentrations. *HVAC & R Research*, *14*(1), 129–140. https://doi.org/10.1080/10789669.2008.10390998

Yurdakul, S., Civan, M., Özden, Ö., Gaga, E., Döğeroğlu, T., & Tuncel, G. (2017). Spatial

variation of VOCs and inorganic pollutants in a university building. *Atmospheric Pollution Research*, *8*(1), 1–12. https://doi.org/10.1016/j.apr.2016.07.001

Liaison report: TC 1.4 (Guideline 36)

Jim Coogan reported:

SGPC has drafted SOO for laboratory rooms. Committee has voted to send to public review. TC 9.10 requested to delay the review. Doesn't seem like that is happening. SGPC chair met with TC officers suggested TC participate actively in review. Also set up Kelley Cramm as "Designated Reviewer", allowing access to draft before public review.

Some topics to explore:

- Priority of air flow drivers in the room
- Potential for excessively negative pressure, trapping occupant when supply system shuts off; and means to address it
- Flow tracking details
- Varying needs for speed and accuracy in air flow control
- Specification issues adjacent to SOO, like qualifying products and contractors
- Features supporting duct pressure reset

Overall, this can be an opportunity to raise the standards in lab control. It might take some effective political work.

Kelley Cramm

From: Ryan Parker <Ryan.Parker@rwdi.com>
Sent: Tuesday, January 23, 2024 4:58 PM
To: Kelley Cramm
Cc: Neetha Vasan
Subject: TC 4.3 Liaison report to TC 9.10

[EXTERNAL EMAIL]

Hi Kelley,

For 4.3: 2 Handbook chapters revisions will be available for review in April. These can be circulated to you for review if you are interested. In particular Chapter 16, Ventilation and Infiltration, had a large re-write and reorganization. You can join TC 4.3 online or reach out to Neetha.Vasan@rwdi.com if you would like to review the chapters.

Volume	Chapter	Lead
2025 Fundamentals	Chapter 16 Ventilation and Infiltration	Marianne Touchie, Cara Lozinsky, Justin Berquist
2025 Fundamentals	Chapter 24 Airflow Around Buildings	Ted Stathopoulos

Ryan Parker, PhD | Senior Engineer
RWDI
Climate & Performance Engineering
601 SW 2nd Avenue, Suite 1140, Portland, OR 97204 USA
T: +1.503.467.4710 ext 5735 | E: ryan.parker@rwdi.com | rwdi.com

Climate and performance expertise. When you need it.

Liaison report: MTG ACR

Kishor Khankari reported:

Focused on preparing a research project. Writing and refining work statement. Combines CFD and physical experiments. Varies size of room. Varies number, type and arrangement of grills and diffusers. Varies air flow rates.

WS will be available to TC 9.10.

Arranging co-funding with Price Industries.

Looking for potential bidders.

Kelley Cramm

From: Ken W. Crooks <kcrooks@newenglandlab.com>
Sent: Tuesday, January 23, 2024 5:11 PM
To: Kelley Cramm
Subject: TC9.10 NFPA45 Liaison Report

[EXTERNAL EMAIL]

Hi Kelley,
I recently changed jobs and have lost some of the important links such as to the ASHRAE page for posting Liaison Reports… Sorry.

Below is the report I gave today during the main TC9.10 committee meeting:

- NFPA45-2024 edition was released in the fall of 2023.
- The 2024 edition includes many minor changes, plus a couple significant changes: laboratories in health care facilities are now included in the scope, and numerous new sections were added for ductless fume hood requirements.
- NFPA45-2027 (next edition) has just entered the Public Input phase. Public input is open until Jan 7, 2025. Go to https://www.nfpa.org/codes-and-standards/4/5/45 to submit input.

Thank you,
Ken

Ken Crooks | Business Development A/E
New England Laboratory Casework Co., Inc.
3 Arrow Drive | Woburn, MA 01801
direct 781.503.8808 | mobile 781.603.5164
kcrooks@newenglandlab.com | www.newenglandlab.com

I2SL

Molecular Foundry building at Lawrence Berkeley National Laboratory;
Source: Berkeley Lab—Roy Kaltschmidt

I2SL

Labs2Zero

Decarbonizing the World's Laboratories

Check out the new look of www.i2sl.org

- **New Branding for I2SL**
- **2024 I2SL Conference – Sept. 29 – Oct 2, 2024 – St. Louis**
  - ✓ **2023 Conference – 585 attendees – 120 presentations**

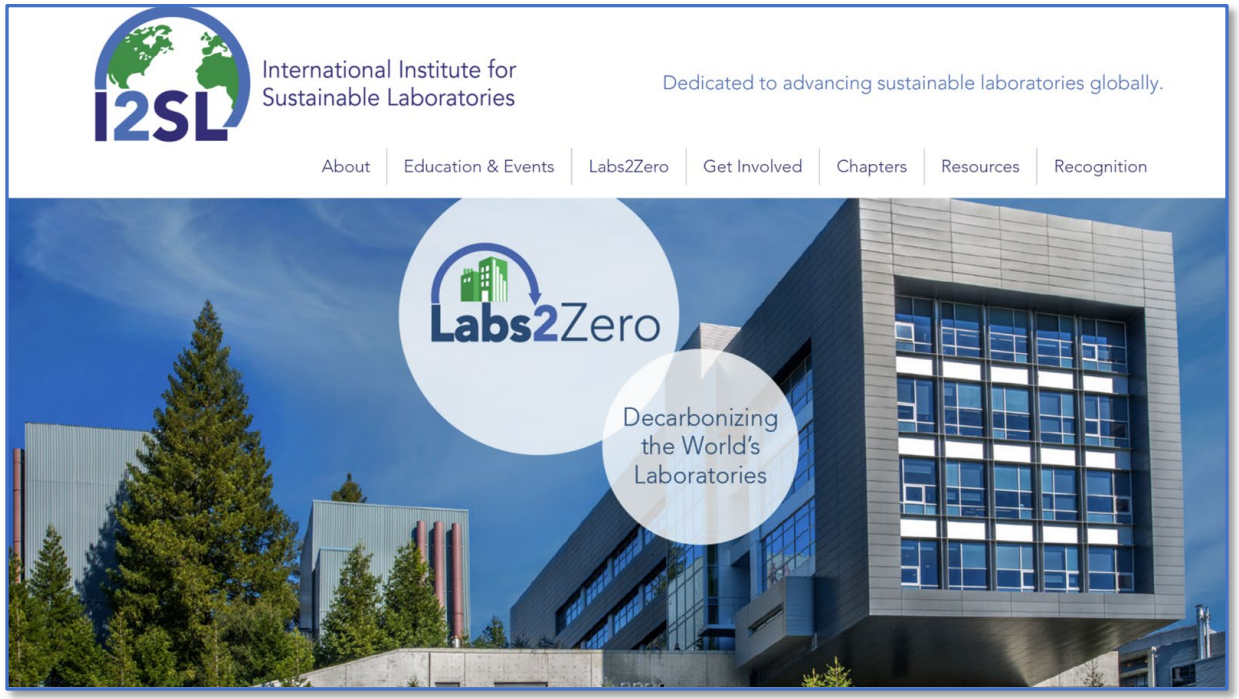

Labs2Zero Elements & Structure:

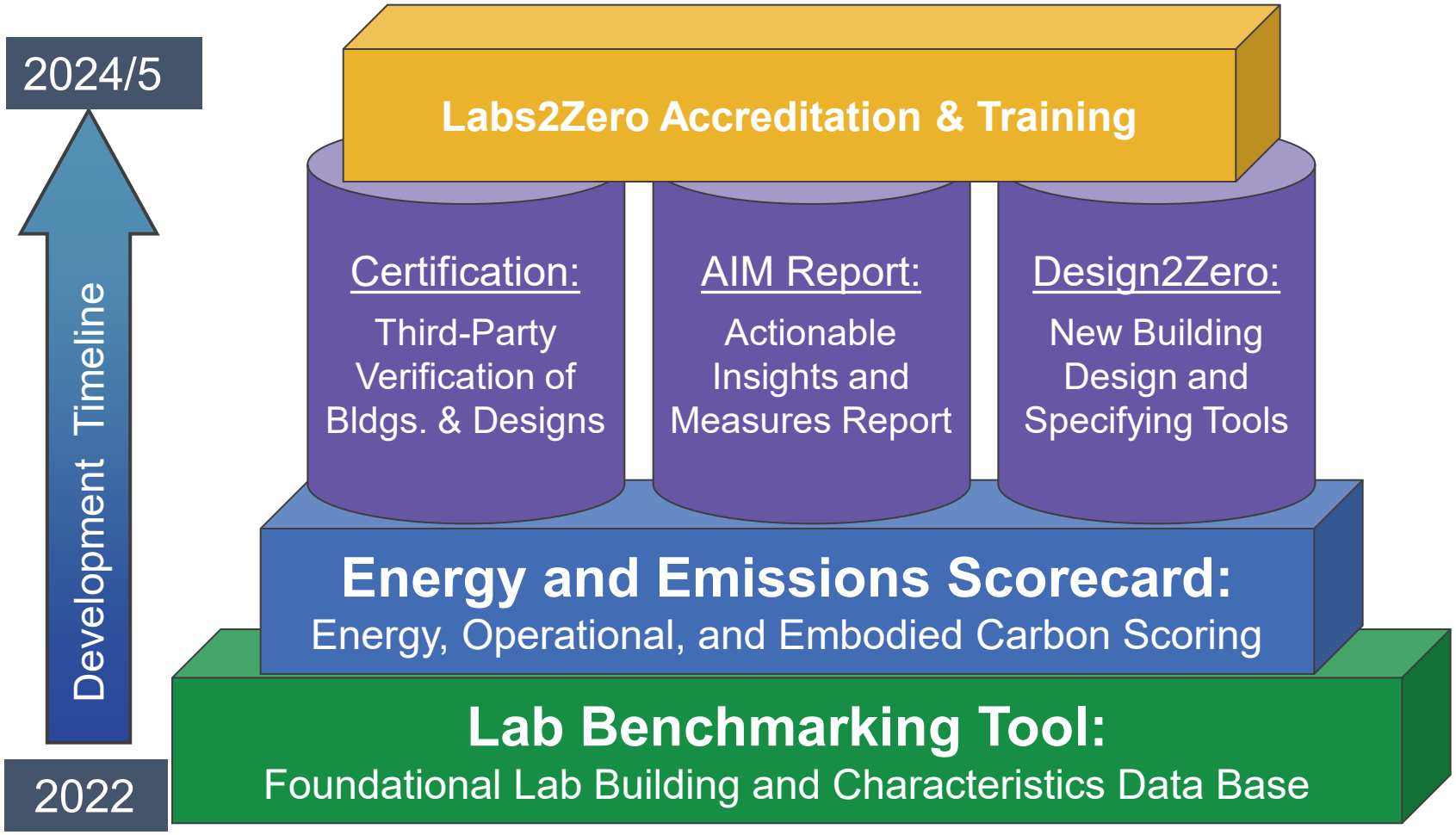

The Labs2Zero Program has six related program elements

2023 Energy & Emissions Score Accomplishments

Energy score pilot released!!

- ✓ Score is a 1 to 100 (best) score based on a percentile value vs. peer labs
- ✓ Similar in concept to Energy Star scores

Embodied carbon benchmarking data call just released

- ✓ If you have done lab building embodied carbon LCA's please contact us!
- ✓ Will provide the foundation for embodied carbon benchmarking & scoring

Operational emissions score focused on location based emissions

Look for pilot operational emissions & embodied carbon scores to be released by Fall 2024

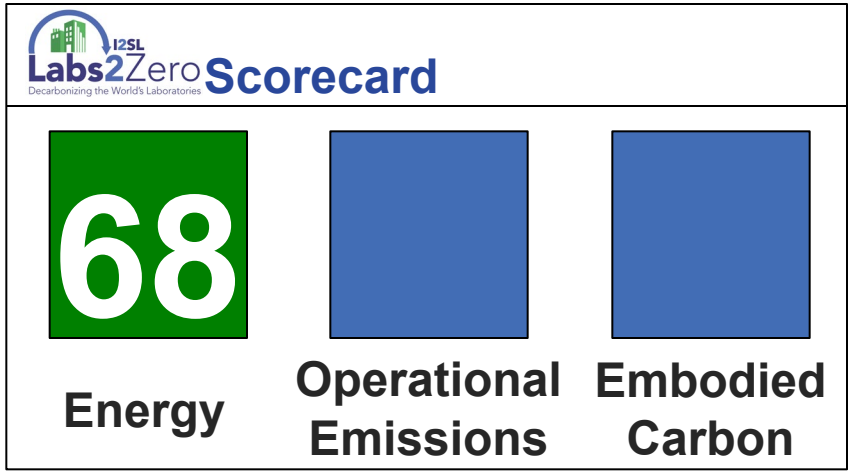

Labs2Zero

Pilot Energy Scores

- **Now displayed for all buildings**
  - 1-100 score, where 100 is best
  - Scores displayed for each user's buildings and for anonymous peer group

Labs2Zero Energy Score

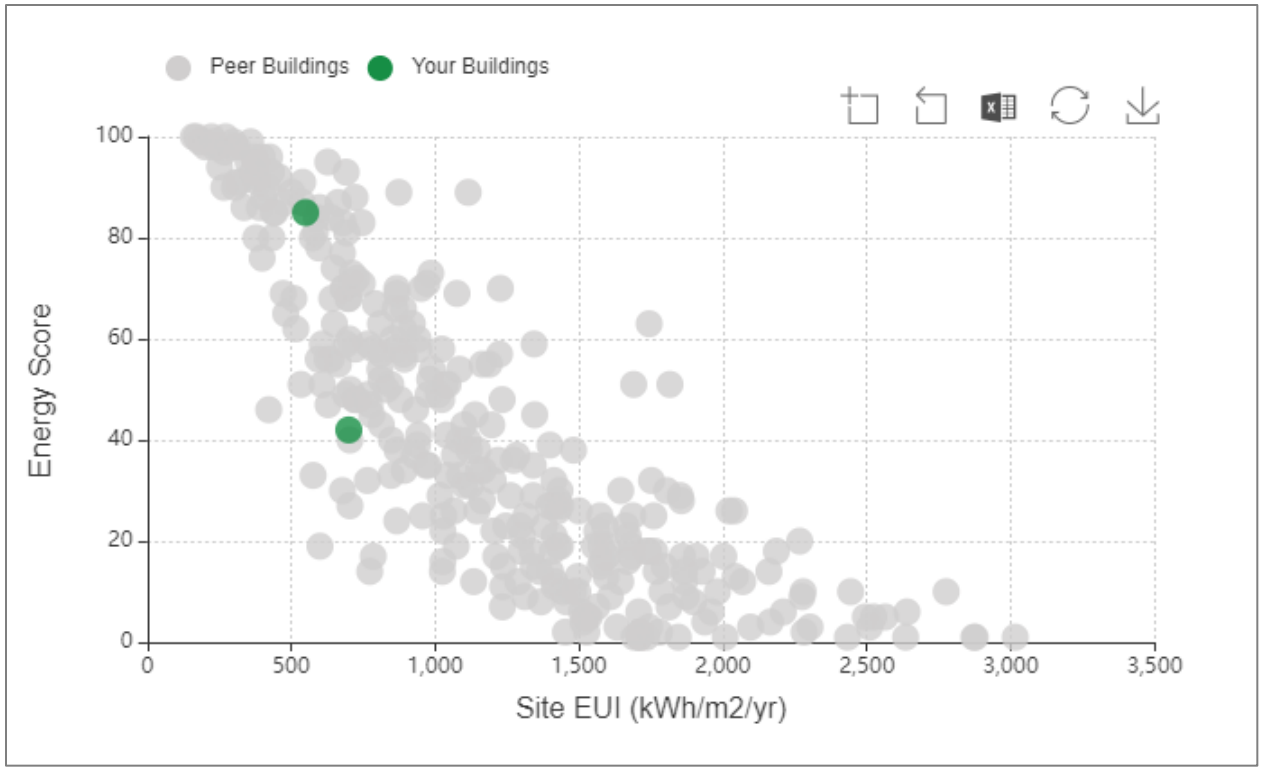

Also New: Longitudinal Benchmarking

- View building **performance over time** for many metrics
  - Only Energy Score is weather normalized

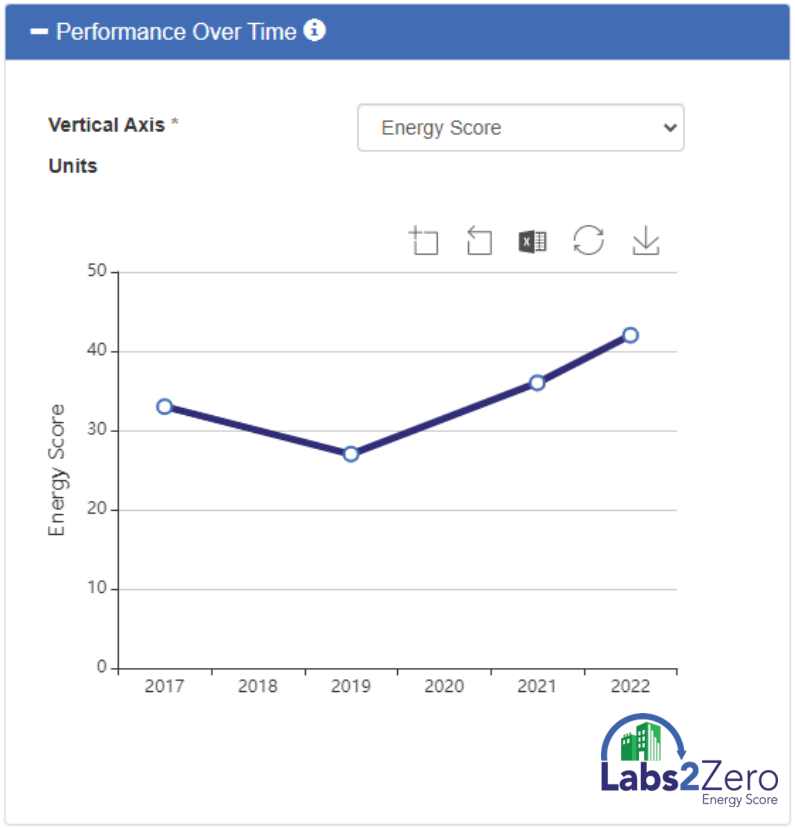

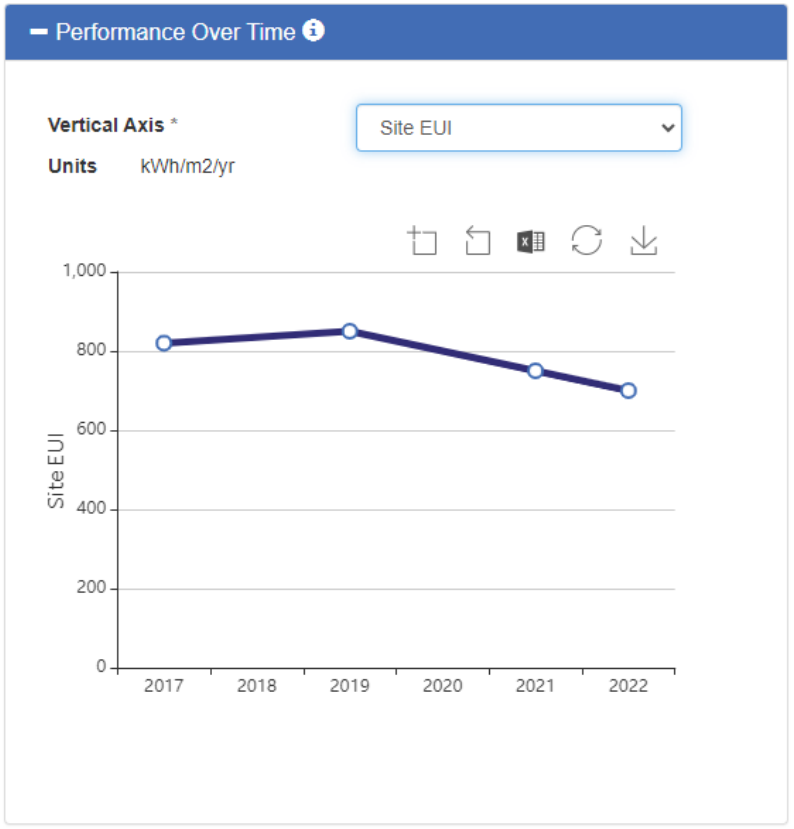

The Energy Score Pilot Phase

- **Post-launch pilot phase October 2023 to mid-2024**
  - ✓ Rev1 score will follow
- **Seeking feedback from you on the Pilot Energy Score**
  - ✓ More data known to be needed for some facility types:
  - ✓ Vivarium, manufacturing, crime labs
  - ✓ Labs in very cold climates

Now is the best time to provide feedback:

1. Enter your data via the LBT (lbt.i2sl.org)
2. View your scores
3. Send us feedback at lbt@i2sl.org

The New Labs2Zero Partner Recognition Program

- **Recognizes organizations that support Labs2Zero:**
  - ✓ **Owner Partners**
    - *Owners that enter their lab data into the LBT annually*
  - ✓ **Consulting Partners**
    - *Architects, engineers & other consultants that supply lab data*
    - *Both for new project designs as well as existing buildings*
    - *Data can be energy, operational emissions, & embodied carbon*
  - ✓ **Promotional Partners**
    - *Organizations that promote and encourage use of the program*

Agree to enter at least some of your labs or your client's labs into the LBT & be recognized as a Labs2Zero Partner!

Labs2Zero Components: The AIM & Design2Zero Reports

- **AIM: Actionable Insights & Measures Report**
  - ✓ **Provides a level 1 audit or screening level report:**
    - *Auto generated 20-40 page report based on LBT inputs*
      - Calculates measure's rough savings, costs & ROI
  - ✓ **Includes relevant case studies for building**
- **Design2Zero report focused on new designs**
- **Standardized, immediate, & objective audits**
  - ✓ **Est. price for AIM Report ~$350 - $500/yr./bldg.**

#	Measure Based Groups
1	Central Heating Plants
2	Central Cooling Plants
3	Ventilation & Heat Recovery
4	Lighting
5	Process/Equipment
6	Demand Response
7	Renewables
8	Building Envelope
9	Electrification
10	Green Lab/Behavioral
11	Bldg. Control System Related
12	Other
13	Embodied Carbon
14	Water Use

AIM & Design2Zero Report Status

2023 Accomplishments:

- ✓ Amassed ~300 energy & emissions measures
- ✓ Developed process & steps to develop reports
- ✓ Developed preliminary software requirements

Next Steps in 2024:

- ✓ Start software & engineering consultant work
- ✓ 4 TAC subgroups will oversee & assist in developing AIM Report Generator

2024 Goal: Rev1 AIM Pilot Report initially focused on energy in existing buildings released by Fall.

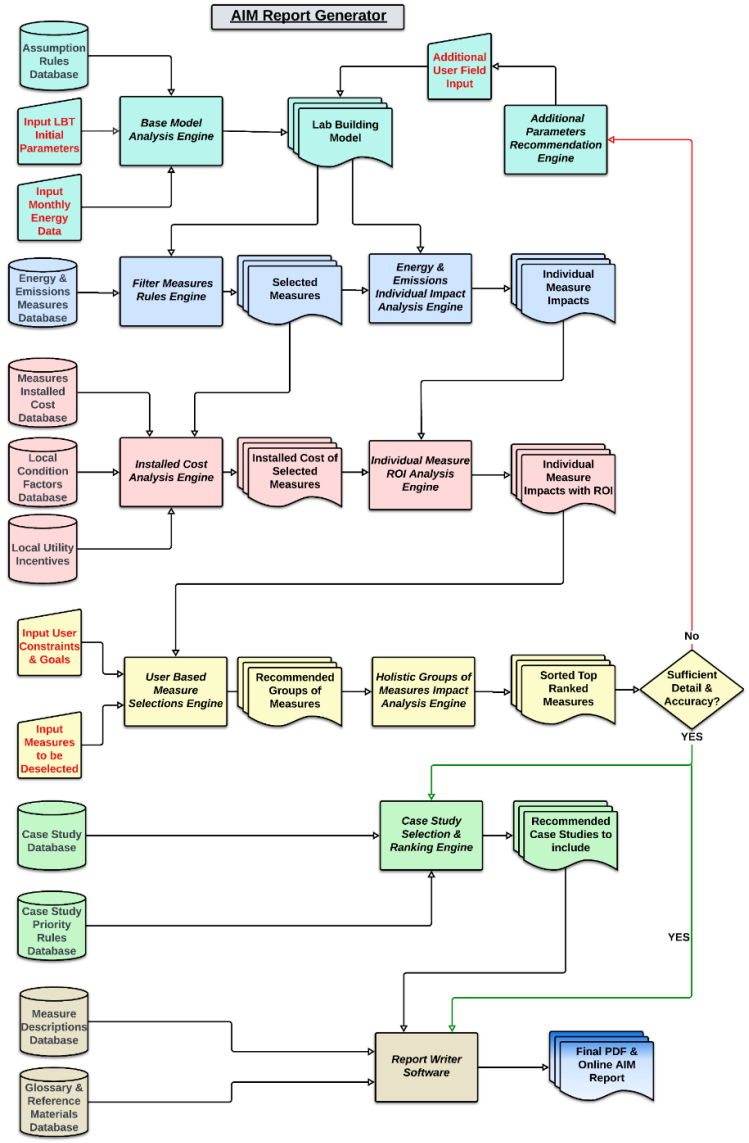

Labs2Zero Program Organization Chart

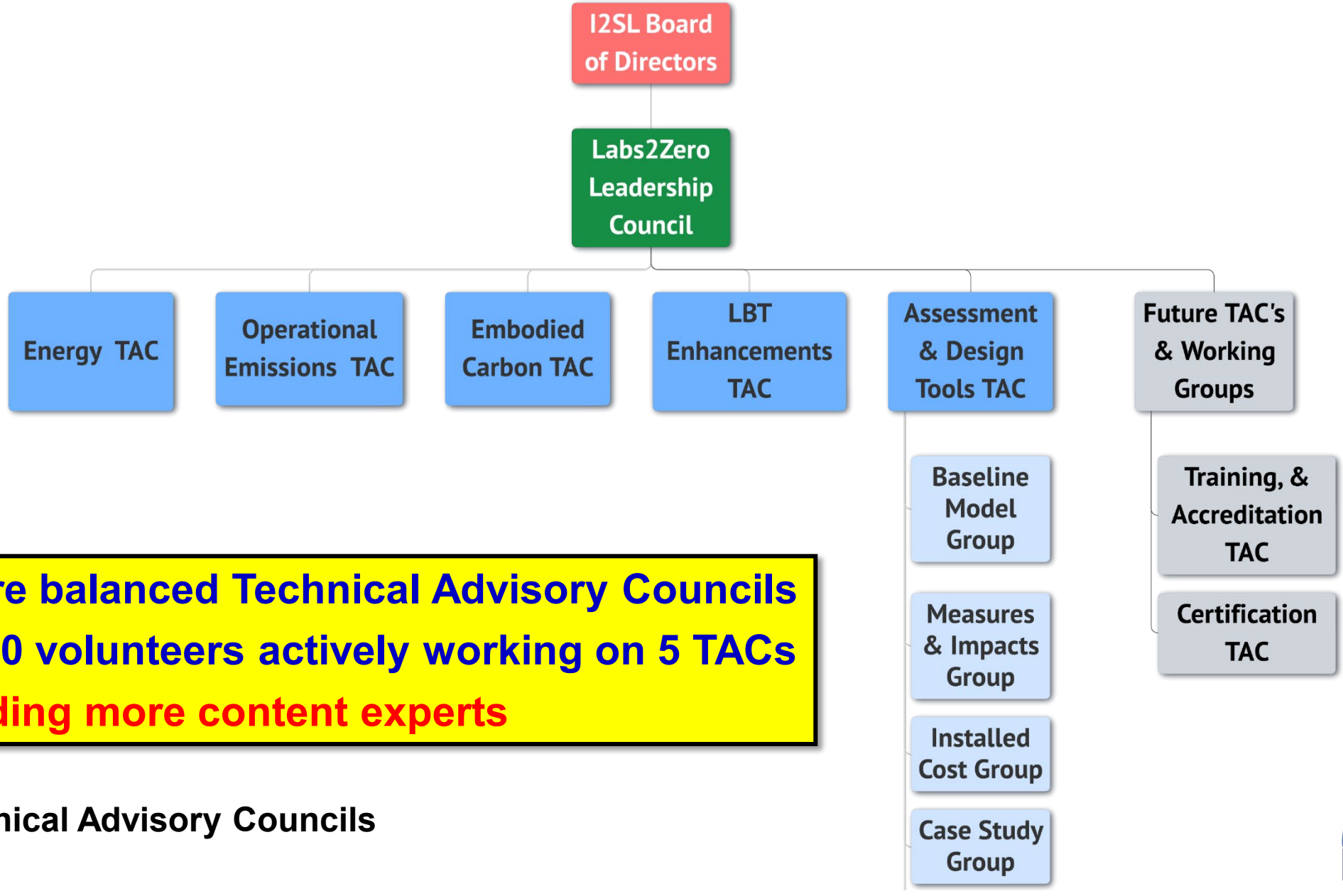

- TACs are balanced Technical Advisory Councils
- Over 100 volunteers actively working on 5 TACs
- Still adding more content experts

*TAC – Technical Advisory Councils

Labs2Zero: A Global Lab Community Wide Program

- **The Labs2Zero Mission:**
  - ✓ Accelerate decarbonizing the world's labs with needed metrics, analysis services, training, and recognition
- **Volunteers needed to help staff TACs & working groups**
  - ✓ I2SL is looking for more volunteers & paid contractors for Labs2Zero
- **Sponsors & financial support still needed for Labs2Zero:**
  - ✓ Looking for additional sponsors

Interested in supporting Labs2Zero? Please contact Gordon Sharp, President@I2SL.org or Kathleen Brady, Kathleen.Brady@erg.com